5164491/2024

VIII

GOVERNMENT OF KERALA

Disaster Management(A)Department

No.DM4/177/2018-DMD

18-04-2024,Thiruvananthapuram

From

Principal Secretary to Government

To

Commissioner
Disaster Management

Sir,

Sub: DMD-SLP(C)10099/16 filed by Dr.Biju Ramesh- Detailed study entrusted to College of Engineering Trivandrum-Reg

Ref: GO(Rt)No.580/2022/DMD dated 22/07/2022

Inviting attention to the reference cited , I am to inform you that as per the order 1st cited, sanction has been accorded to Chief Engineer, IDRB to entrust College of Engineering Trivandrum for conducting a detailed study on the hydrological performance and stability of the Thekkinikkara canal. As such the study report furnished by CET is enclosed herewith for your specific remarks in the matter.

Yours Faithfully,
NISSAR A
UNDER SECRETARY
For Principal Secretary to Government.

Approved for Issue,
Signed by
Veena K V
Date: 20-04-2024 10:27:05
Section Officer.

CONTENTS

List of Figures

List of Figures……contd.

List of Figures……contd.

List of Figures ……contd.

List of Figures ……contd.

List of Tables

HYDRAULIC PERFORMANCE AND STRUCTURAL STABILITY OF THEKKINIKKARA CANAL

1. Introduction

The Irrigation Design and Research Board has requested for conducting a study on the "Thekkinikkara Canal system in Thiruvananthapuram city" Lr. No. 15/92IIDRB/CS(1) dt. 10.11.2020, of Chief Engineer, IDRB, Thiruvananthapuram. The work was taken up as a consultancy project through the Centre for Industrial Training, Consultancy and Sponsored Research (ITC&SR), of the college. The emphasis of the study is to assess the Hydraulic performance and Structural stability of the Thekkinikkara Canal System.

The specific objectives of the study include: (i) Details of all storm water drains connecting the canal (Hydrological and hydraulic particulars) and new canals constructed and connected as part of Operation Anantha (ii) Hydraulic and Hydrological details of Thekkinikkara Canal (Bed level, Top level, cross section, slope, capacity etc.) at salient points (iii) Sedimentation status of existing canal system at salient sections. (iv) Actual Discharge in the canal system for different rainfall events with return period (v) Physical evaluation in the deterioration of the canal structure by field data collection. (vi) Modelling using finite element to assess the stability of the existing structure incorporating the loading and material characteristics (vii) Effect of the earthquake forces on the stability of structure. The details pertaining to the above aspects are presented in the subsequent sections of the report.

2. Organization of Report

The study involves mainly two major components: (i) Hydraulic Performance and (ii) Structural performance, of the Thekkinikkara canal system. Hence the report is presented as two parts: Part A: hydraulic Performance and Part B: Structural Performance, followed by the observations/recommendations from the study.

3. Part A: Hydraulic Performance

The hydraulic performance of the canal system mainly involves assessment of the carrying capacity of the Thekkinikkara canal for the various design rainfall events considered in the study. The study mainly involves in identifying the drainage system of main canal and laterals, delineation of the study area draining to the canal system, data collection for the canal system, assessment of sedimentation status of canal, runoff modelling and routing through canals, performance assessment based on the carrying capacity of canals or flooding at various salient points in the canal stretch.

The alignment of Thekkinikara canal and its cross section was provided by the IDRB. The details pertaining to the catchment, drainage network and associated canal parameters were taken in the field by conducting survey work and other observations. The site was inspected and other details pertaining to the flooding levels, drains, culverts etc., were taken by field survey. The study involves in identifying the sub-basins draining to the natural streams located in the study area, simulation of the runoff from the basins for different rainfall events, routing of runoff/flood flow in the basins and preparation of flood inundation details. The storm water runoff modelling was undertaken using EPA's Storm Water Management Model (SWMM) which is a widely used modelling frame work for planning, analysis and design related to storm water runoff and drainage systems in urban areas. The flooding areas were identified for different rainfall events, The details pertaining to the study area, data used, methodology and the outcome of study are given in the subsequent sections.

3.A.1. Study area

The study area showing the proposed Thekkinikkara canal, major roads, and other prominent establishments is shown in Fig.A.1. A GPS survey was undertaken for locating the canals and drains with GPS points as shown in Fig. A. 2. The main drain of Thekkinikkara canal, lateral drains joining to it (including the drains constructed under operation Anantha) are shown in Fig. A.3. The Thekkinikkara canal is one of the main flood water canals which starts from Karimadom Pond in Karimadom Colony at East Fort and passes through the most populated areas like East Fort, Padmanabhaswamy Temple, Sreevaraham, Muttathara, N H bye pass and ends in Parvathy Puthanar near Puthenpalam. About half of the portion of the canal is covered

with slab and the remaining length of it is kept open. The covered portion of Thekkinikkara canal of length 2.5 km has a width of 2.8 m with an arch on the top with the crown height as 2.5 m. The Thekkinikkara canal was originally envisaged for carrying away the flood water from Karimadom pond, and draining of excess water from the other ponds in and around the Padmanabhaswamy temple. In the course of time, many lateral drains draining the Chalai area, Pazhavangadi temple area, Attakulangara area were constructed under JNNRUM project connected to it at different points enroute of the canal. Moreover, one of the lateral drains is connected to the Pazhavangadi Thodu to drain the excess flood water from it above a particular level. The cross-section of the Thekkinikkara canal is shown in Fig.B.2, with Interior span width = 2800 mm, height of the centre crown = 2500 mm, with the rise of arch at crown = 1000 mm above the rectangular portion having a height 1500 mm. The material: used for arch is country burnt bricks, in three layers. The height of earth fill above crown level of the arch is around 1.5 m. The water flowing in the Thekkinikkara canal occurs mainly during rainfall events and carries very low dry weather flow in other periods, and is highly polluted.

3.A.2. Rainfall data

The duration of rainfall depends on the time of concentration of the basin in the study. In the present case the time of concentration is estimated to be in the range as 1.1 to 1.8 hours for the study area draining to the main outlet at Nandini garden exit. Since no observed hourly rainfall values for the above duration is available, the disaggregation of one day rainfall values to hourly durations is done using the IMD equation $P_t = P_{24}\ (t/24)^{1/3}$, where P_t is the rainfall depth (mm) and t is the desired duration (hr). The rainfall values for the study were taken from PMP Atlas of Western Ghats (PMP atlas-Phase 2(Stage 1): Report of the West flowing rivers of Western Ghats, WAPCOS, New Delhi) [11]. Rainfall maps of Western Ghats, South of River Tadri (Region 101), were adopted for taking rainfall values of 25-year 1 day rainfall: Plate 1; 50-year 1 day rainfall: Plate 14; 100-year 1 day rainfall: Plate 15; 1 day Point PMP rainfall: Plate 11. The one-day rainfall values for the return periods T = 25-year, 50-year, 100-year, and PMP (Probable maximum precipitation) taken from the PMP atlas for the basin are 240 mm, 260 mm, 300 mm, 600 mm respectively. Following the IMD equation, the maximum rainfall corresponding to the duration of rainfall of 1 hr,

for the return periods of T = 25-year, 50-year, 100-year, and PMP (Probable maximum precipitation) were estimated as 83 mm, 90 mm, 104 mm, and 208 mm. Also, the maximum rainfall corresponding to the duration of rainfall of 2 hr, for the return periods of T = 25-year, 50-year, 100-year, and PMP (Probable maximum precipitation) were estimated as 104 mm, 113 mm, 131 mm, and 262 mm. The above rainfall magnitudes were applied for simulation of runoff and derivation of flood hydrographs.

For the simulation of runoff for small return periods (generally adopted in the design of urban drainage systems) daily rainfall magnitudes corresponding to return period T = 5-year, taken as 132 mm [13] and T = 10 year, taken 184 mm [12] were also used in simulations. The corresponding values of 1- hour and 2-hour rainfall for T = 5 year, adopted in simulation are 46 mm and 58 mm respectively. Similarly, the corresponding values of 1 hour and 2-hour rainfall for T = 10 year, adopted in simulation are 64 mm and 80 mm respectively.

3.A.3. Overview of SWMM Modelling Software

The modelling software used for the simulation of flood in the study is EPA's Storm Water Management Model (SWMM) which is a widely used modelling frame work for planning, analysis and design related to storm water runoff and drainage systems in urban areas. This general-purpose urban hydrology cum conveyance system hydraulics software is a dynamic rainfall-runoff simulation model and may be used for single event or long-term (continuous) simulation of runoff quantity and quality from primarily urban areas. The runoff component of SWMM operates on a collection of sub-catchments that contributes runoff and can model its transport through channels/conduits. SWMM has the capability to track runoff contributions from each sub catchment along with corresponding flow rates and flow depth in each channel over multiple simulation time steps. SWMM accommodates spatial variability by dividing a study area into a collection of smaller, homogeneous sub- catchment areas and each having its own fraction of pervious and impervious sub-areas to model overland flow which may then be routed between sub-areas, between sub catchments, or between entry points of a drainage system. SWMM also contains a flexible set of hydraulic modelling capabilities used to route runoff and external inflows through the drainage system network of pipes, channels, storage units and diversion structures. These include the ability to handle drainage networks of unlimited size, use a wide

variety of standard closed and open conduit shapes as well as natural channels, model special elements such as storage/treatment units, flow dividers, pumps, weirs, and orifices, apply external flows and water quality inputs from surface runoff, groundwater interflow, rainfall-dependent infiltration/inflow, dry weather sanitary flow, and user defined inflows, utilize either kinematic wave or full dynamic wave flow routing methods, model various flow regimes, such as backwater surcharging, reverse flow, and surface ponding, apply user-defined dynamic control rules to simulate the operation of pumps, orifice openings, and weir crest levels.

3.A.4. Methodology for the simulation of flood

The study area consisting of the water shed of Thekkinikkara canal was delineated from the topographical maps of Survey of India. The (artificial/natural) drains draining the catchments and their invert levels were identified by field DGPS survey. Also, the cross-sectional parameters of channels (width, depth, invert levels) at salient points were also taken by field survey. The map of the study area was given as input to the SWMM. The entire drainage network was also given as inputs to the model, by specifying the nodes, connecting links between nodes, and the direction of flow. The entire study area is divided into sub-catchments and the runoff from each of them is connected to the nodes in the drainage network. Thus, the entire drainage network of the study area is created in SWMM. The width and depth of drains, invert levels in the direction of flow are also specified as inputs.

The following are the features/details in modelling/simulation of the drains, shown in Fig.A.4.

1. The Thekkinikkara canal starts from Karimadom pond (node : TK66) and ends at outlet of Nandini gardens (node : D5004).
2. Drain constructed on the side of Attakulangara- Killipalam Junction road under Operation Anantha, starting from Killipalam Junction (Node : TK12) and joins the Thekkinikkara canal (Node : TK1)
3. Two drains constructed under Operation Anantha draining the Chalai area (i) TK23 -TK19- TK9 joins operation Anantha drain from Kiiippalam Junction (Node TK9); (ii) TK31-TK67 joining the operation Anantha drain from Killipalam Junction (Node : TK67) (iii) TK7-TK5 joining the operation Anantha drain from Killipalam Junction (Node : TK5).

4. Drain D5003 - TK63 from Attakulangara area joins the Thekkinikkara Canal at TK63.
5. Drain TK381 – TK 442 constructed under operation Anantha, to drain the Putharikandommaidanam area and Chalai area and joins the Thekkinikkara canal (between TK 46 and TK442) inside Govt. High school Attakulangara. This drain is also used to convey the flood water from PazhavangadiThodu above reduced level of + 6.2 m through a canal opening of 2.5 m width and height 0.6 m. The cross-section of canal is 2.2 m wide and 1.5 m depth.
6. Drain TK71 – TK46 from the Pazhavangadi temple area constructed under Operation Anantha joins the Thekkinikkara Canal at TK46.
7. Drain (Node 66 to Node TK50) draining the Transport Bhavan area joins the Thekkinikkara Canal at TK50 near Vazhappally Junction.

The simulation of runoff from the catchments were done by using the SCS curve number method with due consideration to the land use of the area. The calibration of the model was done for observed rainfall patterns and the assessment of model parameters was done with respect to the drain TK381 – TK442. The simulated runoff from the sub-catchments enters into the drainage network at the nearest nodal points to the catchments. The runoff in the drains is routed to the drainage outlet using the dynamic wave flow routing method, incorporating the extreme input conditions. The simulation of flood corresponding to different rainfall events having return periods of 5- year, 10-year, 25-year, and 50-year, 100-year, and PMP were carried out. In undertaking flood simulations, the cross-sectional parameters and invert levels at respective nodes in the flow direction were given, and the hydraulic gradient line of flow in the drains is simulated.

3.A.5. Simulation of flood

The hydraulic simulation of storm water runoff and its routing was done using the SWMM model. The input parameters of the drainage network: layout, shape, dimensions, invert levels were fed into model. The sub-basins draining into the drainage network were also given. The simulation of runoff from the catchments were done by using the SCS curve number method with due consideration to the land use of the area. The calibration of the model was done for observed rainfall patterns of 1 hour duration with magnitudes of 38 mm and 59 mm and the assessment of model

parameters was done with respect to the drain TK381 – TK442. The plot showing the actual and computed depth of flow at TK42 node (in the stretch TK381 – TK 442) is shown in Figure A.5. The land use of the study area is more or less similar, highly urbanized with 90 % area impervious in nature, which assigns curve numbers CN in the range 90 to 95 in calibration. The simulation of flood corresponding to rainfall events having return periods of 5-year, 10-year, 25- year, and 50-year, 100-year, and PMP were carried out. The simulated hydrographs at the salient nodal points in the network were generated, and maximum value hydraulic gradient at each of the locations were noted. The assessment of the capacity of canal to carry the discharge was thus done for the situations simulated.

3.A.6. Results and Discussion

The outputs of the study in consonance with the objectives of the study are summarized.

(a) **Details of all storm water drains connecting the canal (Hydrological and hydraulic particulars) and new canals constructed and connected as part of Operation Anantha :**The drainage network indicating the Thekkinikkara canal and the main canals constructed as a part of JNURUM project used in the simulation study are shown in Figure A. 3. The details of linked canals which are rectangular in cross-section (width, depth and invert levels) at salient points are presented in Table A.2.

(b) **Hydraulic particulars of the Thekkinikkara canal System** : The hydraulic particulars indicating the cross-sectional parameters at salient points for the canal system used in simulation at the nodal points are summarized in Table. A.1.

(c) **Sedimentation status of existing canal system at salient sections**: The existing invert levels at the salient points in the Thekkinikkara main system is given in Table A.1. The sedimentation profile in the canal is plotted as in Fig.A.17.

(d) **Hydraulic Simulation of flood in the Canal system:** Discharge in the canal system for different rainfall events occurred during the study period were simulated. The flood hydrographs at the nodal points were simulated for typical rainfall events during the study period. The simulated discharge hydrograph at the salient points of the canal system for rainfall durations tr = 1 hour for return periods T = 5-year, 10-year, 25-year, 50-year, 100-year and PMP are shown in Figures Fig.A.6, Fig.A.8, Fig.A.10, Fig.A.12, Fig.A.14 and Fig.A.16 respectively.

Also, the simulated discharge hydrograph at the salient points of the canal system for rainfall durations tr = 2 hour for return periods T = 5-year, 10-year, 25-year, 50-year, and PMP are shown in Figures. Fig.A.7, Fig.A.9, Fig.A.11, Fig.A.13, Fig.A.15, and Fig.A.17 respectively. The hydraulic grade line (HGL) of runoff flow in canals corresponding to the rainfall durations of tr = 1 hour for return periods of T= 5-year, 10-year, 25-year, 50-year, 100-year and PMP at the salient points of the canal system are given in Table A.3. Similarly, the hydraulic grade line (HGL) of runoff flow in canals corresponding to the rainfall durations of tr = 2 hour for return periods of T= 5-year, 10-year, 25-year, 50-year, 100-year and PMP at the salient points of the canal system are given in Table A.4. The plot of the HGL indicating the maximum permissible water level and the simulated water levels corresponding to tr = 1 hour rainfall for different return periods of T = 5, 10, 25, 100 years and PMP is shown in Fig.A.19. Also, the plot of the HGL indicating the maximum permissible water level and the simulated water levels corresponding to rainfall duration tr = 2 hour for different return periods of T = 5, 10, 25, 100 years and PMP is shown in Fig.A.20. For the different reaches of Thekkinikkara canal, corresponding to rainfall duration tr = 2 hour, the plot of HGL for different return periods, is given in Fig.A.21, Fig.A.22, Fig.A. 23, and Fig.A.24. At some of the nodal points (where lateral inflow enters into the canal system) a sudden increase in HGL is observed for higher intensity rainfall cases. It can be observed that for T= 5-year, and T=10-year, flooding occurs only at the starting node (Karimadom pond area); and all other nodes in the stretch of the canal, the HGL is below the permissible HGL values, thereby no flooding. Also, for rainfall values corresponding to return periods T = 25-year, 50-year, 100-year, and PMP, it can be observed that in majority of nodes (except few at the downstream end), the HGL for the cases is above the permissible limits, thereby flooding occurs, as the capacity of canal is exceeded.

(e)Simulation of Flash flood due to cloud burst phenomena

In recent times the occurrence of flash flood situation created due to the cloud burst phenomena has been reported. According to IMD, if the rainfall is more than 100 mm in one hour the event is termed as cloud burst phenomena and if the rainfall is between 50 to 100 mm it is termed as mini cloud burst phenomena. In the present study the magnitude of rainfall considered for runoff and flood simulation is more than 100 mm in situations of T= 100 year and PMP. Both simulation of flood similar to cloud burst/mini-cloud burst situations are considered in the study. Hence it is not necessary to conduct a separate simulation for the case, since it is already incorporated.

(f) Physical evaluation in the deterioration of the canal structure by field data collection: The Thekkinikkara canal was originally constructed as a closed canal with rectangular bottom covered with an arch on the top (bottom width = 2.8 m, depth from the crown of arch = 2.5 m, height of rectangular portion = 1.5 m, radius of arch portion above the rectangular portion = 1.0 m). The side walls of canal are of rubble work 0.6 m thick and the top cover is by brick arch of 0.3 m thick. The portion of the canal from the Karimadom pond to the node TK68 by the side of Attakulangara-Killippalam road was renovated as a part of Operation Anantha and converted into a rectangular drain of 2.8 m width and 2.5 m depth, covered by RCC slabs. The major length of the canal from Node TK68 to TK50 (near Vazhappally temple junction) is a closed canal with rectangular bottom covered with brick arch on the top, being the original constructed canal. In the above stretch of the canal there are only few openings for accessing the canal; (i) Manhole in the compound of Vaikuntam Kalyana Mandapam owned by Padmanabha swamy temple trust; (ii) broken portions of canal by the side of Karimpinel arcade (one near to the fort wall by the side of MG Road, and another one by the side of road connecting Transport Bhavan to Padmanabhaswamy temple east nada). Also, at two locations inside the Government High School Attakulangara compound (in the stretch TK1-TK441-TK46) the canal section was opened and covered with slabs. At one of the locations the canal section was seen in a damaged state due to the growth of tree roots. The water flowing in the canal is highly polluted with sewage and with less DO. It is difficult to enter into the closed canal without proper ventilation and thereby dangerous, as there exist very few manholes.

3.A.7. Observations from the study

1. It is seen that around fifteen lateral canals draining the study area were constructed under Operation Anantha and other scheme and are connected to the main Thekkinikkara canal at different reaches. Also, a lateral diversion to divert excess flood water from the Pazahavangadi Thodu (when the flood level exceeds +6.2 m) was constructed under Operation Anantha, joining the Thekkinikkara Canal inside the Attakulangara school.
2. The major stretch of the Thekkinikkara canal is silted up thereby having lesser carrying capacity when compared to its design carrying capacity.
3. It is observed that the existing network of Thekkinikkara canal is not subjected to flooding (except Karimadom pond area) for the return period of rainfall of 5-year, 10-year, being the usually adopted return period for storm drainage design practices.
4. Also, it is observed that the majority of the nodes in the existing network of Thekkinikkara canal is subjected to flooding for higher values of return period of rainfall of 25-year, 50-year and 100-year and PMP values.
5. The simulation of flood was carried out on the basis of design hydraulic parameters of canal, without considering the sedimentation status in canals. The magnitude of flood may be more in sediment deposited canal stretches.

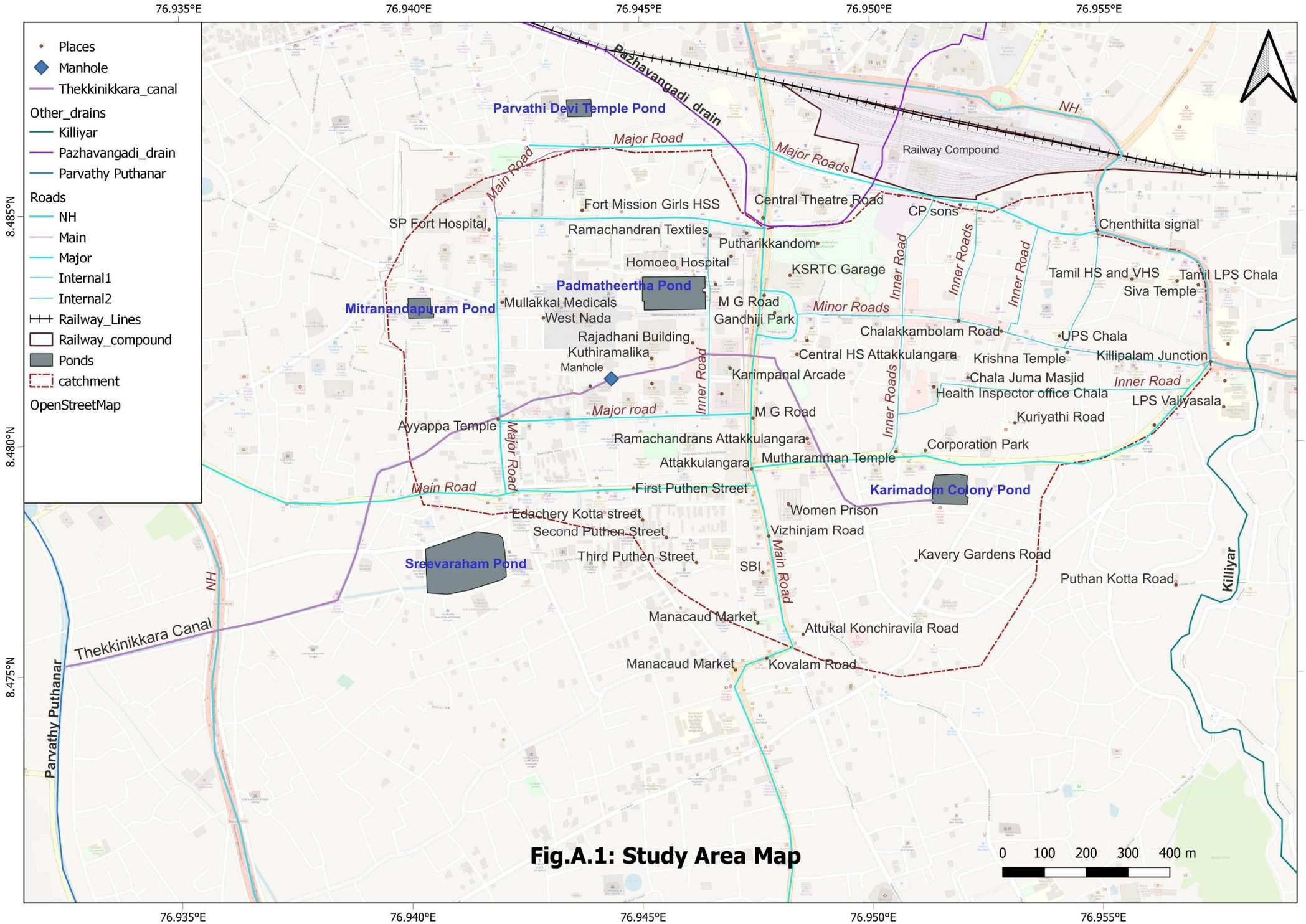

Fig.A.1: Study Area Map

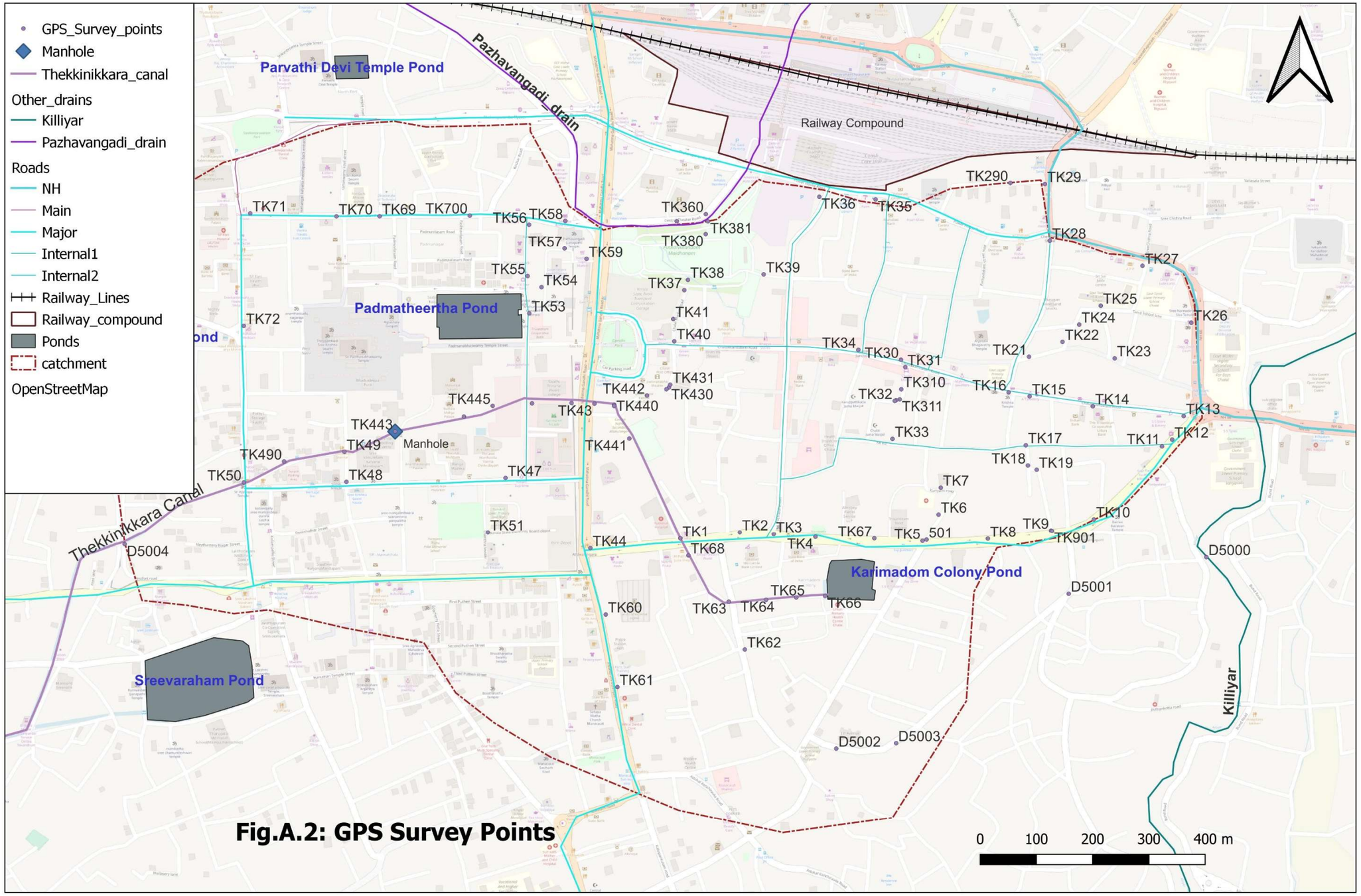

Fig.A.2: GPS Survey Points

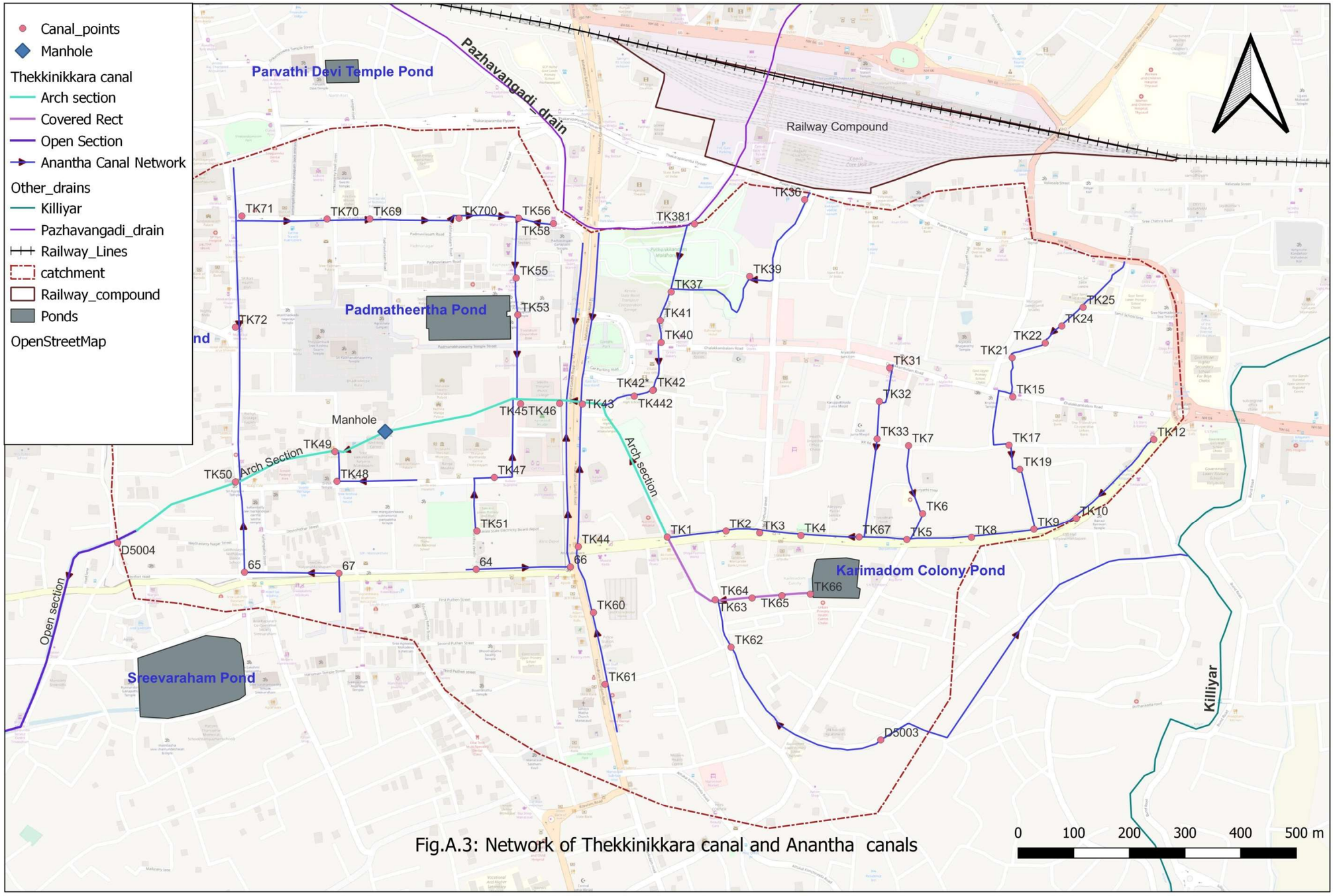

Fig.A.3: Network of Thekkinikkara canal and Anantha canals

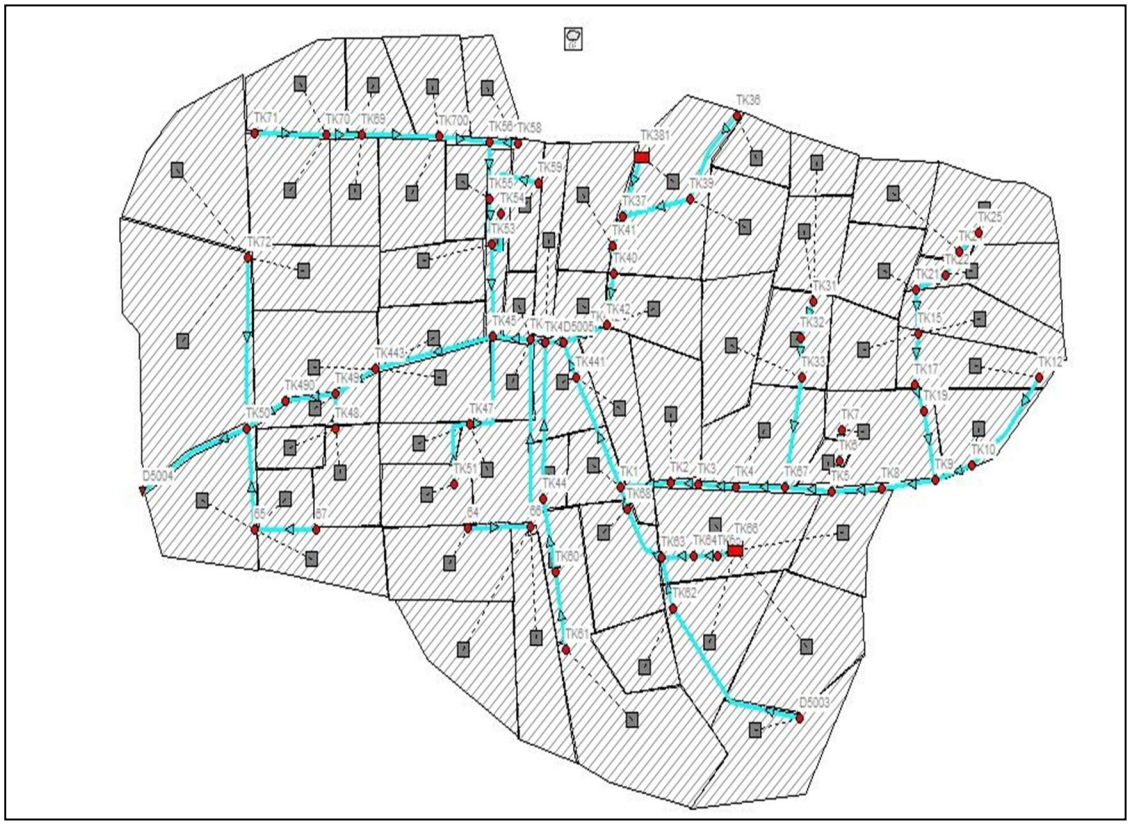

Fig.A. 4 : Drainage network of Thekkinikkara Canal and Operation Anantha Canals

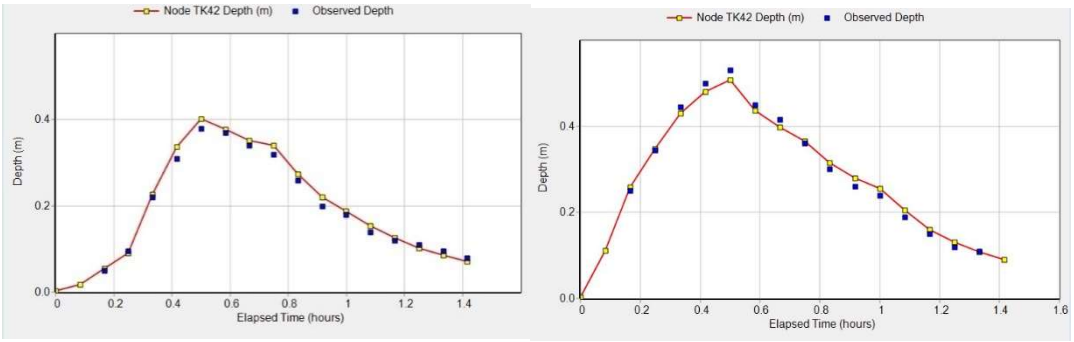

(a) (b)

Fig. A.5 : Plot of computed and actual depth of flow at TK42 node for rainfall events (a) 38 mm and (b) 59 mm

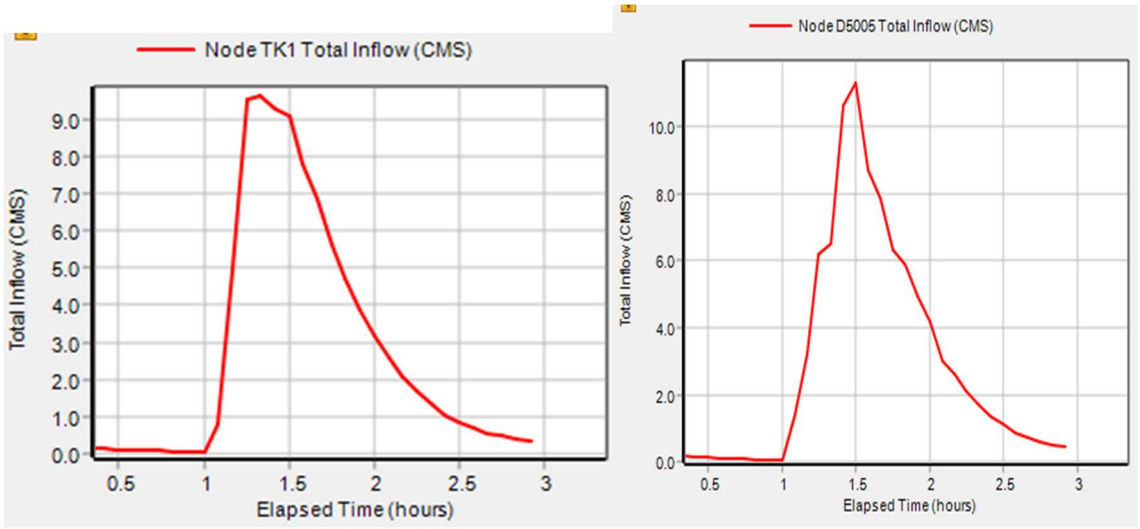

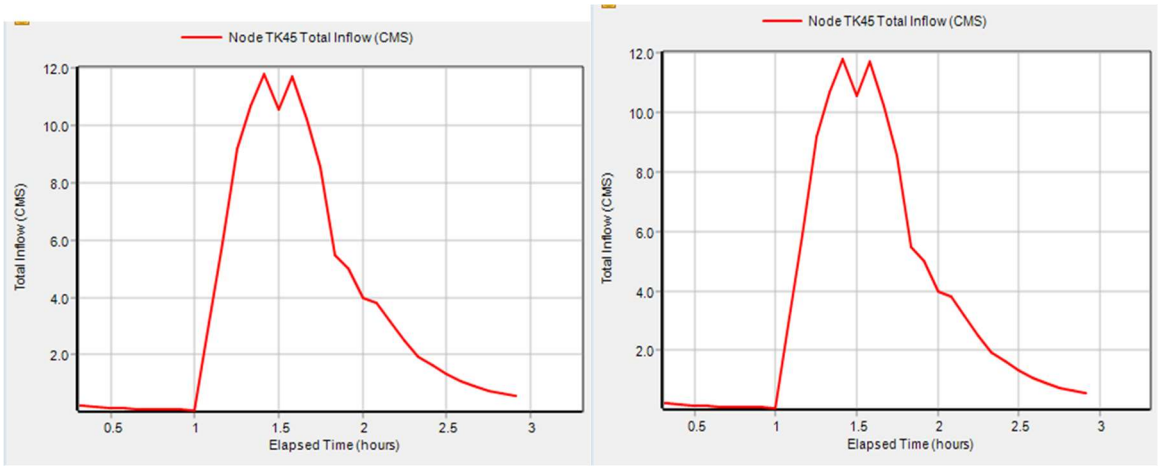

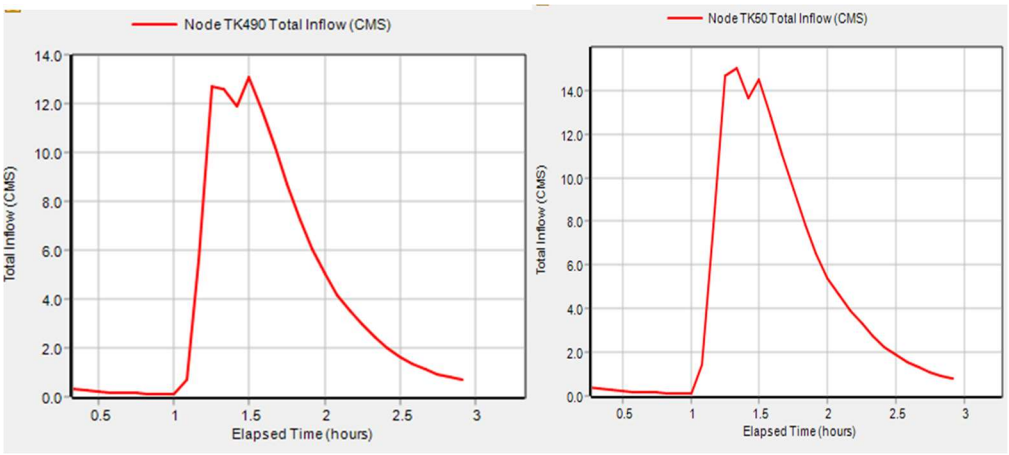

Fig. A.6. Simulated hydrographs at typical nodes for rainfall duration tr = 1 hr, for T = 5 year

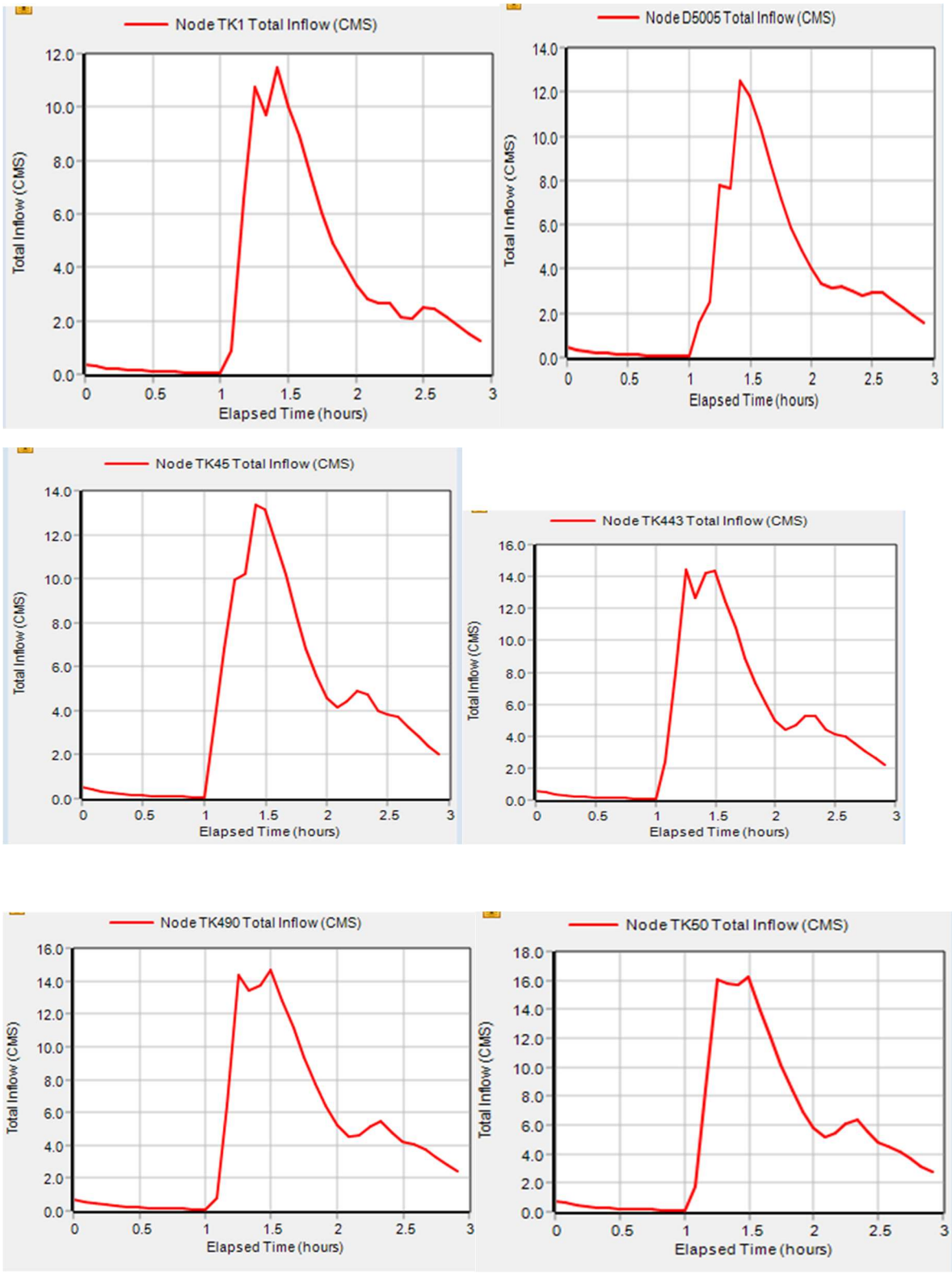

Fig. A.7. Simulated hydrographs at typical nodes for rainfall duration tr = 2 hr., for T = 5 year

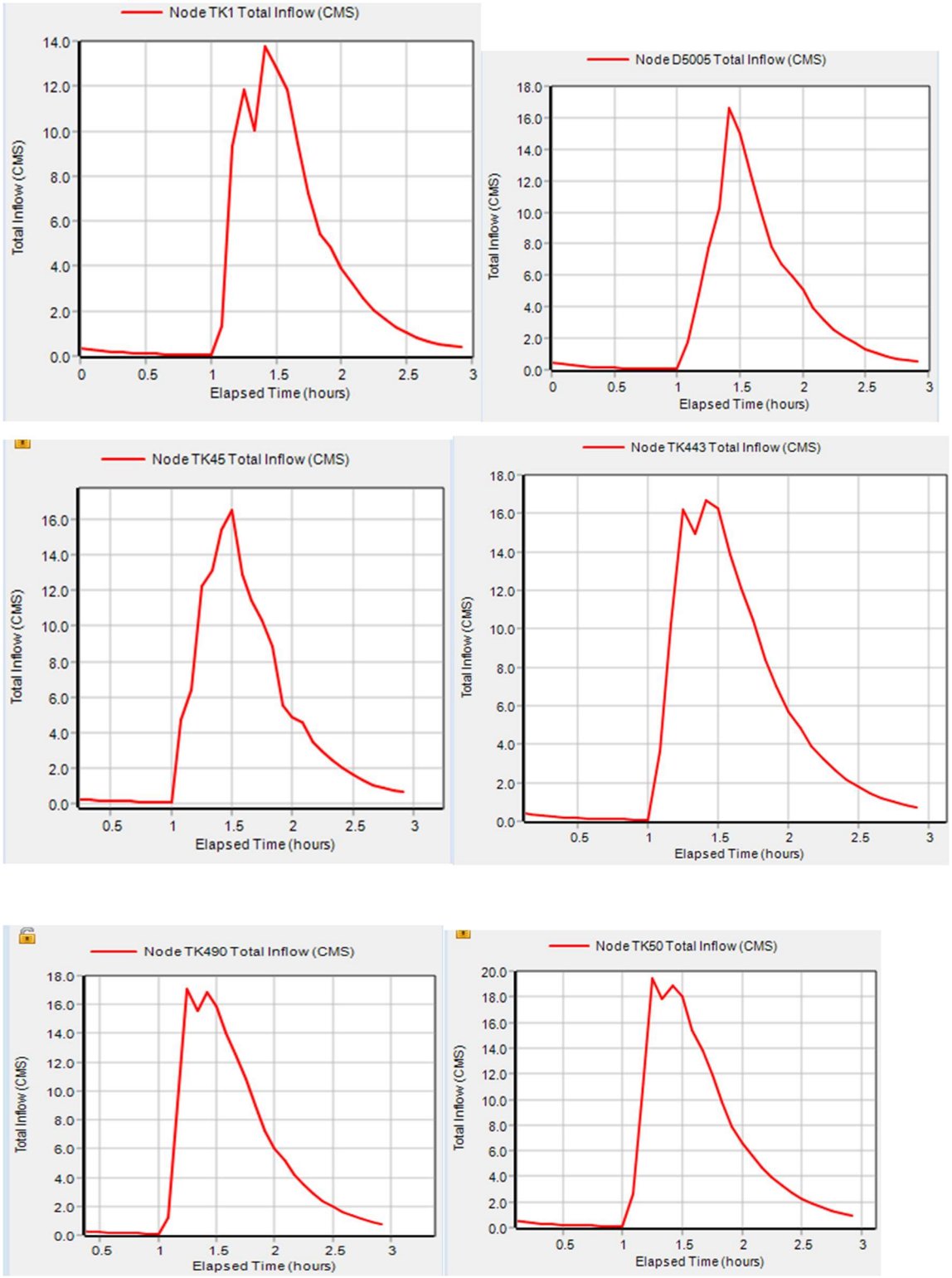

Fig. A.8. Simulated hydrographs at typical nodes for rainfall duration tr = 1 hr., for T = 10 year

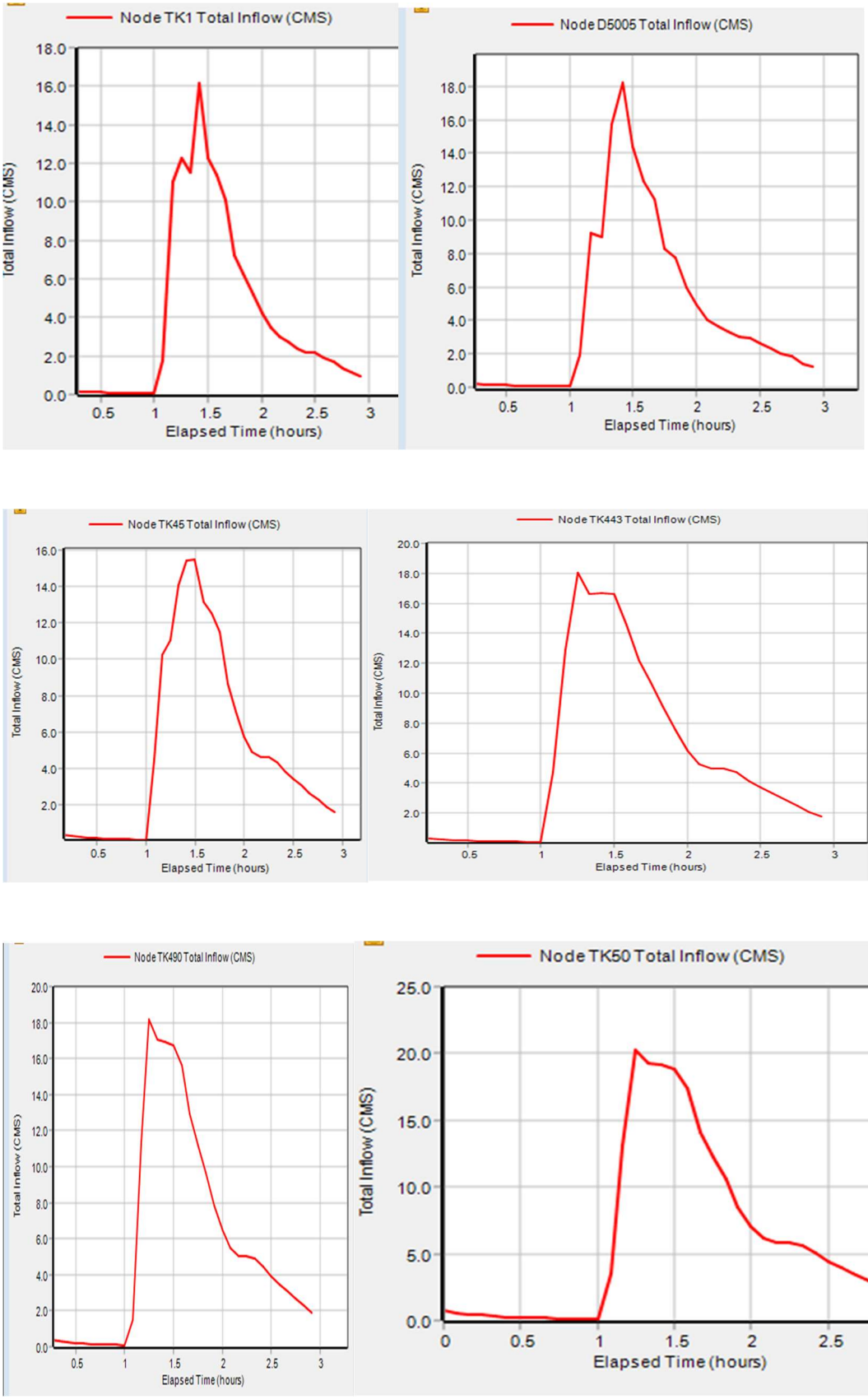

Fig. A.9. Simulated hydrographs at typical nodes for rainfall duration tr = 2 hr., for T = 10 year

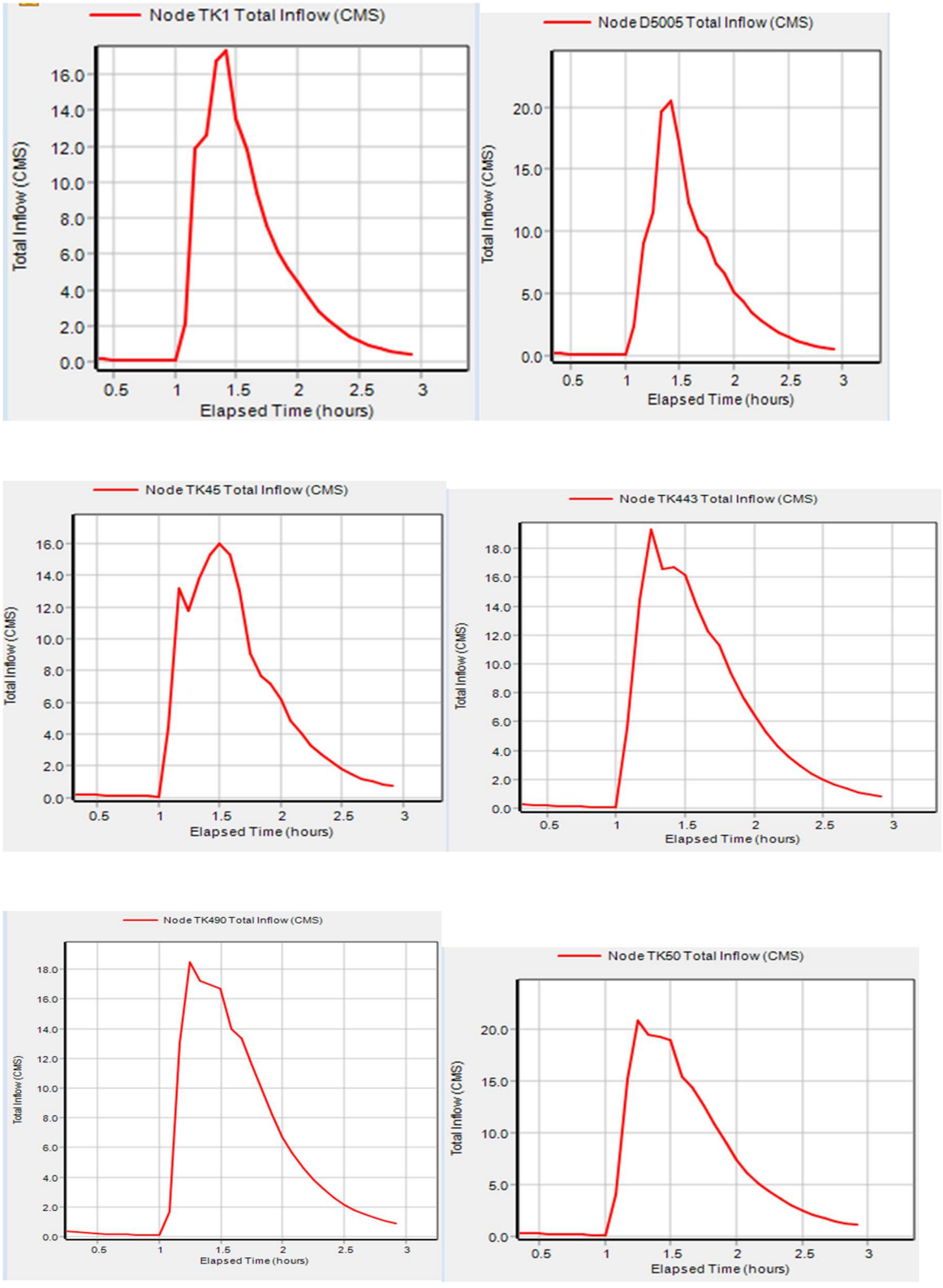

Fig. A.10. Simulated hydrographs at typical nodes for rainfall duration tr = 1 hr., for T = 25 year

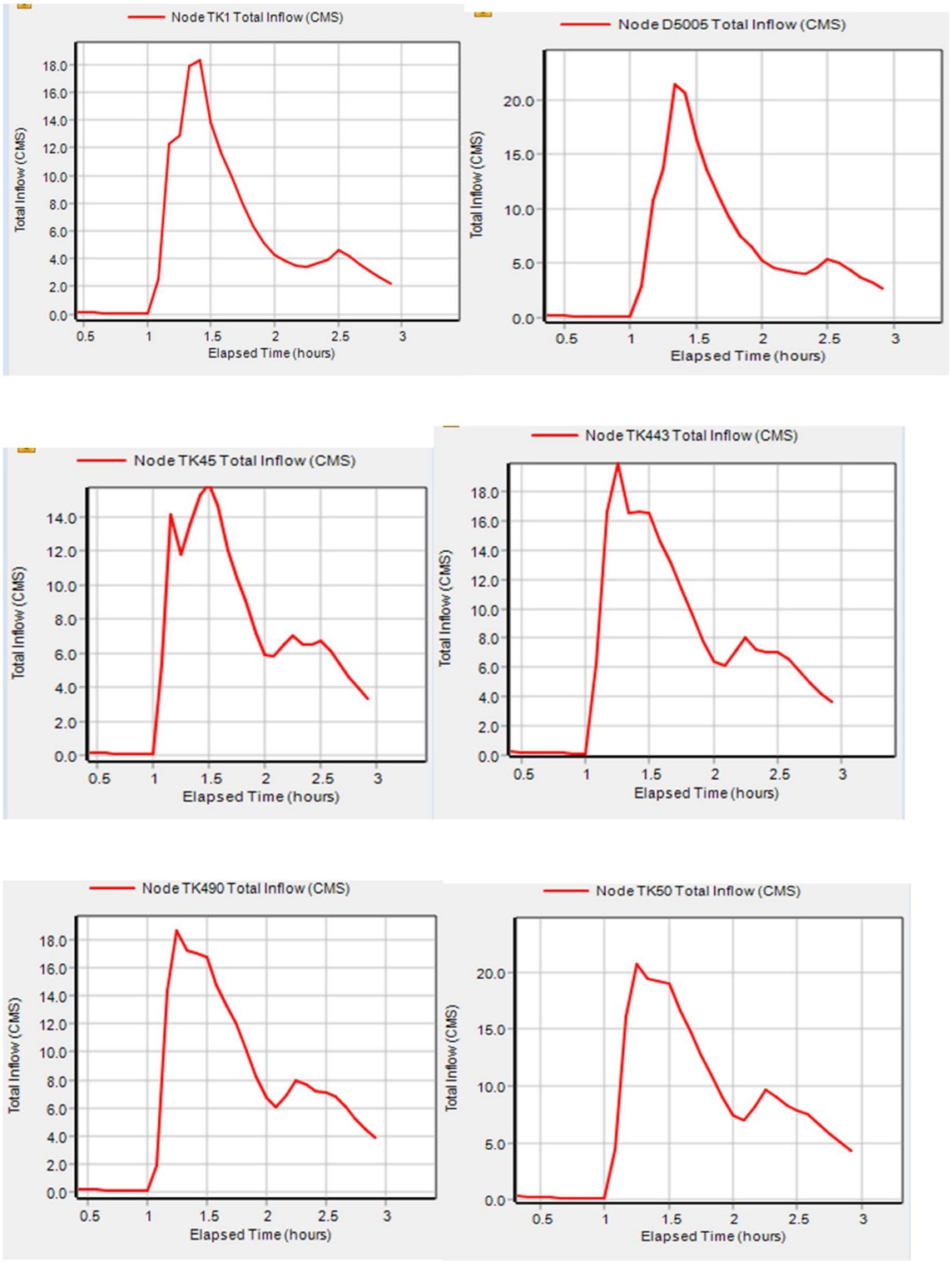

Fig. A.11. Simulated hydrographs at typical nodes for rainfall duration tr = 2 hr., for T = 25 year

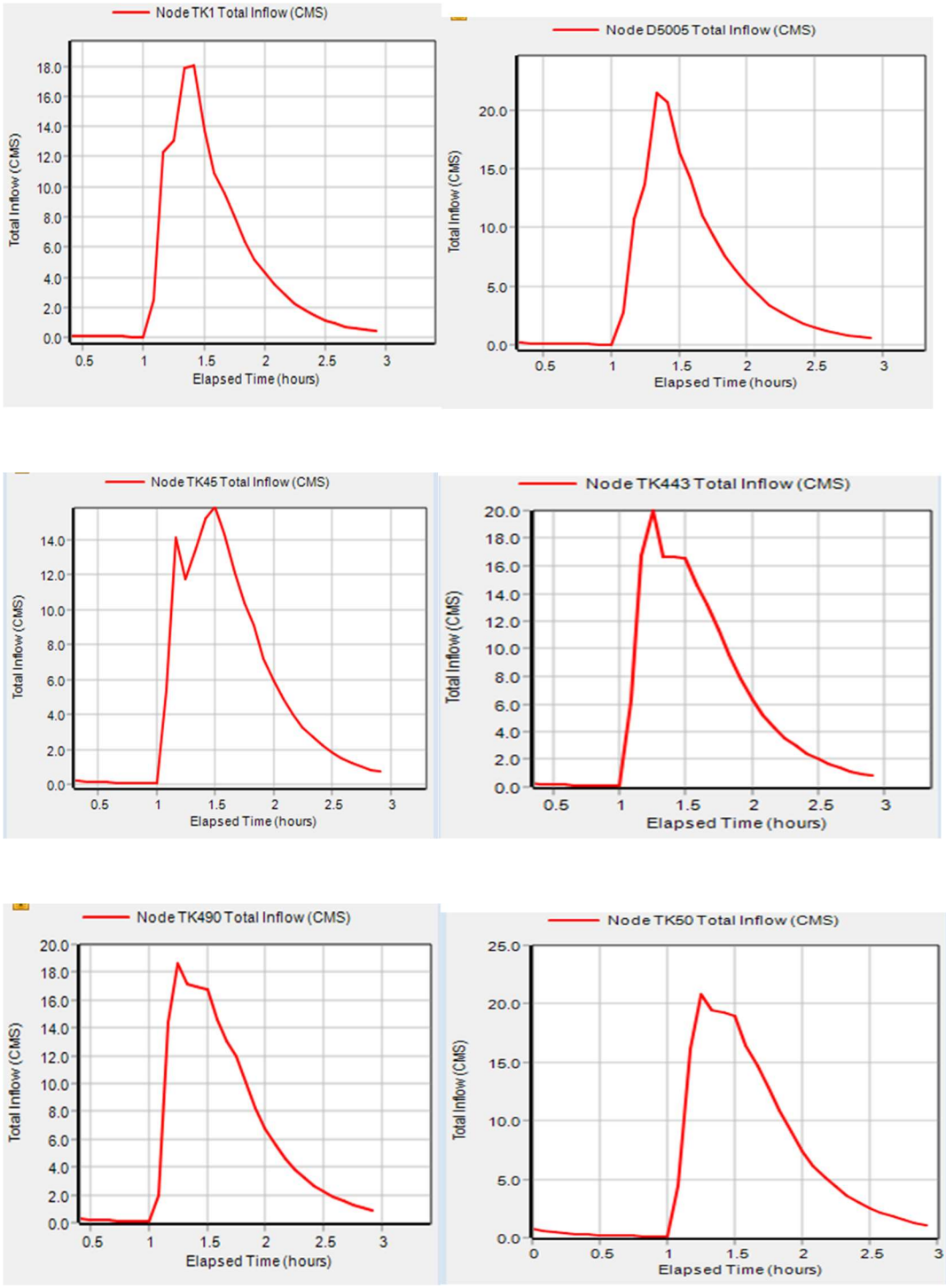

Fig. A.12. Simulated hydrographs at typical nodes for rainfall duration tr = 1 hr., for T = 50 year

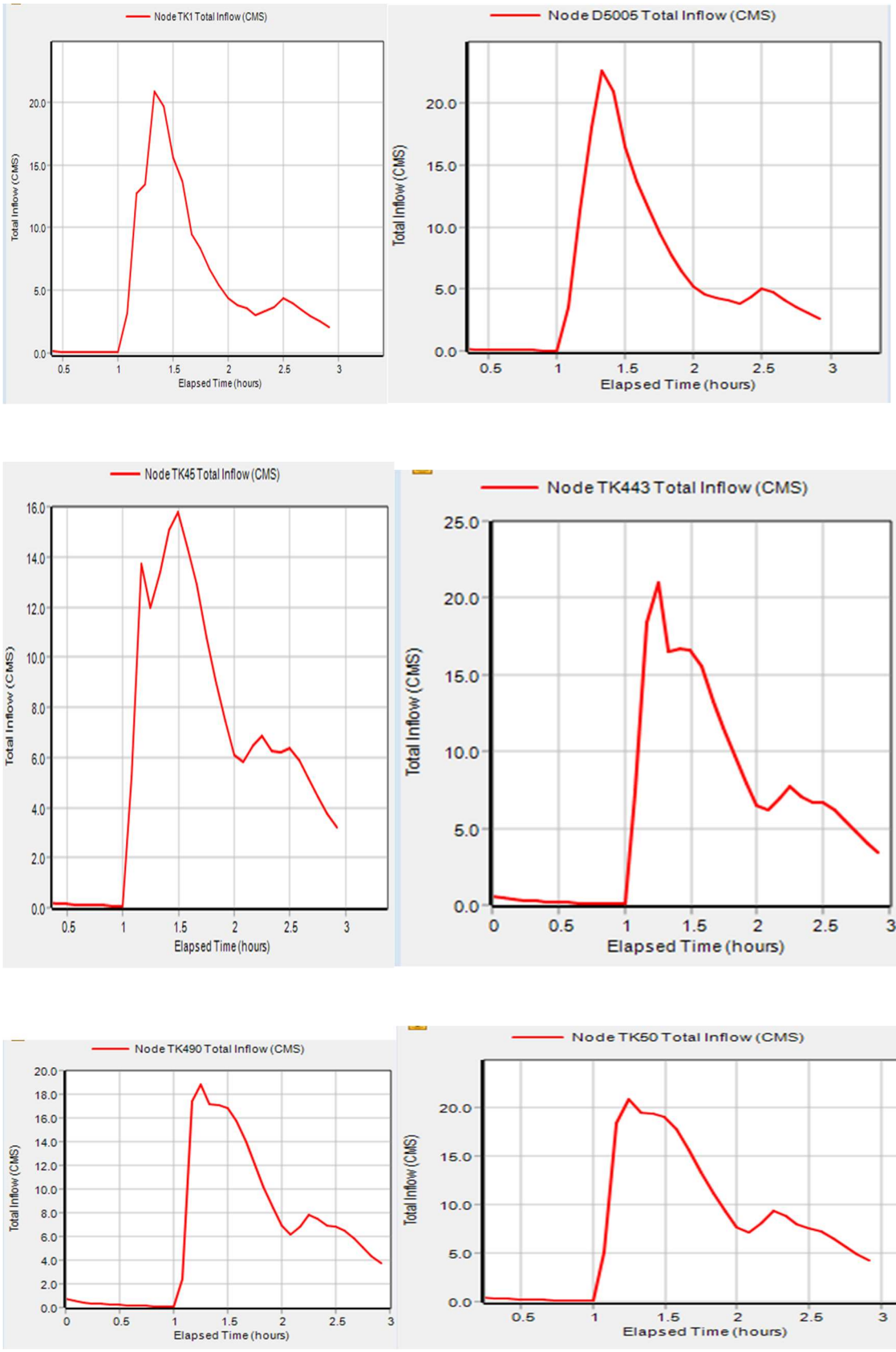

Fig. A.13. Simulated hydrographs at typical nodes for rainfall duration tr = 2 hr., for T = 50 year

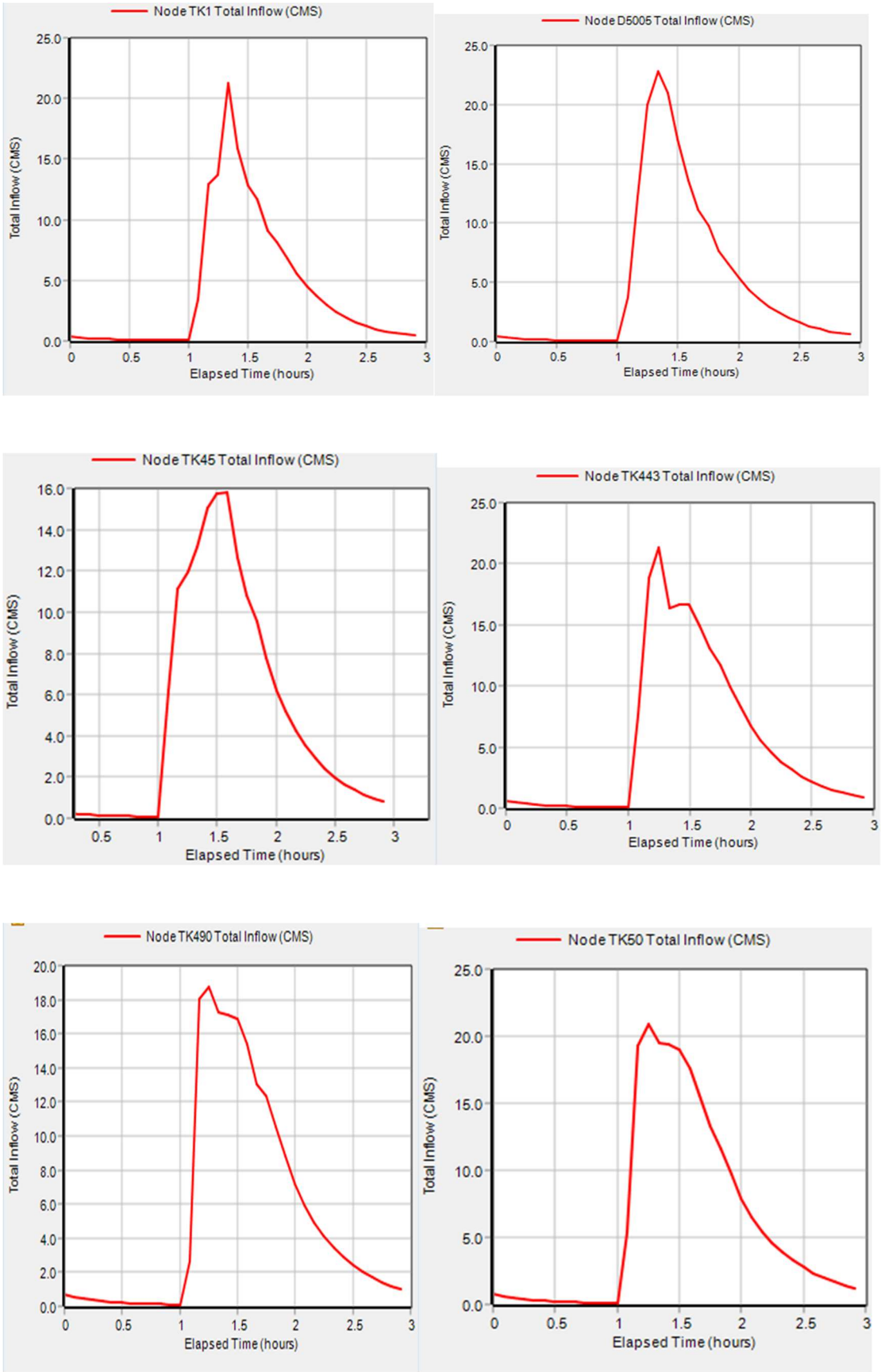

Fig. A.14.Simulated hydrographs at typical nodes for rainfall duration tr = 1 hr., for T = 100 year

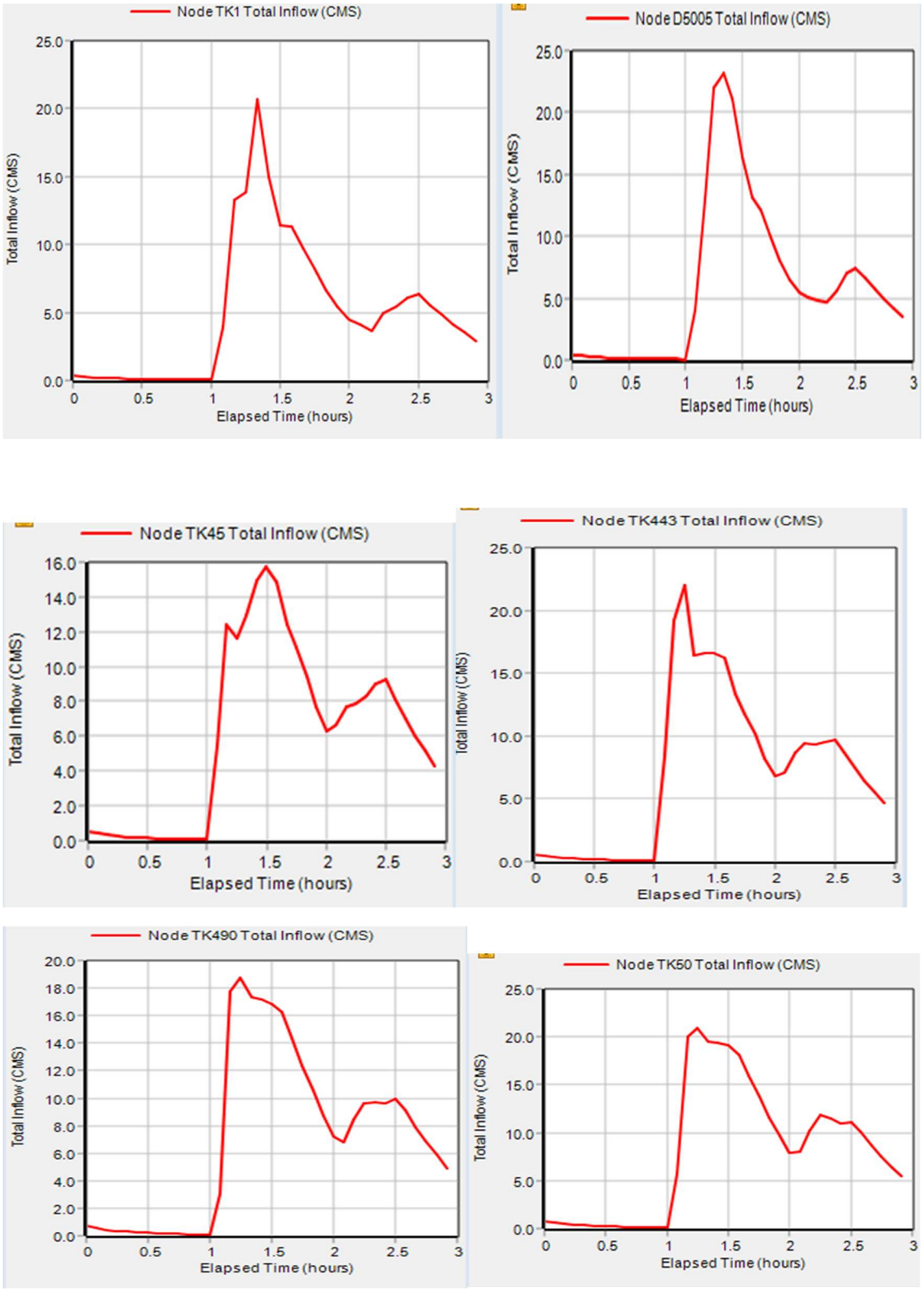

Fig. A.15. Simulated hydrographs at typical nodes for rainfall duration tr = 2 hr., for T = 100 year

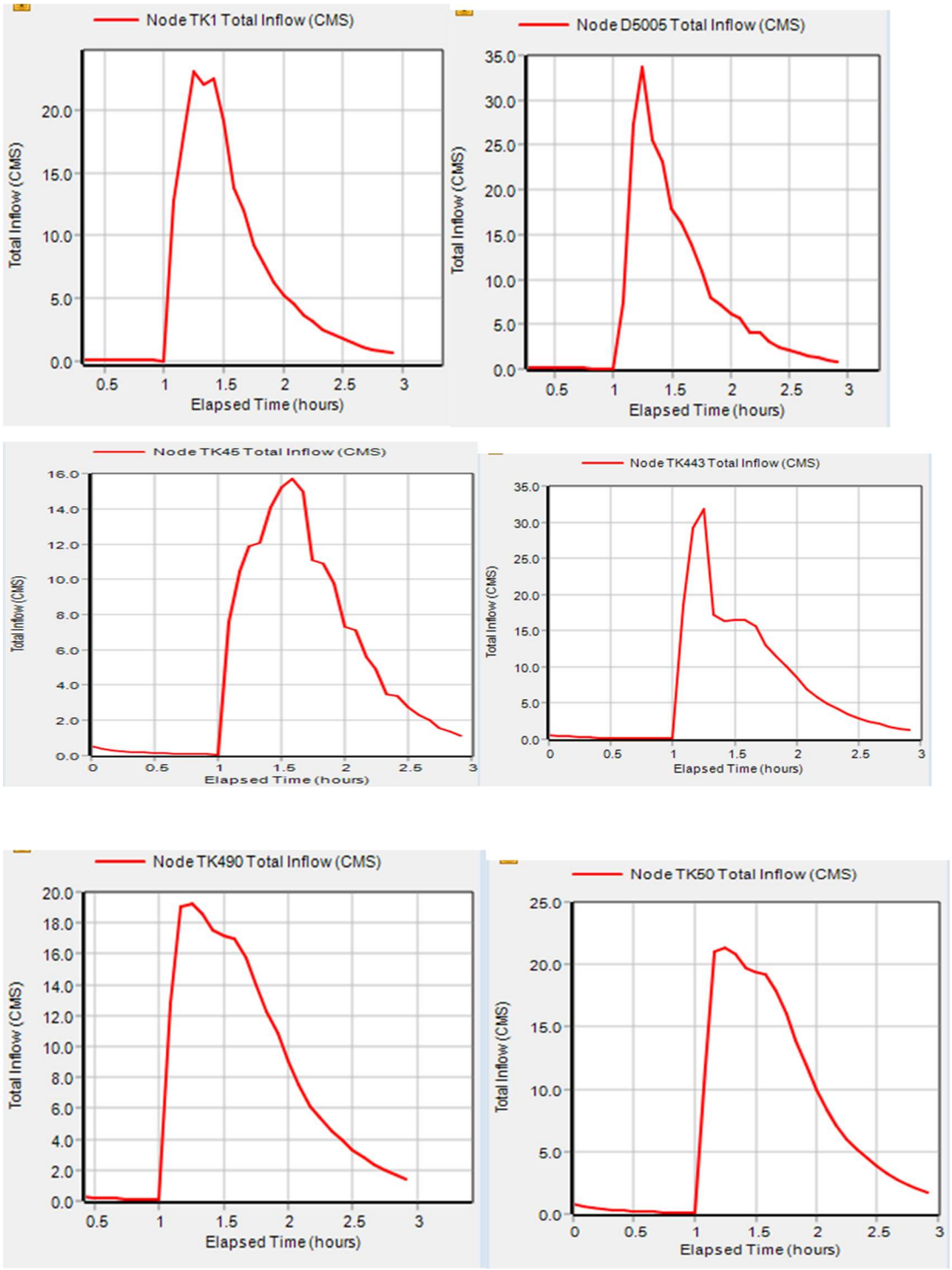

Fig. A.16. Simulated hydrographs at typical nodes for rainfall duration tr = 1 hr., for PMP

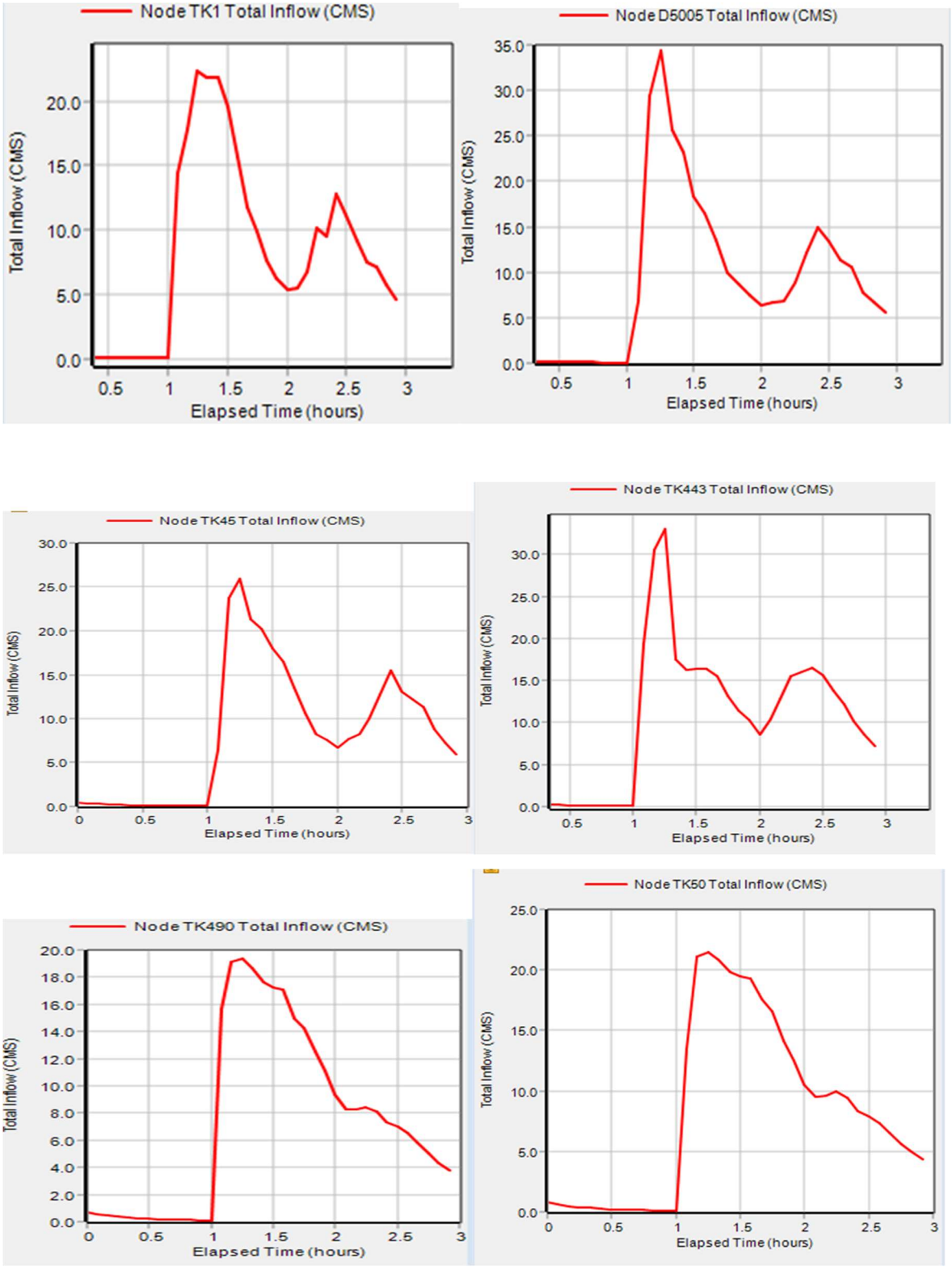

Fig. A.17. Simulated hydrographs at typical nodes for rainfall duration tr = 2 hr., for PMP

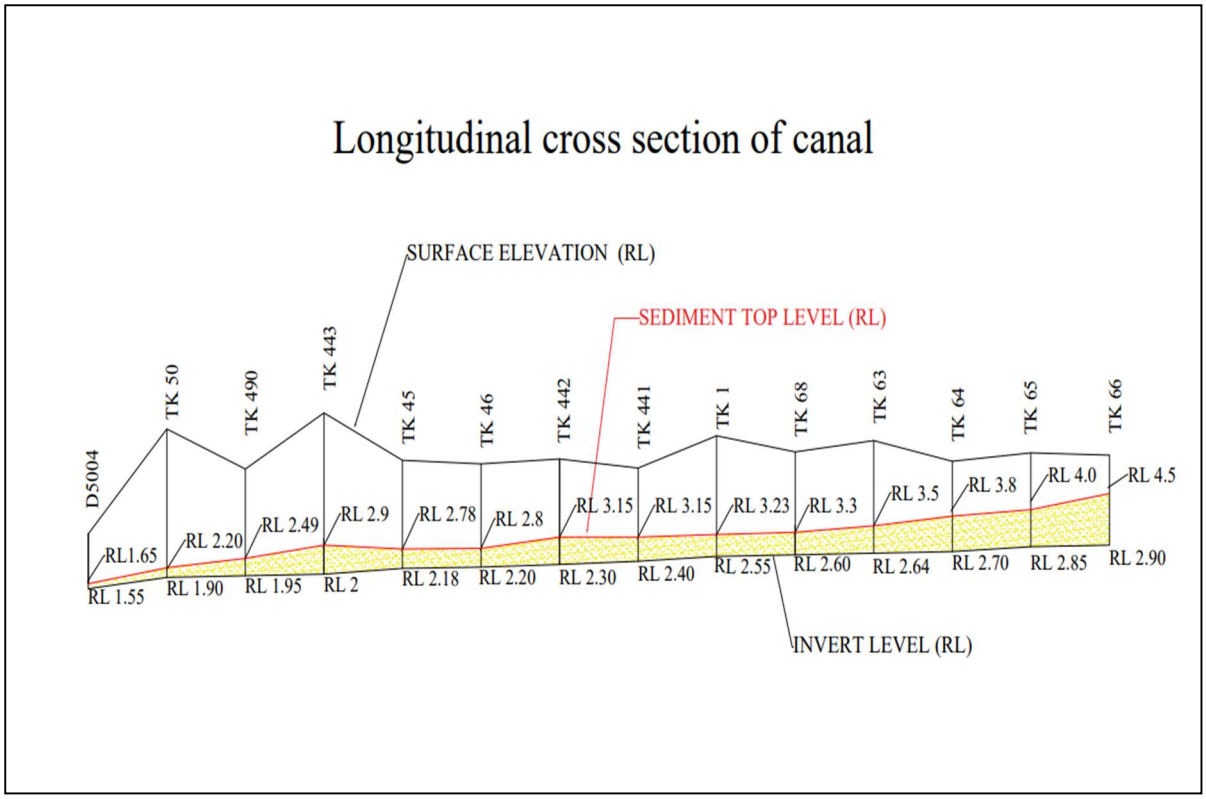

Figure A.18 : Longitudinal profile-status of sedimentation in Thekkinikkara Canal

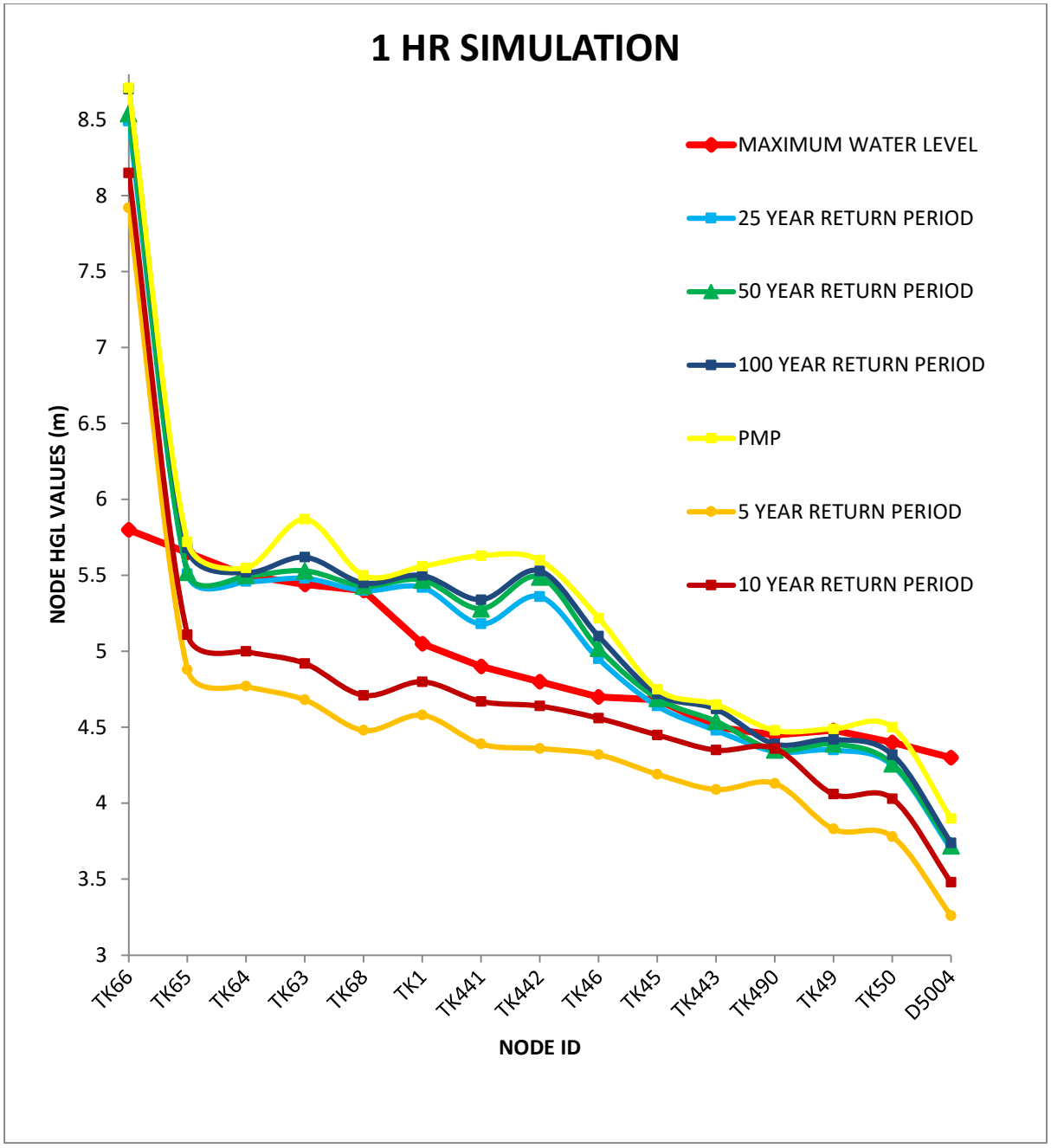

Fig A.19 : Plot of HGL along the Thekkinikkara Canal for tr = 1 hour for different return periods of rainfall

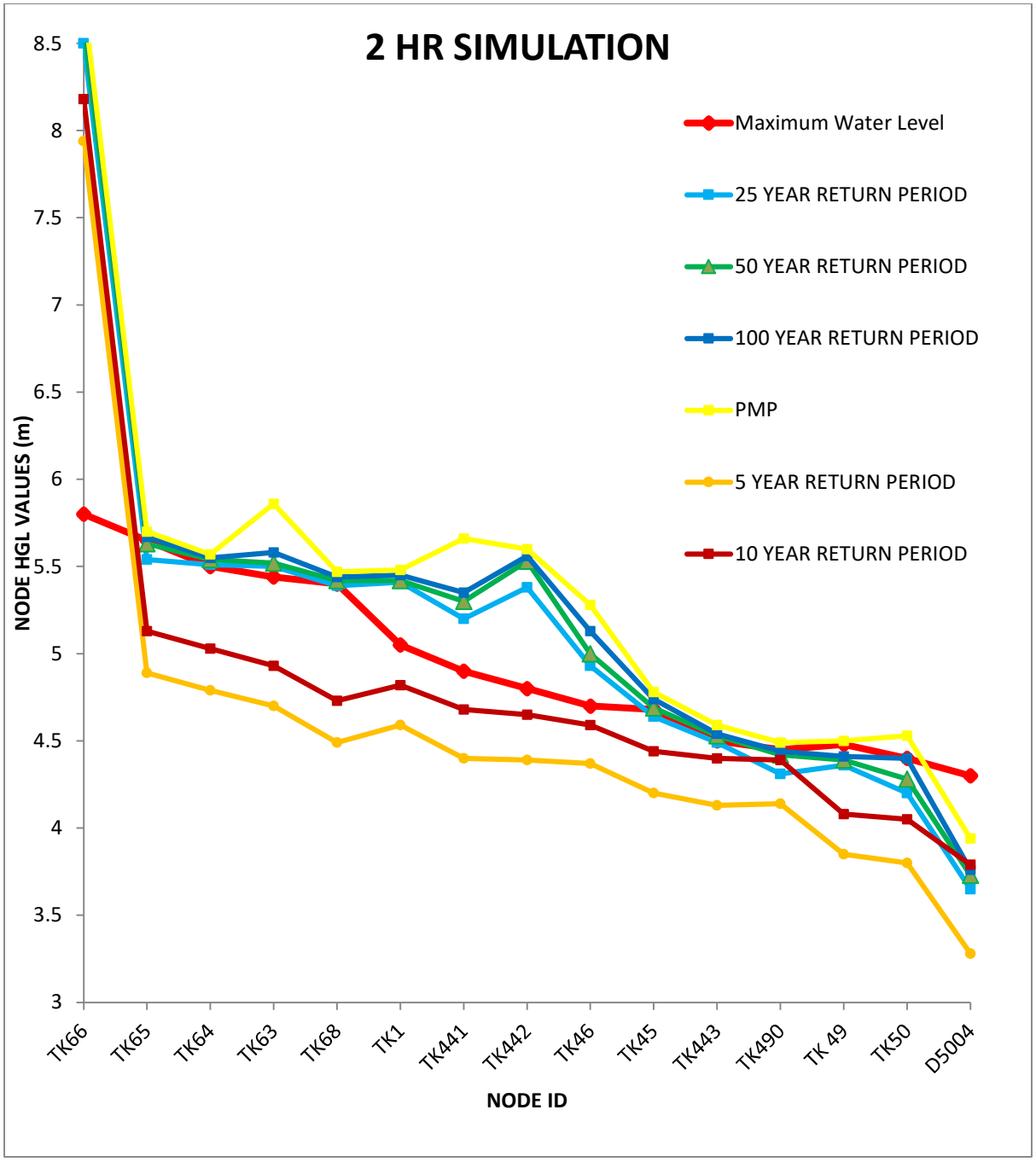

Fig A.20 : Plot of HGL along the Thekkinikkara Canal for tr = 2 hour for different return periods of rainfall

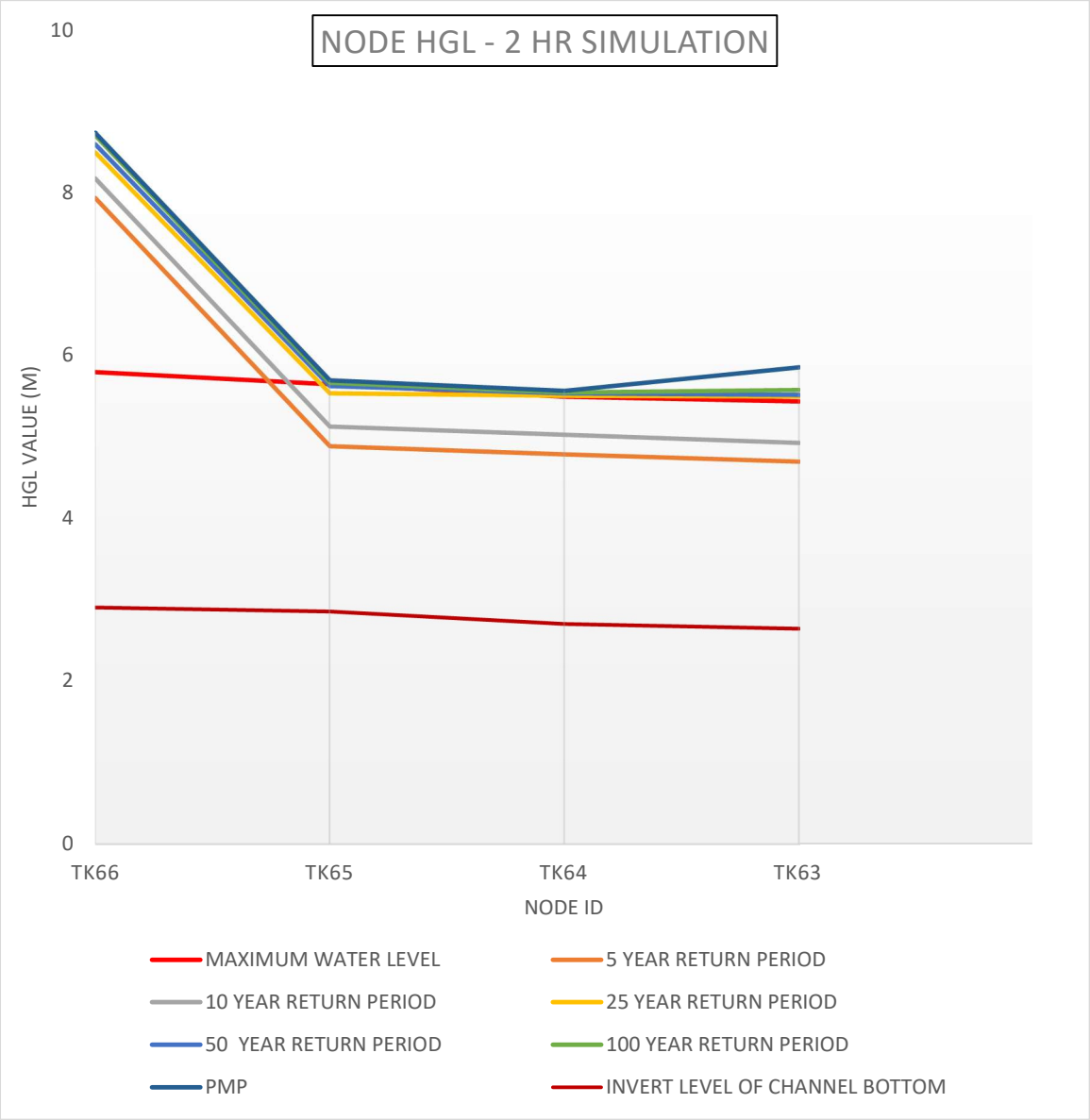

Fig A.21 : Plot of HGL for the reach TK66 to TK63 of Thekkinikkara Canal for tr = 2 hour for different return periods of rainfall

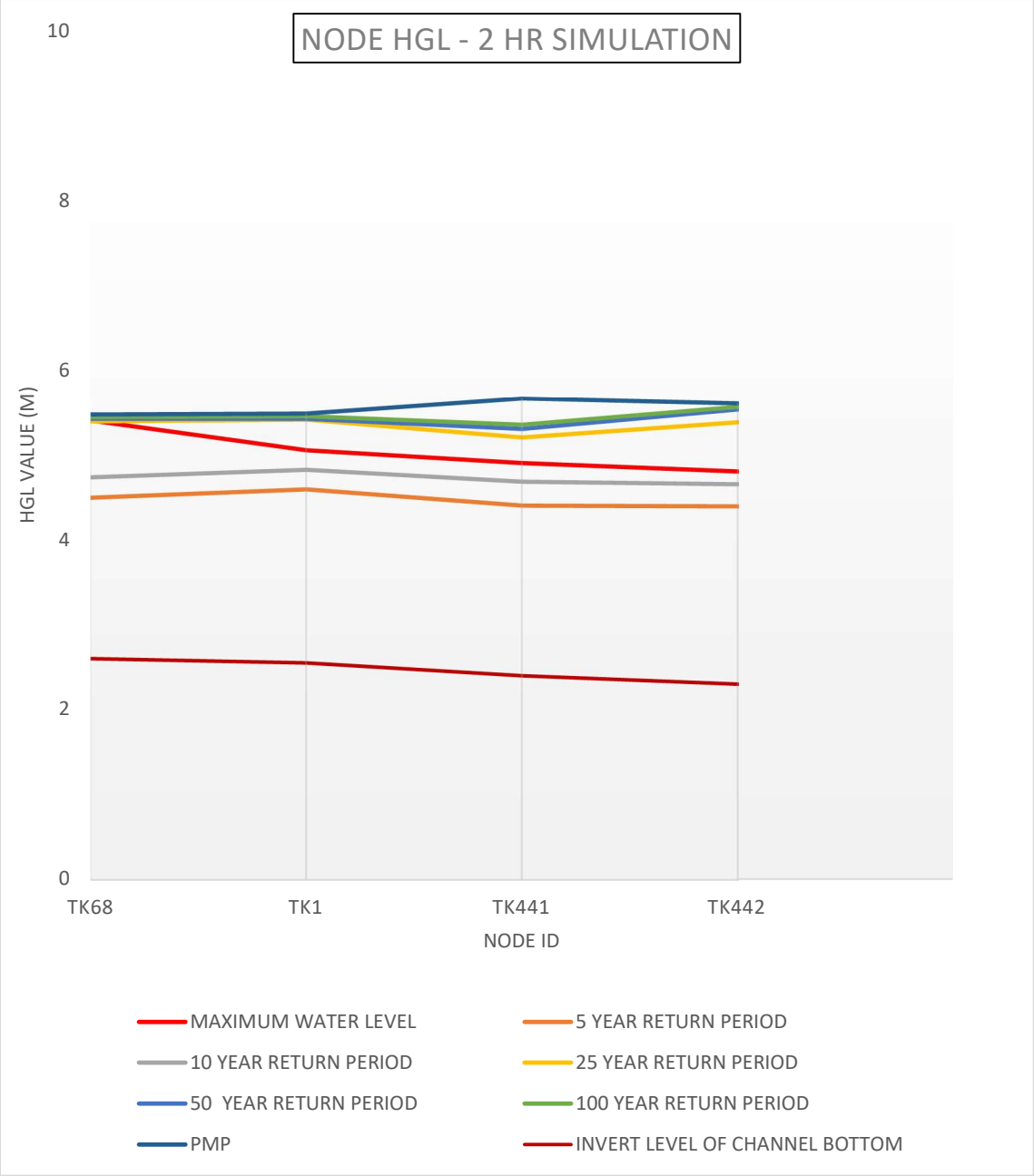

Fig A.22 : Plot of HGL for the reach TK68 to TK442 of Thekkinikkara Canal for tr = 2 hour for different return periods of rainfall

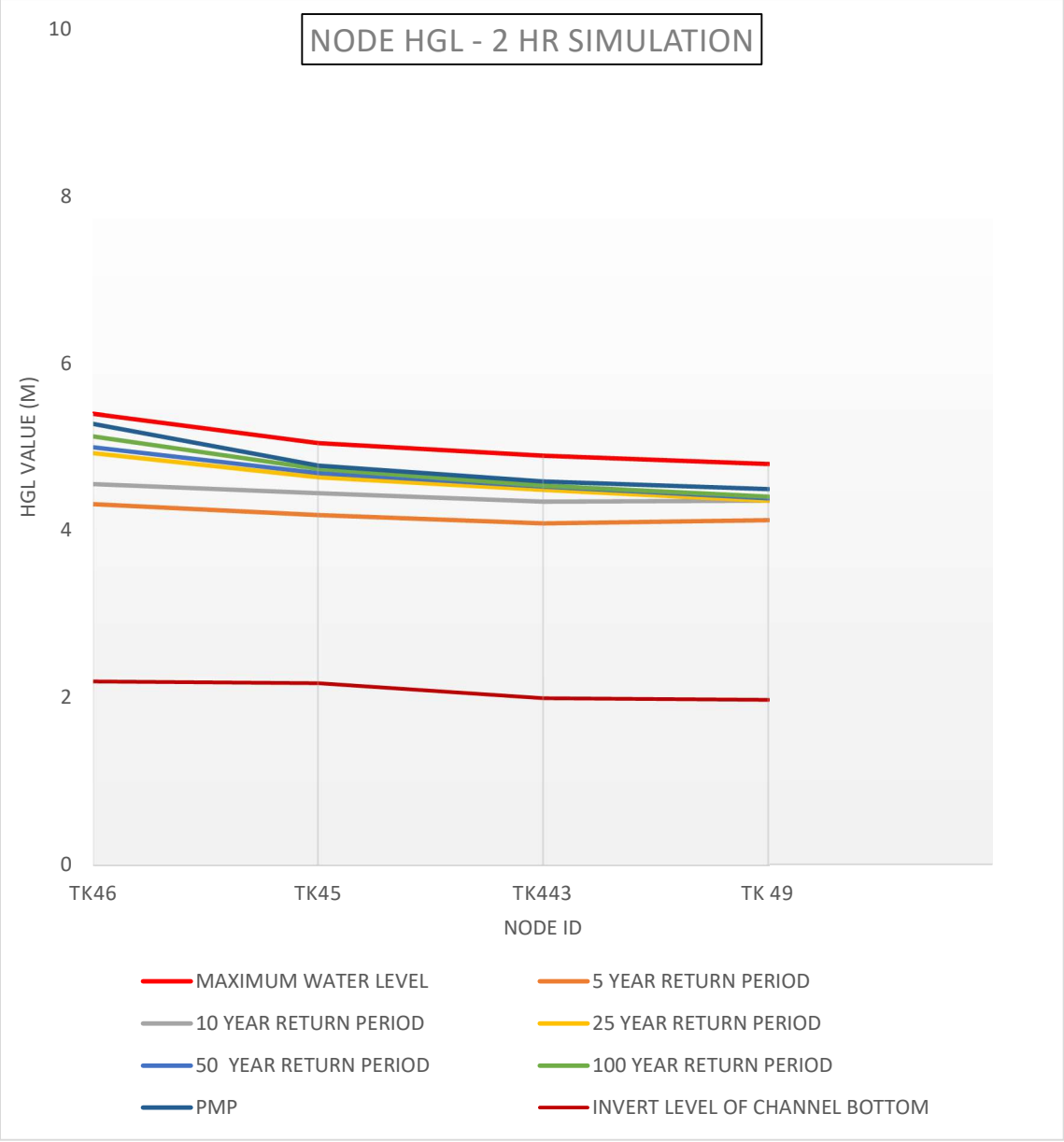

Fig A.23 : Plot of HGL for the reach TK46 to TK49 of Thekkinikkara Canal for tr = 2 hour for different return periods of rainfall

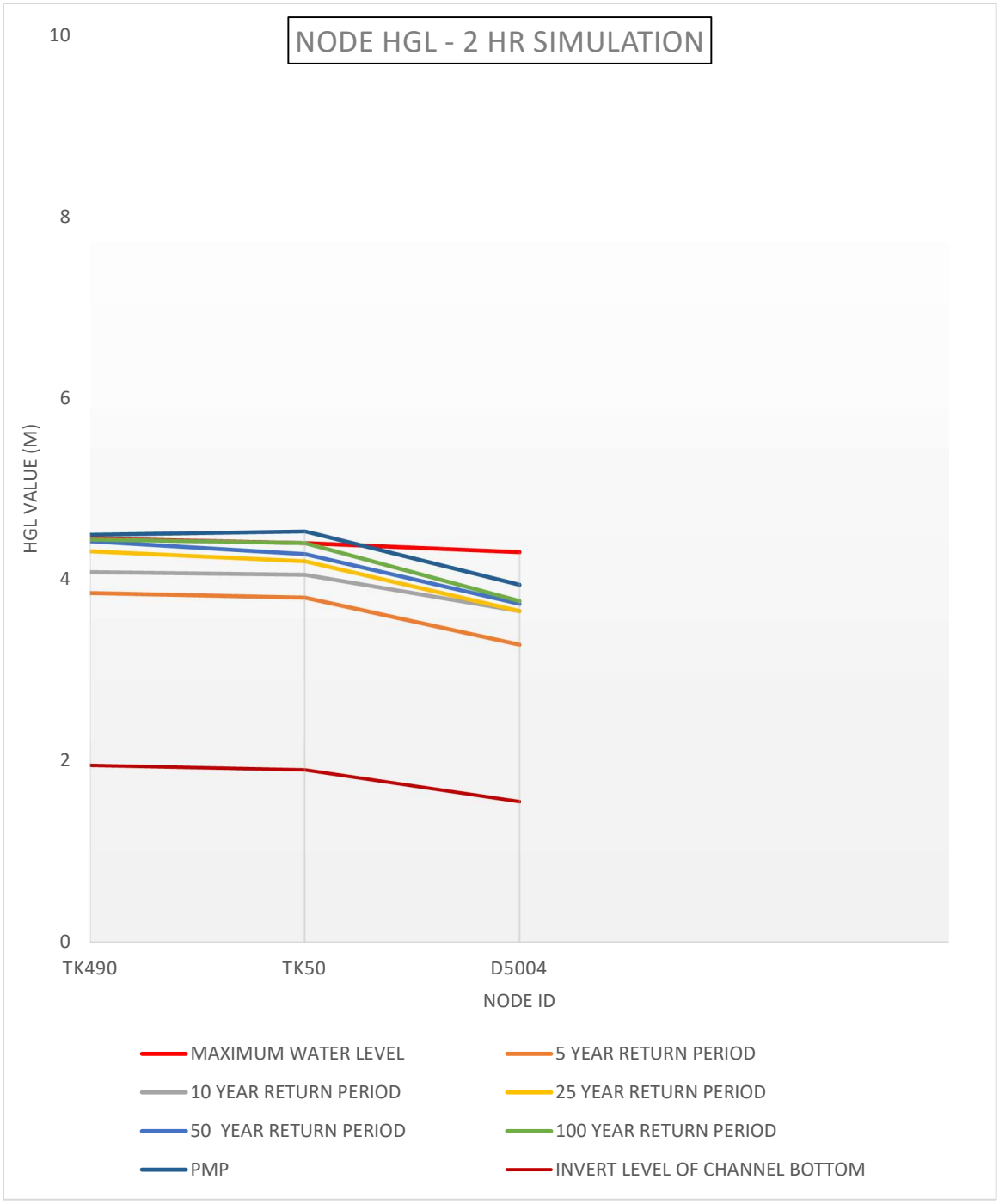

Fig A.24 : Plot of HGL for the reach TK490 to D5004 of Thekkinikkara Canal for tr = 2 hour for different return periods of rainfall

Table A.1 : Salient Parameters of Thekkinikkara Canal

Link	C/s details		Starting node	End node	Starting node		End node	
	Width (m)	Depth at crown(m)			Invert level (m)	Sediment level(m)	Invert level(m)	Sediment level(m)
1	2.8	2.5	TK 66	TK 65	2.90	4.50	2.85	4
2	2.8	2.5	TK 65	TK64	2.85	4	2.70	3.8
3	2.8	2.5	TK 64	TK 63	2.70	3.8	2.64	3.5
4	2.8	2.5	TK 63	TK 68	2.64	3.5	2.60	3.3
5	2.8	2.5	TK 68	TK 1	2.60	3.3	2.55	3.23
6	2.8	2.5	TK1	TK441	2.55	3.23	2.40	3.15
7	2.8	2.5	TK 441	TK 46	2.40	3.15	2.20	2.8
8	2.8	2.5	TK 442	TK 46	2.30	3.15	2.20	2.8
9	2.8	2.5	TK46	TK 45	2.20	2.8	2.18	2.78
10	2.8	2.5	TK45	TK443	2.18	2.78	2	2.9
11	2.8	2.5	TK443	TK490	2	2.9	1.95	2.49
12	2.8	2.5	TK490	TK50	1.95	2.49	1.90	2.20
13	2.8	2.5	TK50	D5004	1.90	1.7	1.55	1.65

Table A.2. Details of link canals joining the Thekkinikkara Canal, constructed under operation Anantha Project

Canal Link and Length (m)	Node	Cross-section		Invert Elevation (m)
		Base width (m)	Depth (m)	
TK71-TK45 650 m	TK71	0.75	0.7	7.10
	TK 70			6.56
	TK 69			6.26
	TK 700			5.3
	TK 56			4.85
	TK 55			4.52
	TK 53			3.7
	TK 45			2.18
TK58-TK56 66 m	TK58	0.75	0.7	5
	TK56			4.85
TK381- TK442 355 m	TK381	2.2	1.5	6.2
	TK 37			4.95
	TK 41			4.72
	TK 40			4.5
	TK 42			3.98
	TK 42*	1.5	1.5	3.90
	TK 442			2.30
TK 36- TK37 423 m	TK 36	0.75	0.7	5.8
	TK 39			5.7
	TK 37			4.95
TK7- TK5 178 m	TK 7	2	1.5	4.7
	TK 6			4.5
	TK 5			4.05

Table A.2. Details of link canals joining the Thekkinikkara Canal, constructed under operation Anantha Project (Contd.)

Canal Link and Length (m)	Node	Cross-section		Invert Elevation (m)
		Base width (m)	Depth (m)	
TK 25- TK 9 667 m	TK 25	2	1.5	5.4
	TK 24			5.32
	TK 22			5.2
	TK 21			5.15
	TK 15			4.99
	TK 17			4.86
	TK 19			4.79
	TK 9			4.35
TK 12- TK 1 941 m	TK 12	2	1.5	5.25
	TK 10			4.54
	TK 9			4.35
	TK 8			4.15
	TK 5			4.05
	TK 67			3.95
	TK 4			3.85
	TK 3			3.82
	TK 2			3.75
	TK 1			2.55
D5003-TK63 506 m	D5003	2.65	1.65	4.42
	TK62			4.29
	TK63			2.64
TK61-TK43 604 m	TK61	0.75	0.70	9.96
	TK60			8.83
	TK44			6.51
	TK43			2.25

Table A.2. Details of link canals joining the Thekkinikkara Canal, constructed under operation Anantha Project (Contd.)

Canal Link & Length (m)	Node	Cross-section		Invert Elevation (m)
		Base width (m)	Depth (m)	
TK51-TK45 341 m	TK51	0.75	0.7	9.07
	TK47			7.5
	TK45			2.18
TK 48-TK49 54 m	TK48	0.65	0.6	6.9
	TK49			1.98
TK 72-TK50 278 m	TK72	0.65	0.6	9.82
	TK50			1.90
67-TK50 336 m	67	0.65	0.6	3
	65			2.5
	TK50			1.90
64-TK46 354 m	64	0.75	0.7	3.5
	66			3.25
	TK46			2.20
TK31-TK67 326 m	TK31	0.75	0.7	4.99
	TK32			4.72
	TK33			4.47
	TK67			3.95

Table A.3 : Simulated Hydraulic gradient at nodal points for rainfall duration tr = 1 hour, for different return periods

Node ID	Permissible HGL (m)	Simulated HGL (m)					
		T= 5 yr.	T= 10yr.	T = 25 yr.	T= 50 yr.	T= 100yr	T = PMP
TK66	5.8	7.92	8.15	8.49	8.54	8.70	8.71
TK65	5.65	4.88	5.11	5.51	5.52	5.68	5.72
TK64	5.5	4.77	5.00	5.46	5.5	5.52	5.55
TK63	5.44	4.68	4.92	5.48	5.53	5.62	5.87
TK68	5.4	4.48	4.71	5.4	5.43	5.45	5.5
TK1	5.05	4.58	4.80	5.42	5.47	5.5	5.56
TK441	4.9	4.39	4.67	5.18	5.28	5.34	5.63
TK442	4.8	4.36	4.64	5.36	5.49	5.53	5.6
TK46	4.7	4.32	4.56	4.95	5.02	5.10	5.22
TK45	4.68	4.19	4.45	4.64	4.69	4.72	4.75
TK443	4.5	4.09	4.35	4.48	4.54	4.62	4.65
TK490	4.45	3.83	4.06	4.34	4.35	4.39	4.48
TK50	4.4	3.78	4.03	4.25	4.26	4.32	4.5
D5004	4.3	3.26	3.48	3.7	3.72	3.74	3.9

Table A.4 : Simulated Hydraulic gradient at nodal points for rainfall duration tr = 2 hour, for different return periods

Node ID	Permissible HGL (m)	Simulated HGL (m)					
		T= 5 yr.	T= 10yr.	T = 25 yr.	T= 50 yr.	T= 100 yr	T = PMP
TK66	5.8	7.94	8.18	8.50	8.60	8.71	8.74
TK65	5.65	4.89	5.13	5.54	5.63	5.67	5.70
TK64	5.5	4.79	5.03	5.51	5.54	5.55	5.57
TK63	5.44	4.70	4.93	5.50	5.52	5.58	5.86
TK68	5.4	4.49	4.73	5.39	5.42	5.44	5.47
TK1	5.05	4.59	4.82	5.41	5.42	5.45	5.48
TK441	4.9	4.40	4.68	5.20	5.30	5.35	5.66
TK442	4.8	4.39	4.65	5.38	5.53	5.56	5.60
TK46	4.7	4.37	4.59	4.93	5.00	5.13	5.28
TK45	4.68	4.20	4.44	4.64	4.69	4.74	4.78
TK443	4.5	4.13	4.40	4.49	4.53	4.54	4.59
TK490	4.45	3.85	4.08	4.31	4.42	4.44	4.49
TK50	4.4	3.80	4.05	4.20	4.28	4.40	4.47
D5004	4.3	3.28	3.79	3.65	3.73	3.76	3.94

4. Part B : Structural Stability of Thekkinikkara Canal

The Thekkinikkara canal is a rectangular shaped canal with sidewalls of rubble masonry and brick masonry arch section on the top. This part of the study discusses the modelling of the canal section incorporating the loading and material characteristics, so as to assess the stability of the structure under static loading condition and loading with consideration of earth quake forces acting on it. The details pertaining to the methodology used, analysis of the problem and the results of the study are discussed subsequently.

4. B.1. Methodology for assessment of Structural Stability

For the structural stability analysis, the region of the canal which is subjected to maximum loading was considered. This include (i) Rajadhani multistoried building complex and (ii) the road in front of it. The loadings on the arch portion of the canal were estimated based on (i) alignment of the canal and the building location details and (ii) alignment of canal and the design traffic load on the road above it. The estimation of collapse load of the arch was done following the limit analysis of masonry arch structures, considering the parameters of soil, masonry and that of the structures interacting with it. The collapse load was also estimated for vehicular loading condition for the road passing over the canal. This is followed by the Finite element model formulation of the arch, using a macro-modelling approach. The finite element model was simulated using the finite element software ABAQUS. The stress contours on the arch rings for the two cases(i) building over the canal and (ii) road over the canal were simulated. The analysis was done for static loading condition and also by incorporating loading due to earth quake effects.

4. B.2. Details of Canal

The cross-section of canal is rectangular of clear span 2.8 m, with side walls of rubble masonry, and covered by a brick arch on the top. The rubble masonry wall is well packed and is intact as observed in the field. It is the arch portion which is critical and the modelling is done for the arch portion. The photograph showing the canal during a renovation done is presented in Figure B.1. The canal cross-section as supplied by the client is shown in Figure B.2. The height upto the crown of arch is 2.5 m from the

canal bottom with arch rise of 1.0 m above the top of side wall on verification in the field, and adopted in the study.

Fig.B.1. Thekkinikkara Canal during a renovation (shared by client)

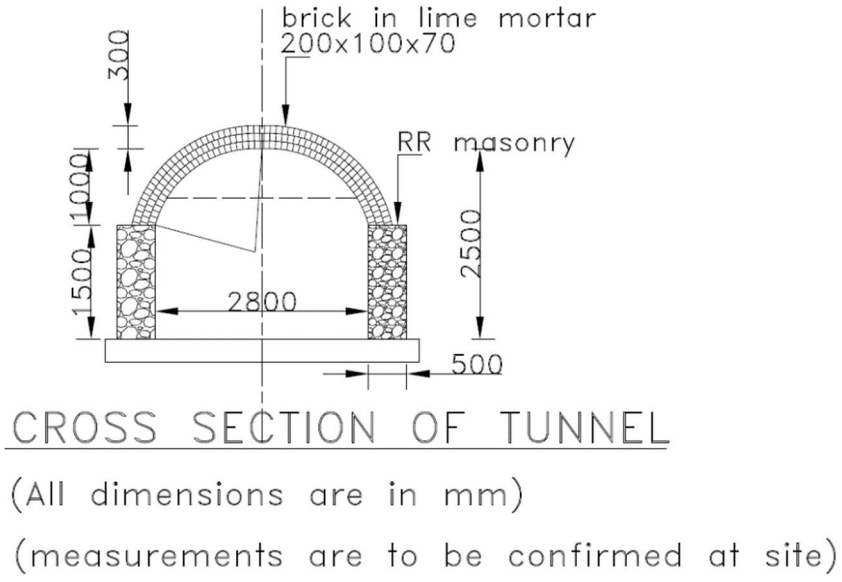

Fig.B.2. Cross-section details of Thekkinikkara Canal (as obtained from the client)

Details of masonry arch.

Clear span: 2800 mm

Arch rise: 1000 mm clear

Material: country burned bricks of size 200 mm x100 mm x70 mm

Number of brick layers in the arch rings: 3 (total thickness of 300mm)

Height of earth fill above crown level of the arch: 1.5 m (Approximate: field analysis & photograph)

4. B.3. Collapse load estimation of masonry arch of the tunnel portion under external column loads

4. B.3.1. Column load estimation

From the canal layout superimposed over the building plan, it is seen that around seven column (footing) rest above or close to the arch of the canal. Since the foundation details were not provided, it is unclear the type of foundation, how and at what depth the said column foundations are positioned. The type foundation of column is assumed as spread footings.

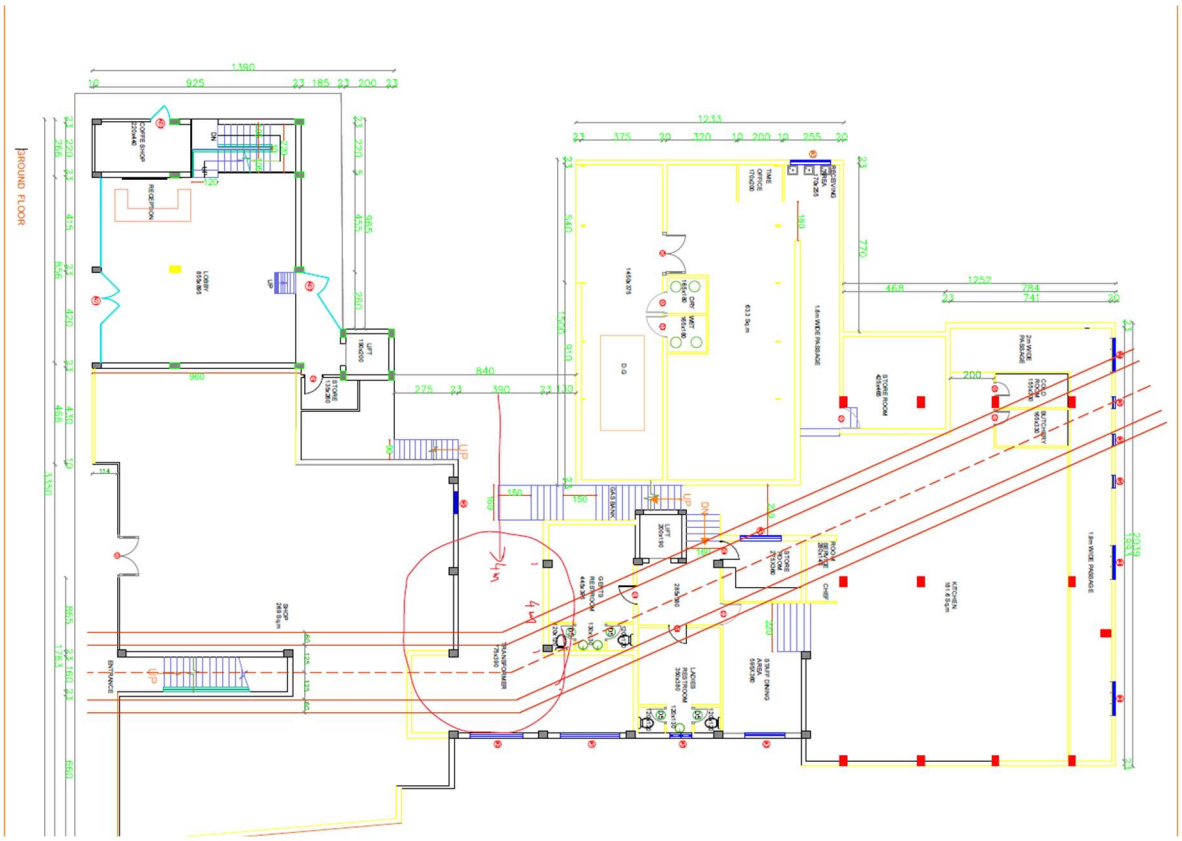

Fig.B.3. Canal layout with building GF plan (supplied by client)

For estimation of column loads (for columns positioned over the canal layout as per the drawing supplied), it was decided to consider the columns circled in red in Figure B.3., since the column spacing for those alone could be read from the drawing supplied. Approximate spacing for those columns was taken as 4 m in both directions (Figure B.4).

NB: the spacing of column in the stair region seems to be higher, but the lateral spacing of columns could not be ascertained from the drawings.

Taking the spacing of columns to be 4 m (for columns with footing over or near to canal)

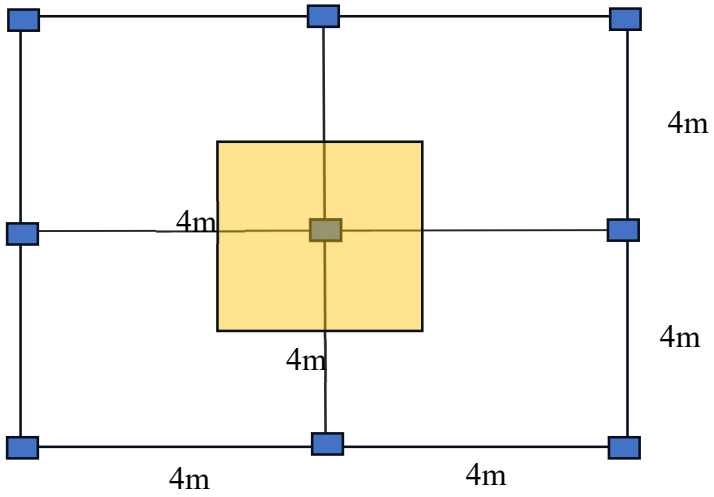

Fig.B.4. Approximate layout considered for load estimation.

For load calculation, only ground floor plan drawing is available and hence plan shown in fig B4 is considered for first, second and third floors.

1. Live load = 4 kN/m^2 (IS 875 part 2)

   Thickness of the slab and layout and size of beams are also not available. The thickness of slab is taken as 120 mm and load due to finishes is taken as 0.75kN/ m^2.

2. Dead load on slab = 0.12 x 25 + 0.75 = 3.75 kN/m^2

   (DL + LL = 7.75 kN/m^2)

Hence total load on column from slab weight and LL = 4 x 4 x 7.75 = 124 kN

(DL of slab = 4 x 4 x 3.75 = 60 kN , LL from slab = 4 x 4x 4 = 64 kN)

3. Self-weight of beams = 0.23 x 0.5 x 1 x 25 = 2.875 kN/m

(beam cross section is not available, assumed as 230mm x 500mm)

Total load on column as four support reactions from beam = 4 x 2 m x 2.875 = 23 kN.

4. Weight of masonry wall

   (considering the floor height to be 3.5 m) = 0.23 x 3.5 x 1 x 20 = 16.1 kN/m

There are 3 wall segments in the slab influence area (shaded) of the column.

Total load on column as 4 support reactions from beam = 3 m x 2 m x 16.1 = 96.6 kN.

5. Weight of column assuming column size 350 mm x 350 mm

   Self-weight of column = 3.5 x 0.35 x 0.35 x 25 = 10.75 kN

Total load per floor ≅ 256 kN.

Hence total service loads (unfactored) from four floors: 256 x 4 = 1024 kN

NB: Gravity load effects alone has been considered in arriving at the above column base reaction. To account for the additional loads due to beam moments from gravity load effects (and also due to lateral load effects) an approximate allowance of 10 % is made. Hence the overall column reaction approximately comes to 1.1 x 1024 = 1130 kN.

Assuming an SBC of 150 kN/m^2, approximate size of column footing = 3 m (to be confirmed at site by excavation)

4. B.3.2. Estimation of collapse load of arch

Accurate estimation of masonry properties was beyond the scope of the present investigations. Hence, the first stage analysis of collapse load of the arch was made based on the concept of limit analysis of masonry structures. For estimation of masonry compressive strength, laboratory tests were done on masonry brick samples (3 no.'s) taken from the canal arch section. The test results are shown in Table B.1

Table B.1. Test on Brick specimens for Mechanical properties

Sample no.	Size (cm)	Dry Wt. (gm)	Wet Wt. (gm)	Water absorption (%)	Failure Load (kN)	Failure stress (N/mm^2)	Unit weight (kN/m^3)
1	21.5 x 9.5 x 7	2531	2930	15.76	210	10.28*	17.7*
2	22 x 10 x 7	2897	3230	11.49	140	6.36	20.26
3	22.5 x 10 x 7	2896	3254	12.36	150	6.67	20.26
					Avg	6.52	20.26

* discarded

4. B.3.2.1. Concept of Limit Analysis of Masonry Structures

Masonry arches are statically indeterminate compression structures which resist external applied loads primarily as a result of the friction between various blocks, their inherent self-weight and external passive resistance offered by the surrounding soil. Limit analysis, originally developed for steel structures, was extended to the case of

collapse load estimation of masonry structures [1,2,3]. In limit analysis, masonry arch structures are idealized as an assemblage of rigid blocks. The collapse mechanism of such systems consists of rotation of individual blocks about theoretical hinge points or through sliding. Hinge points are those locations were the resultant thrust line meets the exterior faces of the arch. The eccentricity of thrust line from the centroid of arch cross-section is obtained as the ratio of moment at any section to the axial thrust. Formation of sufficient number of hinges (or planes of sliding) leads to collapse.

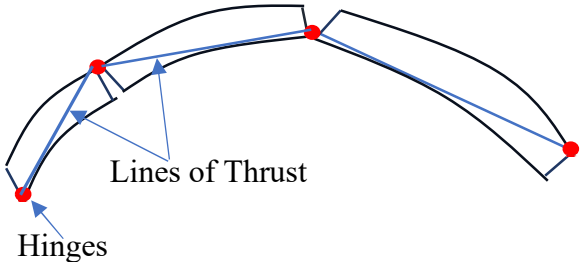

Fig.B.5 Thrust line and formation of hinges in Limit analysis of masonry arch structures

In limit analysis of masonry gravity structures, in addition to basic equilibrium considerations, the following conditions are used to test for ultimate collapse (assuming both hinging and sliding failures at masonry joints between two blocks).

Yield condition: The yield condition is deemed to be satisfied if the line of thrust satisfies the following conditions (i) falls entirely within the masonry (ii) does not cross any joint between two blocks at a subtended angle (θ) less than $tan^{-1}(\mu)$; where μ is the sliding friction coefficient.

Mechanism condition: The mechanism condition is deemed to be satisfied provided the line of thrust either touches the exterior faces of masonry block and/or crosses sufficient joints at an angle (θ) of $tan^{-1}(\mu)$ to create the releases required to transform the structure into a mechanism.

The *lower bound theorem* for the collapse load estimation of masonry arches can be stated as: if the thrust line satisfies the equilibrium and yield conditions, then the true plastic collapse load cannot be less than the applied load.

The *upper bound theorem* for collapse load estimation of masonry arches can be stated as: if the line of thrust satisfies both equilibrium and mechanism condition, then the collapse load cannot exceed the applied load.

By choosing an appropriate collapse mechanism and using equilibrium or virtual work method, the limit analysis can be performed by hand. But in case of arches, the procedure is complicated. Hence in the present study, the limit analysis software for

arches - Limit State RING (Limit State inc. and University of Sheffield UK.) was used for the purpose. The software is properly validated against experimental/field test results [4].

The software accounts for lateral passive earth pressure offered by surrounding soil as well as the load dispersion through soil fill above the arch. Boussinesq type distribution model, with a limiting distribution angle specified by the user, is used for dispersion of vertical live loads over the arches through the soil fill above the arch.

One dimensional bar elements (compression elements) are used to model passive restraints experienced by sections of the arch moving towards the backfill soil, thus offering a passive resistance.

The output from the software is the adequacy factor (AF). AF < 0 means the arch is even unstable under the influence of dead loads (and hence cannot carry live loads). An AF between 0 and 1 indicates the arch is stable under its own weight, but unable to carry additional load. An adequacy factor greater than one indicates the arch is able to carry additional live loads (other than self-weight) and the collapse load being given by applied load multiplied by AF. The software also provides the optimal collapse mechanism along with the formation of hinges and thrust line.

4. B.3.2.2. Input parameters for arch modelling.

Since material properties relating to arch masonry, surrounding soil, applied load nor load position was available, bounds of collapse loads were estimated using appropriate practical bounds of material parameters.

Masonry properties

Unit weight of masonry = 20 kN/m^3

Compressive strength= 4 MPa.

Friction coefficient to model sliding between blocks in same ring = 0.4. [9]

Friction coefficient to model inter-ring sliding = 0.35 [9]

Backfill soil properties

Unit weight = 18 kN/m^3

Angle of friction (ϕ) = 30°

Cohesion, c = zero

4. B. 3.2.3. Collapse load estimation based on column loading

Column load and position

For the estimation of collapse load using limit analysis, a unit load is applied as the column load. The actual collapse load obtained from the analysis as the product of the applied unit load and adequacy factor (AF) was compared with the column load corresponding to service load conditions from the building.

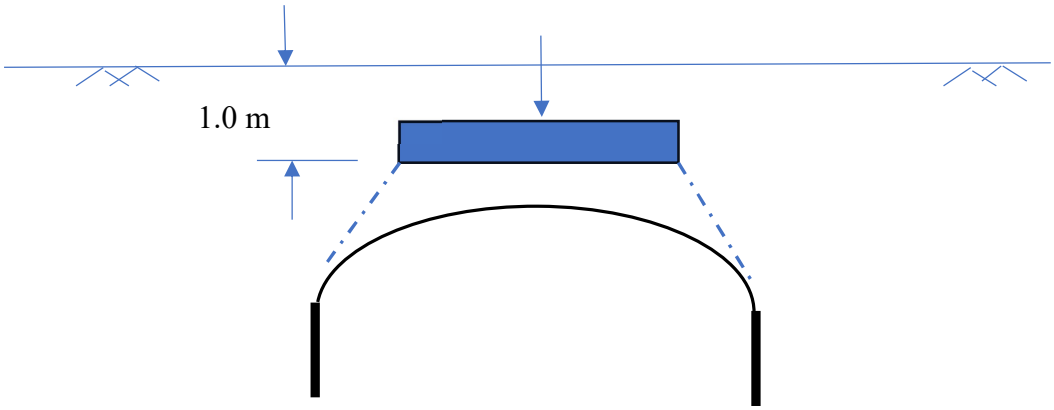

Fig. B.6. Schematic of column load application over tunnel arch

Size of footing and the lateral position (from the arch left support) were varied since the exact column and foundation positions were not provided by the client. Depth of footing for all cases were considered as 1.0 m from the surface.

As the footing size is not clear from drawings, 3 footing sizes: 1.5 m x 1.5 m, 2 m x 2 m and 3 m x 3 m were tried in the analysis. Also 3 different column positions viz column at support, quarter span and mid span, were also considered in the analysis.

4. B.3.2.3.1: Case 1: Footing size 1.5 m x 1.5 m; Column position at left support of arch

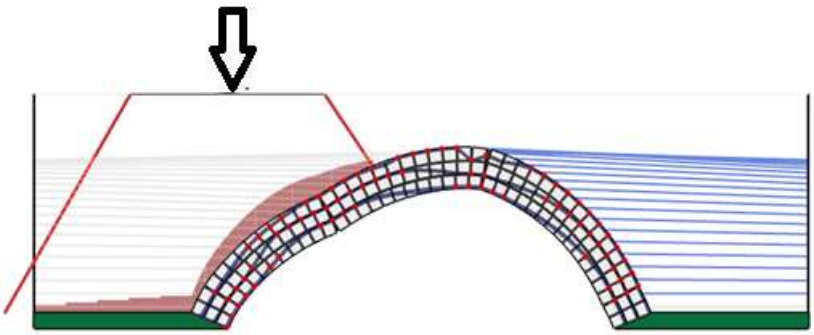

Fig.B.7. Collapse mechanism for arch loaded by 1.5 m square footing, column position at left support of arch.

4. B.3.2.3.2. Case 2: Footing size 1.5 m x 1.5 m. Column position at arch quarter span position

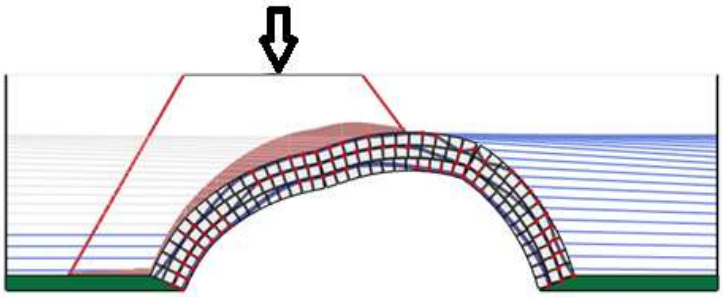

Fig.B.8. Collapse mechanism for arch loaded by 1.5 m square footing, column position at arch quarter span.

4. B.3.2.3.3 :Case 3: Footing size 1.5 m x 1.5 m. Column position at arch midspan

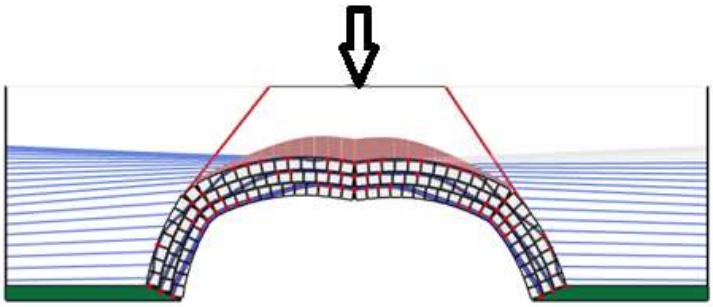

Fig.B.9. Collapse mechanism for arch loaded by 1.5 m square footing, column position at arch mid-span

4. B.3.2.3.4. Case 4: Footing size 2 m x 2 m. Column position at arch left support

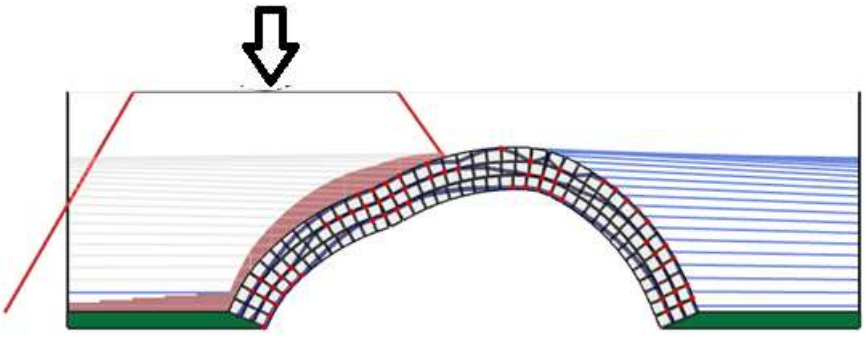

Fig.B.10. Collapse mechanism for arch loaded by 2 m square footing, column position at arch left support

4. B.3.2.3.5. Case 5: Footing size 2 m x 2 m. Column position at arch left quarter span

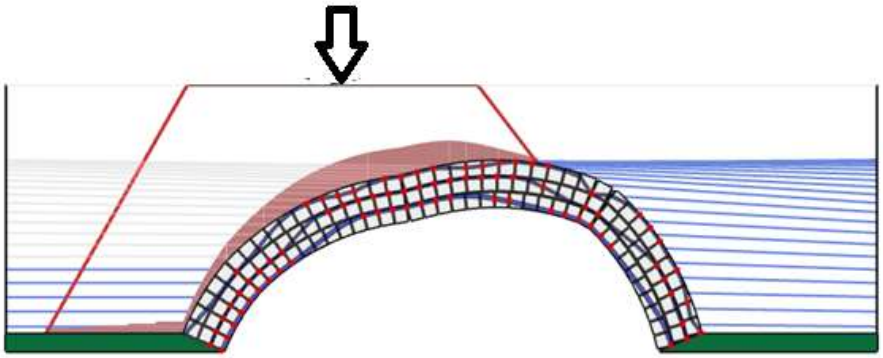

Fig.B.11. Collapse mechanism for arch loaded by 2 m square footing, column position at arch left quarter-span.

4. B.3.2.3.6. Case 6: Footing size 2 m x 2 m. Column position at arch mid- span

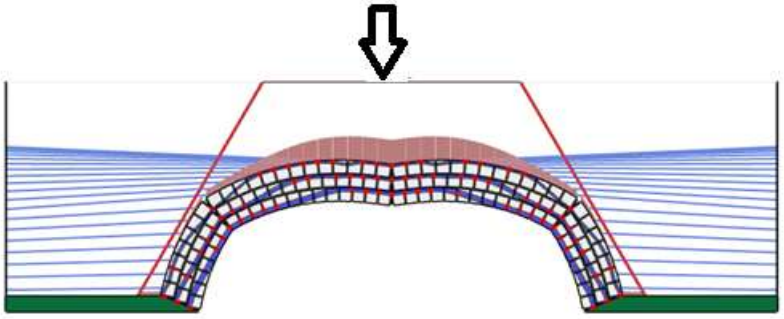

Fig.B.12. Collapse mechanism for arch loaded by 2 m square footing, column position at arch mid-span

4. B.3.2.3.7: Case 7: Footing size 3 m x 3 m. Column position at arch left support

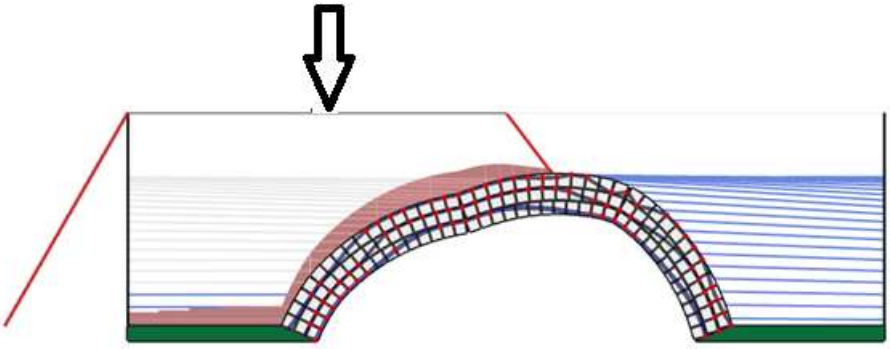

Fig.B.13. Collapse mechanism for arch loaded by 3 m square footing, column position at arch left support

4. B.3.2.3.8. Case 8: Footing size 3 m x 3 m. Column position at arch left quarter-span

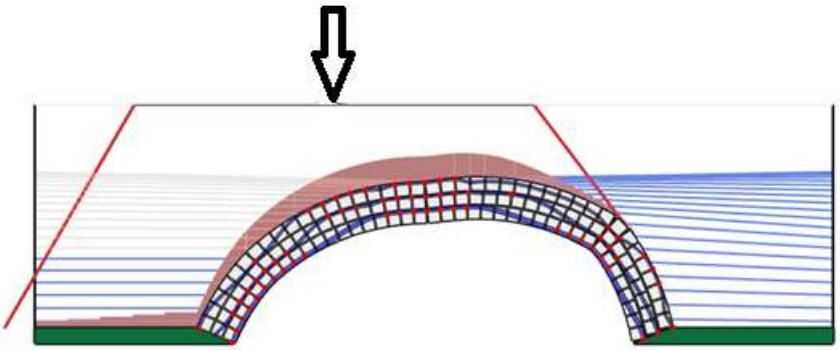

Fig.B.14. Collapse mechanism for arch loaded by 3 m square footing, column position at arch left quarter-span.

4. B.3.2.3.9. Case 9: Footing size 3 m x 3 m. Column position at arch mid-span

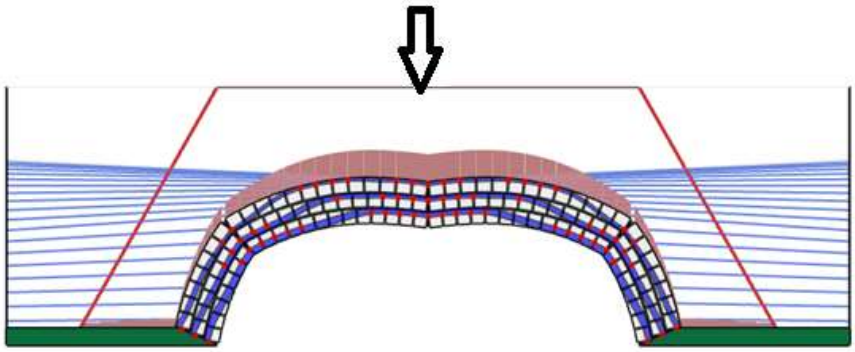

Fig.B.15. Collapse mechanism for arch loaded by 3 m square footing, column position at arch mid-span.

Table B. 2. Collapse load of masonry arch tunnel for various footing sizes and footing/column positions

Case	Footing size	Column position	Collapse load (kN)
1	1.5 m x 1.5 m	Arch left support	517
2	1.5 m x 1.5 m	Arch left quarter-span	365
3	1.5 m x 1.5 m	Arch mid-span	651
4	2 m x 2 m	Arch left support	560
5	2 m x 2 m	Arch left quarter-span	464
6	2 m x 2 m	Arch mid-span	1140
7	3 m x 3 m	Arch left support	703
8	3 m x 3 m	Arch left quarter-span	1030
9	3 m x 3 m	Arch mid-span	2480

4. B.3.2.4. Inferences:

Considering the various load positions and footing sizes in Table B.2, for most cases, the collapse load is below the service load of column i.e., 1130 kN.

Only for a column with footing size 3 m x 3m, with load position being at the mid-span, the collapse load of arch (2480 kN) exceeds the service load of column (1130 kN) with a factor of safety of 2. The safety margin for case 9, being sufficient, it is the lone case where the arch stability can be deemed to be safe.

The masonry arch tunnel is seen to be unstable for column footings with size 1.5 m x 1.5 m and 2 m x 2 m, and even for footing with 3 m size with column position non-coincident with arch mid-span.

4. B. 3.2.5. Collapse load estimation based on Vehicular loading

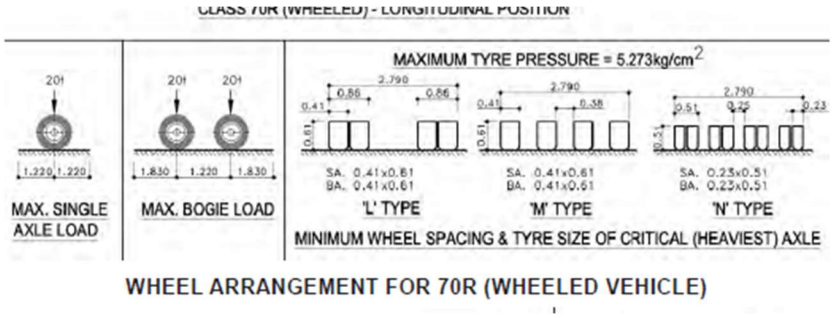

Fig.B.16. IRC Class 70 R Wheeled vehicle configuration considered in the analysis

For analysis, IRC class 70R Wheeled load as shown in Fig B.16 is considered.

Heaviest axle load (single axle load) = 200 kN

Hence one wheel load (single axle load) = 100 kN.

Tyre contact patch dimensions = 860 x 610 mm

Heaviest bogie load = 200 + 200 kN

Hence one wheel load (single axle load) = 100 + 100 kN.

Tyre contact patch dimensions = 860 x 610 mm

Bogie axle spacing = 1.23 m.

To simulate this loading on the road surface in software, 100 kN load with contact dimensions 860 mm x 610 mm was applied at the ground level.

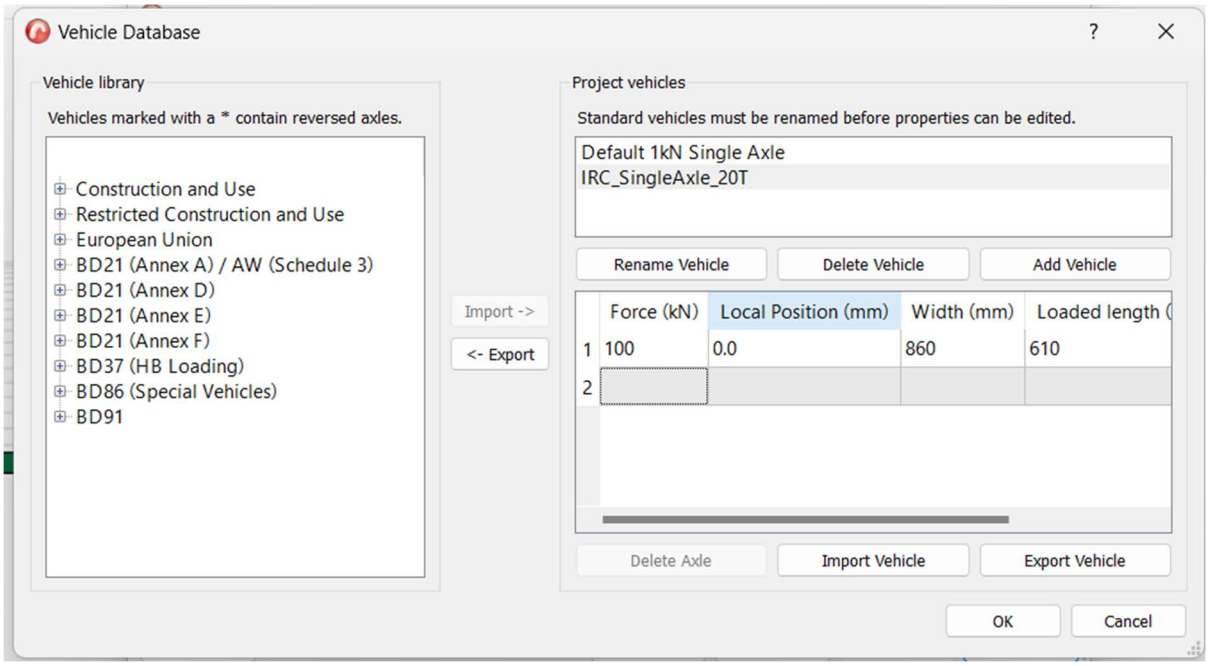

Fig. B. 17. Generation of single axle (70R) wheel load in software

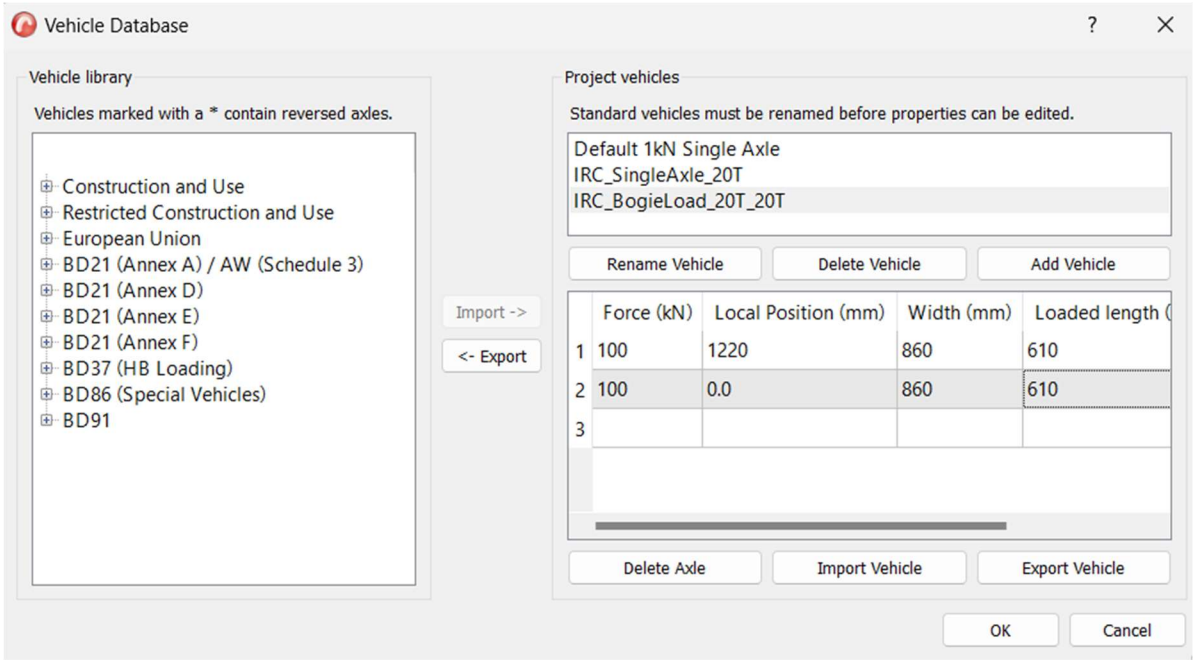

Fig.B.18. Generation of Bogie Load (70R) in software

4.B.3.2.5.1. Case 1: Single axle (100 kN wheel load) at arch left support

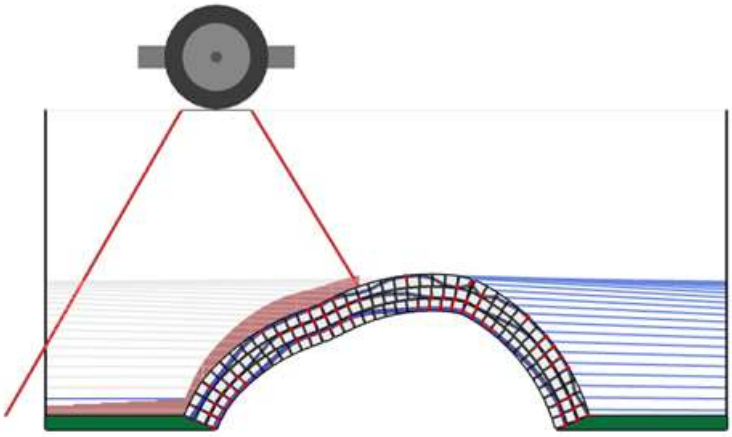

Fig.B.19. Collapse mechanism of arch tunnel due to single axle load of 100 kN (wheel load) at arch left support

4. B.3.2.5.2. Case 2: Single axle (100 kN wheel load) at arch left quarter-span

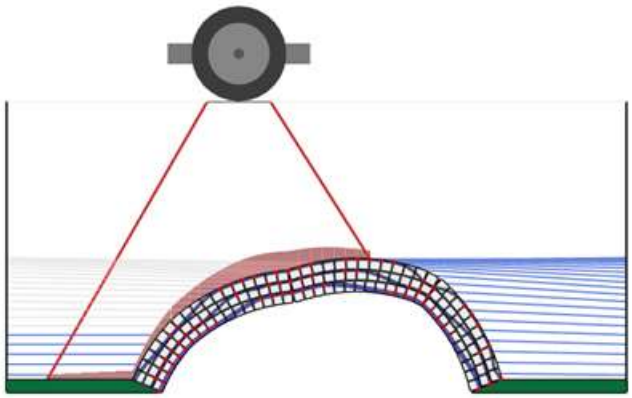

Fig.B. 20. Collapse mechanism of arch tunnel due to single axle load of 100 kN (wheel load) at arch left quarter-span

4. B.3.2.5.3. Case 3: Single axle (100 kN wheel load) at arch middle-span

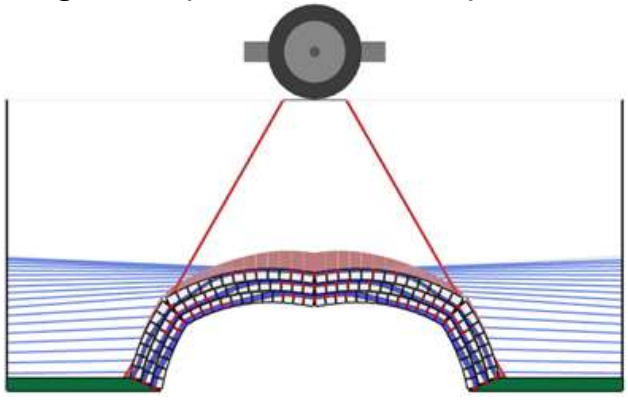

Fig.B.21. Collapse mechanism of arch tunnel due to single axle load of 100 kN (wheel load) at arch mid-span

4.B.3.2.5.4. Case 4: Bogie load (100 kN each wheel load @ 1.23 m c/c), with C.G. of load position coinciding with left arch support.

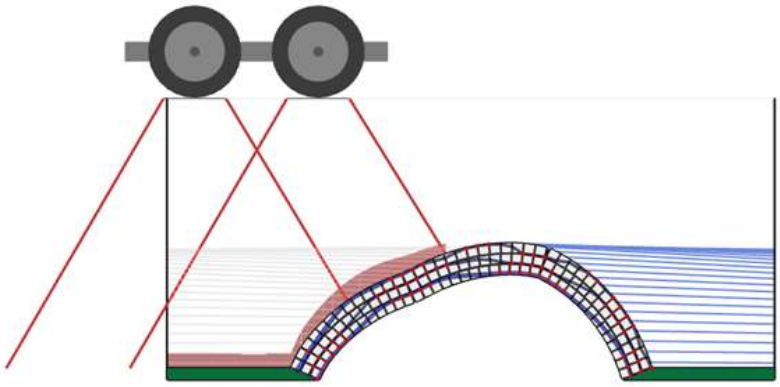

Fig.B.22. Collapse mechanism of arch tunnel due to bogie load of 100 kN (each wheel load) with C.G. of load system coincident with arch left support.

4.B.3.2.5.5. Case 5: Bogie load (100 kN each wheel load @ 1.23 m c/c), with C.G. of load position coinciding with arch left quarter-span position.

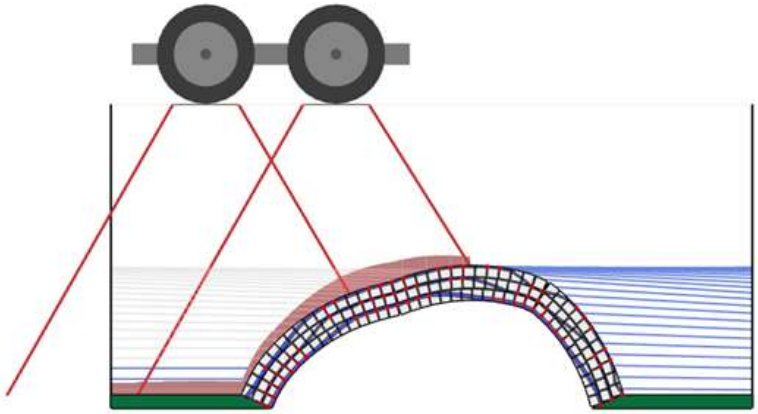

Fig.B.23. Collapse mechanism of arch tunnel due to bogie load of 100 kN (each wheel load) with C.G. of load system coincident with arch left quarter-span.

4. B.3.2.5.6. Case 6: Bogie load (100 kN each wheel load @ 1.23 m c/c), with C.G. of load position coinciding with arch mid-span position.

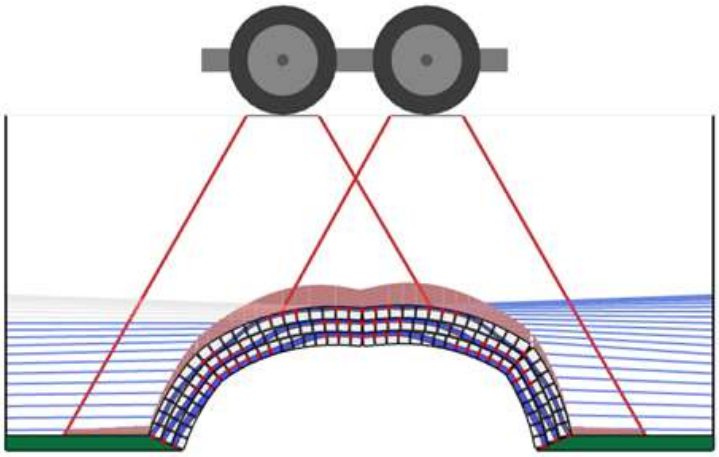

Fig.B.24. Collapse mechanism of arch tunnel due to bogie load of 100 kN (each wheel load) with C.G. of load system coincident with arch mid-span.

Table B.3. Collapse load of masonry arch tunnel for various axle loads and positions

Case	Axle load	Load position	Collapse load (kN)
1	Single axle 100 kN	Arch left support	1050
2	Single axle 100 kN	Arch left quarter-span	791
3	Single axle 100 kN	Arch mid-span	1740
4	Bogie load (200 kN)	CG of load coincident with arch left support	2040
5	Bogie load (200 kN)	CG of load coincident with arch left quarter-span	1360
6	Bogie load (200 kN)	CG of load coincident with arch mid-span	1896

4.B.3.2.6. Inferences:

Lowest collapse load from the various load positions for single heaviest axle load, considered in Tables B. 3 is 791 kN. This exceeds IRC class 70R single axle wheel load of 100 kN and even 110 kN (considering an impact factor of 1.1 to account for the dynamic effects of running traffic).

Lowest collapse load from the various load positions for bogie load, considered in Tables B. 3 is 1360 kN. This exceeds IRC class 70R single axle wheel load of 200 kN

and even 220 kN (considering an impact factor of 1.1 to account for the dynamic effects of running traffic).

Hence, from the results of the present study, it is inferred that the arch is capable of carrying the traffic loads of IRC class 70R loading with a factor of safety 3.5.

4. B.4. Finite Element Analysis of Masonry Arch Tunnel

Finite element modelling of the masonry tunnel, including the back-fill and surcharge soil was done in FE package ABAQUS. A macro modelling approach was adopted for the masonry arch. A 2D (plane strain) idealization was used for the purpose.

Since detailed soil investigations were outside the scope of the work, information on soil characteristics from nearby areas was utilized in the investigations. Accordingly, soil backfill was taken to be of silty-sand type. For the analysis, the surrounding soil was modelled as a 2D continuum with the following parameters [5]: E = 50 MPa and $\nu = 0.25$. Mohr-Coulomb plasticity model with friction angle 35°, dilation angle 5° was used in modelling. Inelastic material properties were used in the modelling of masonry arch. Drucker-Prager model with **compression hardening behaviour** with the following model parameters were used in the modelling of masonry [8] : E = 3654 MPa; $\nu = 0.15$; Friction angle, $\emptyset = 35^{\circ}$; flow stress ratio = 0.8; Dilatancy angle $\Psi = 15^{\circ}$. 2D plane strain elements with 2 dof (translations) per node were used in the discretization of masonry tunnel arch. Details of loading and boundary conditions specified are shown in Figure B. 25

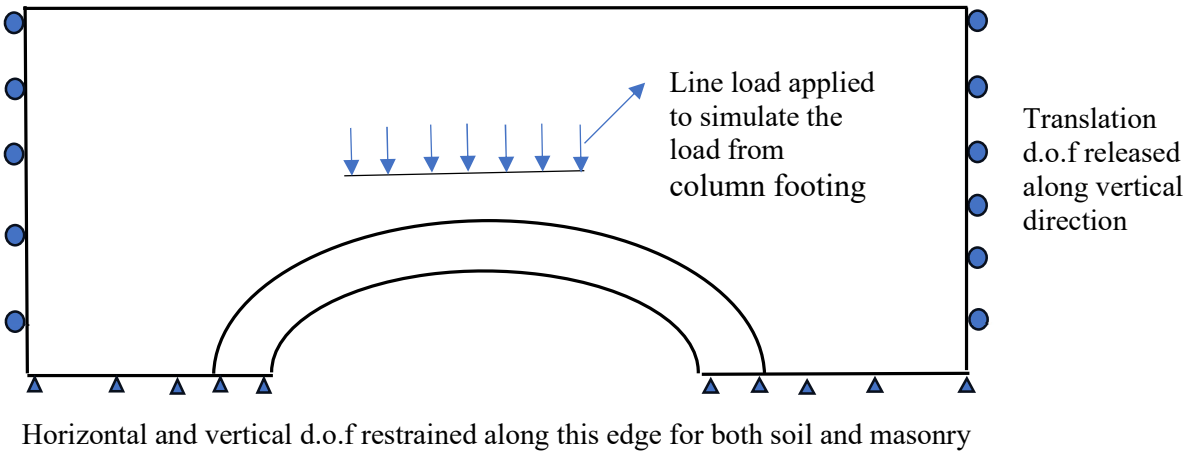

Fig. B. 25. Schematic diagram of the FE model developed.

Effect of column loads were applied as a line load of length equal to the width of column footing at a level of 1 m from the ground level (consistent with the loading in limit analysis)

Effect of precompression in masonry tunnel resulting from the passive pressure exerted by soil backfill was included in the analysis through geostatic step, where the soil effects were modelled as body forces.

4.B.4.1. Model Validation studies

For validation of the modelling procedure adopted, an under-ground concrete tunnel of Delhi metro, at a depth of 18 m below ground level was modelled and results were compared with the reported one in literature [7].

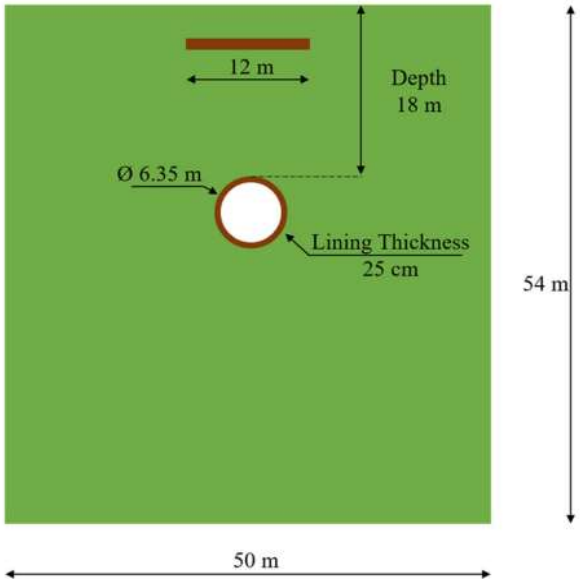

Fig.B.26. Geometry details of soil continuum and concrete tunnel lining considered for modelling

The results from the present non-linear FE analysis performed using ABAQUS software is compared with the results reported in literature [7] as in Table B.4.

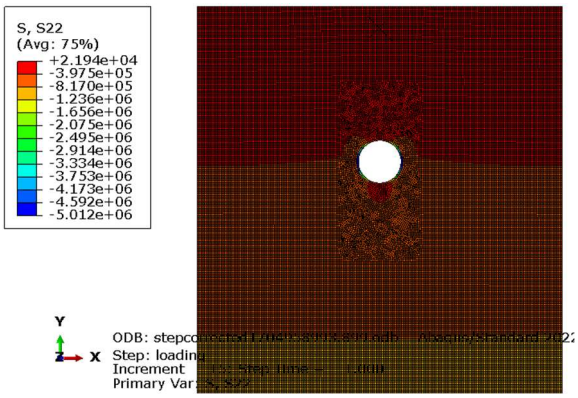

Fig.B.27.a.Vertical stress contour from ABAQUS

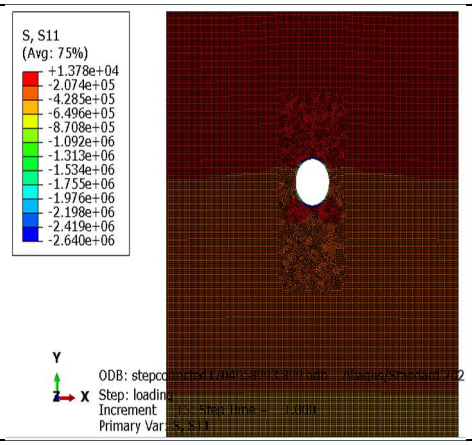

Fig.B.27.b.Horizontal stress contour from ABAQUS

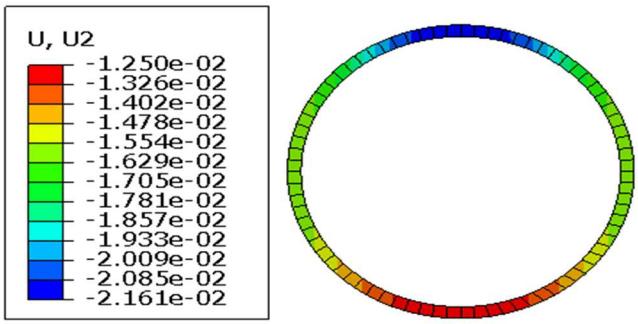

Fig.B.27. Vertical displacement component (m) in tunnel lining from ABAQUS

Table B.4. Comparison of results from present study and literature [Naqvi et al.(2020)]

Response quantity	Present study	Naqvi et al. (2020)	Error
Maximum vertical stress in the soil (at the bottom)	980.19 kPa	982.48 kPa	0.23%
Maximum horizontal stress in the soil (at the bottom)	488.28 kPa	489.46 kPa	0.24%
Maximum displacement in tunnel - At Crown	21.6 mm	21 mm	2.85%

Various response quantities from the present non-linear finite element analysis study of the underground concrete tunnel model considering soil-structure interaction effects performed using FE package ABAQUS is compared with the results in literature developed using finite element package OptumG2. From Table 4, it can be seen that the prediction of all response quantities using the modelling procedure adopted using ABAQUS matches well with the results reported in literature.

4. B.4.2. Analysis of masonry tunnel using FEA

The validated modelling procedure is now used for performing FE analysis of masonry arch tunnel. Static analysis is performed considering the dead load and live load combination. Under dead load category, the dead load effects of masonry arch, soil back fill and dead load and imposed dead load component of column load were considered. Under live load, the live load component of the column load has been included in the study. The self-weight effects of soil backfill was included in the analysis using the geostatic step in ABAQUS model. A multi-step analysis procedure was used in the present study, which includes an initial step where the boundary conditions are introduced, followed by step 1 which is the geostatic step where the stabilizing effects due to soil backfill is included in the analysis by considering the soil gravity effects as body forces. Geostatic step in ABAQUS ensures that the equilibrium of soil masonry system is ensured before the application of column load effects. Interaction between the soil and masonry was ensured through the use of appropriate interaction models in ABAQUS. For non-linear soil and masonry material models, the parameters discussed in section 4.B.4, were used in the analysis. Four noded quadrilateral plain strain element was used in the discretization of continuum. Careful meshing of the continuum was ensured by proper partitioning of the various parts of the model.

Since the actual footing size was not provided by the client, analysis was performed for three sizes of column footing- (i) square footing of size 1.5 m (ii) square footing of size 2 m (iii) square footing of size 3 m. For all the footing sizes, the depth of footing was taken as 1 m below ground level. For the static analysis, a load combination of 1.5 (Dead load + Live load), consistent with the design specifications, was used.

Two column load positions have been considered in the present study, consistent with the limit analysis performed, i.e., (i) Symmetric loading of arch, with the column and footing symmetrically placed at the mid-span of the tunnel (ii) unsymmetric loading of the arch, with the column load position coinciding with the left quarter-span position of the tunnel.

4.B.4.3. Results of FEM Analysis for gravity loads

Contours of maximum and minimum principal stress corresponding to various load positions are presented in this section. Sign convention for stress contour is Tension T: +ve and Compression C : -ve.

4. B.4.3.1.Case 1. Symmetric loading (mid-span loading) of tunnel with 1.5 m x 1.5 m size footing

Total pressure corresponding to 1.5 (DL + LL) combination = 0.8 MPa.

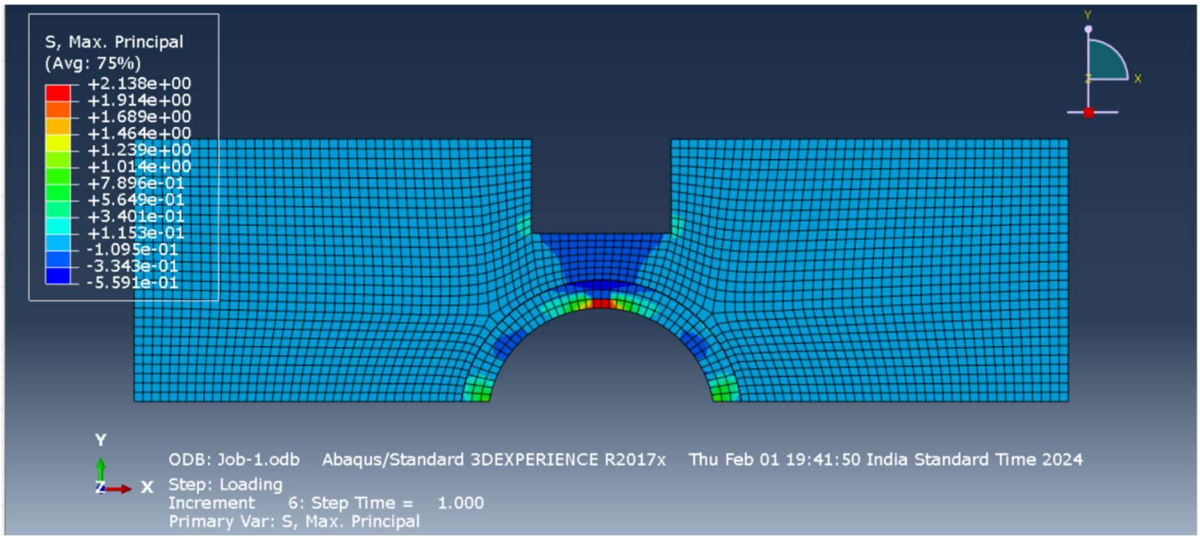

Fig.B.28. Maximum principal stress (MPa) contour corresponding to symmetric loading by footing of size 1.5 m x 1.5 m

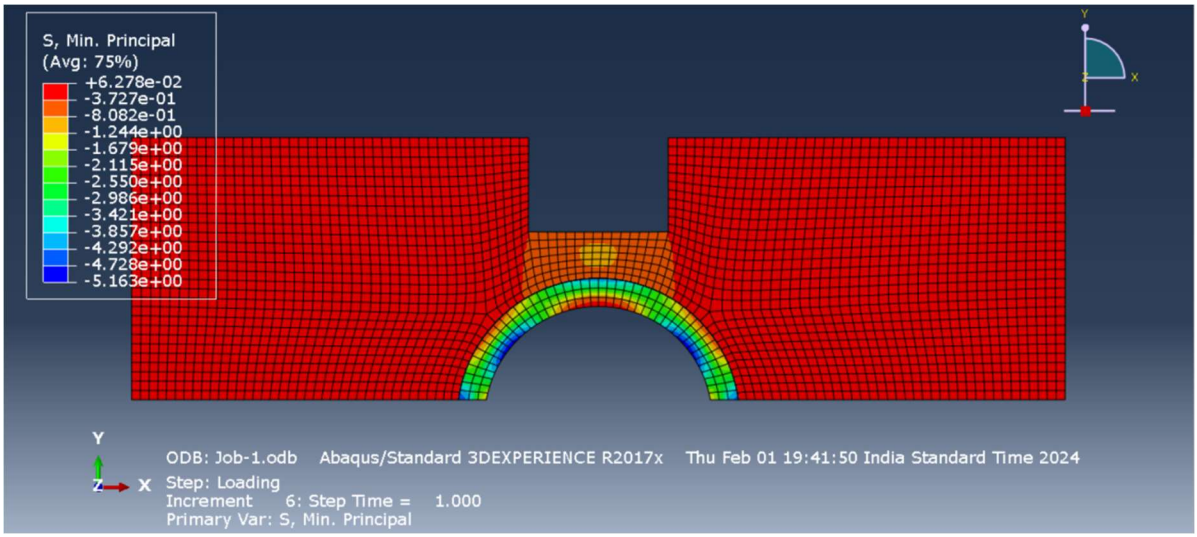

Fig. B.29. Minimum principal stress (MPa) contour corresponding to symmetric loading by footing of size 1.5 m x 1.5 m

4. B.4.3.2. Case 2: Unsymmetric loading of masonry tunnel using footing of size 1.5 m X 1.5 m

Total pressure corresponding to 1.5 (DL + LL) combination = 0.8 MPa.

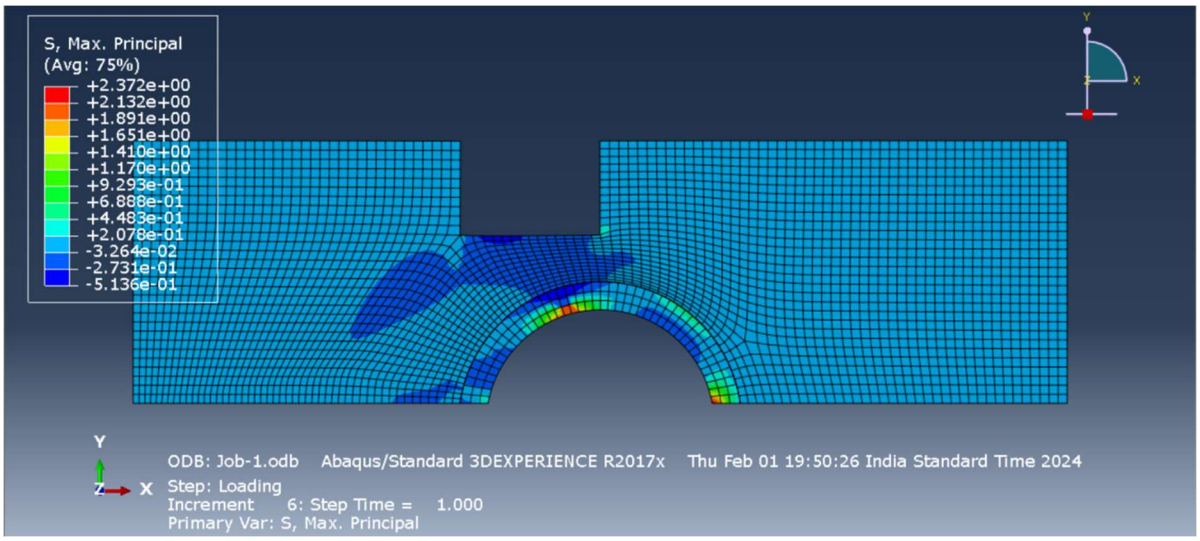

Fig.B.30. Maximum principal stress (MPa) contour corresponding to unsymmetric loading by footing of size 1.5 m x 1.5 m

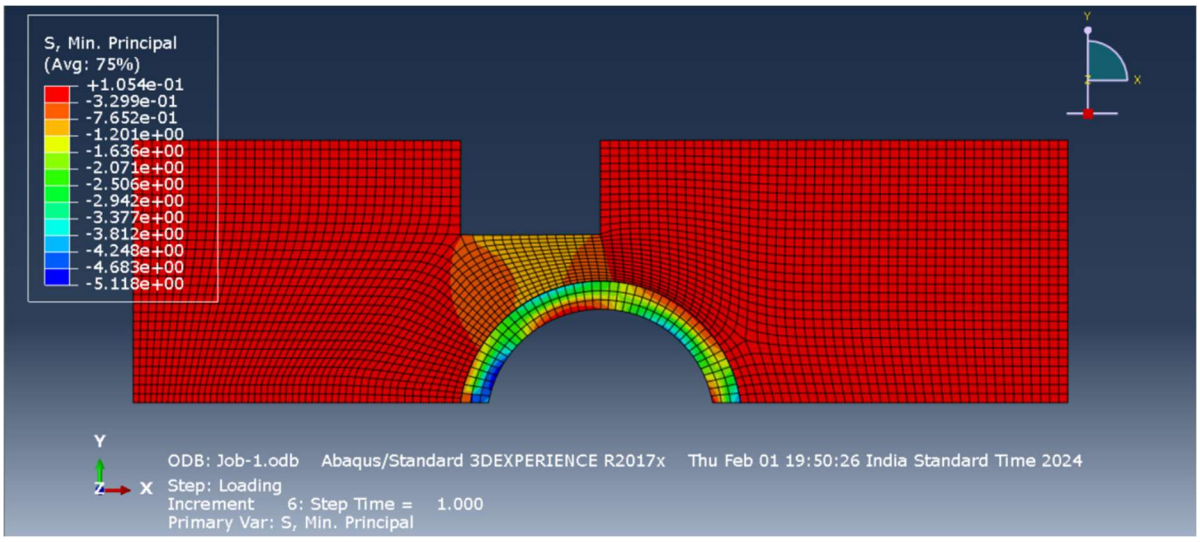

Fig.B.31. Minimum principal stress (MPa) contour corresponding to unsymmetric loading by footing of size 1.5 m x 1.5 m

4.B.4.3.3.Case 3: Symmetric loading of masonry tunnel using footing of size 2.0 m x 2.0 m

Total pressure corresponding to 1.5 (DL + LL) combination = 0.45 MPa.

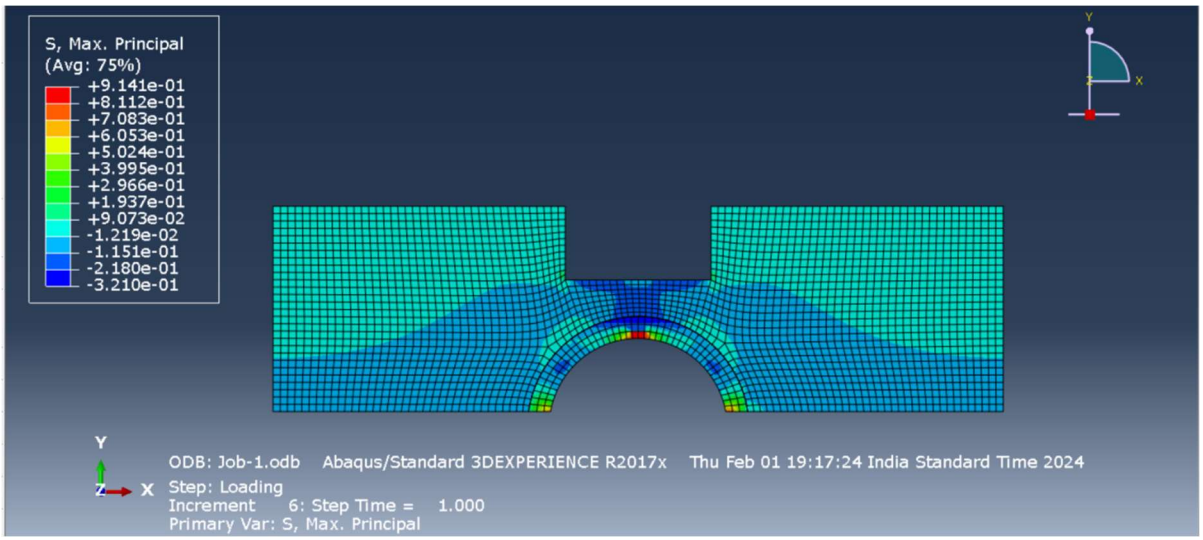

Fig.B.32. Maximum principal stress (MPa) contour corresponding to symmetric loading by footing of size 2 m x 2 m

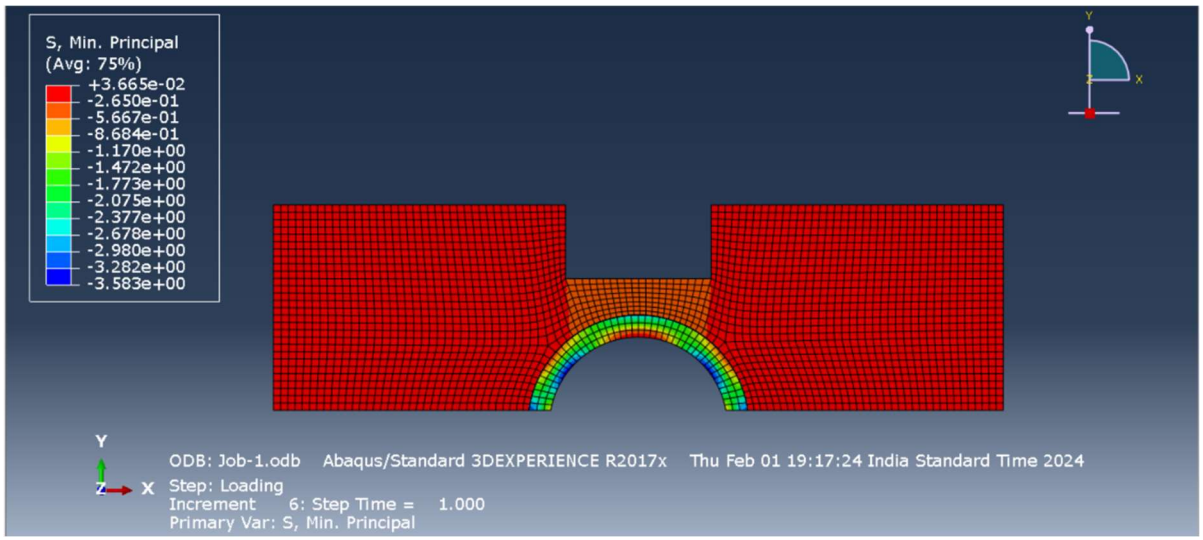

Fig.B.33. Minimum principal stress (MPa) contour corresponding to symmetric loading by footing of size 2 m x 2 m

4.B.4.3.4. Case 4: Unsymmetric loading of masonry tunnel using footing of size 2.0 m X 2.0 m

Total pressure corresponding to 1.5 (DL + LL) combination = 0.45 MPa.

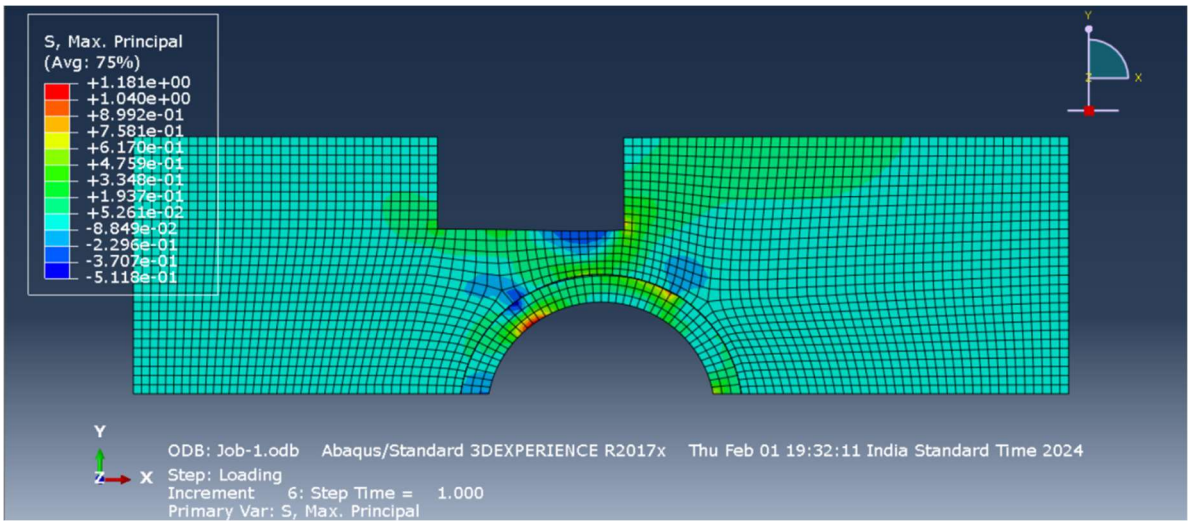

Fig.B.34 Maximum principal stress (MPa) contour corresponding to unsymmetric loading by footing of size 2 m x 2 m

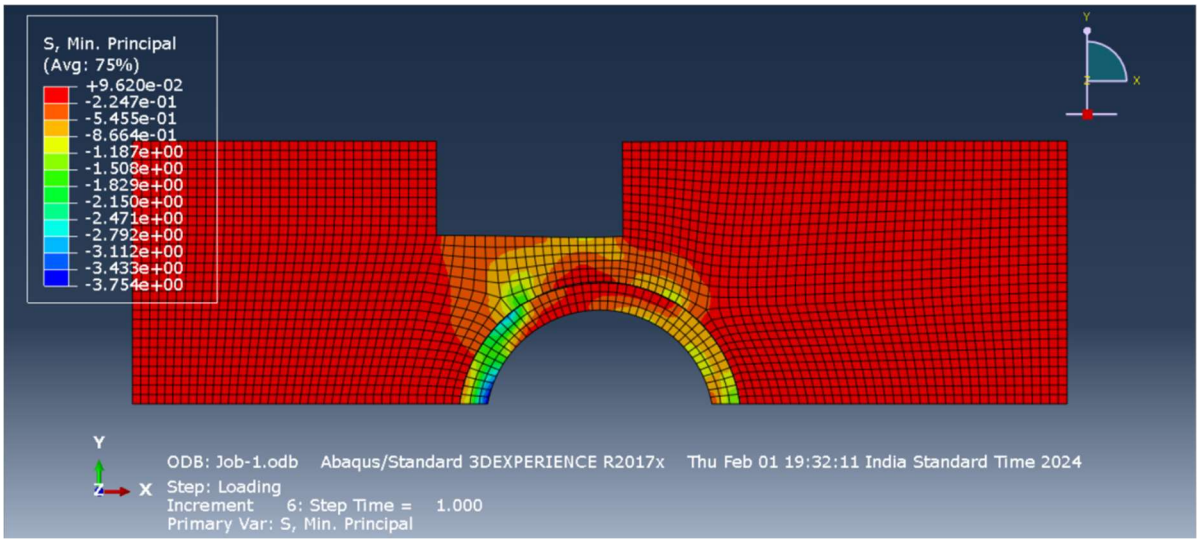

Fig.B.35. Minimum principal stress (MPa) contour corresponding to unsymmetric loading by footing of size 2 m x 2 m

4.B.4.3.5. Case 5: Symmetric loading of masonry tunnel using footing of size 3.0 m x 3.0 m

Total pressure corresponding to 1.5 (DL + LL) combination = 0.20 MPa.

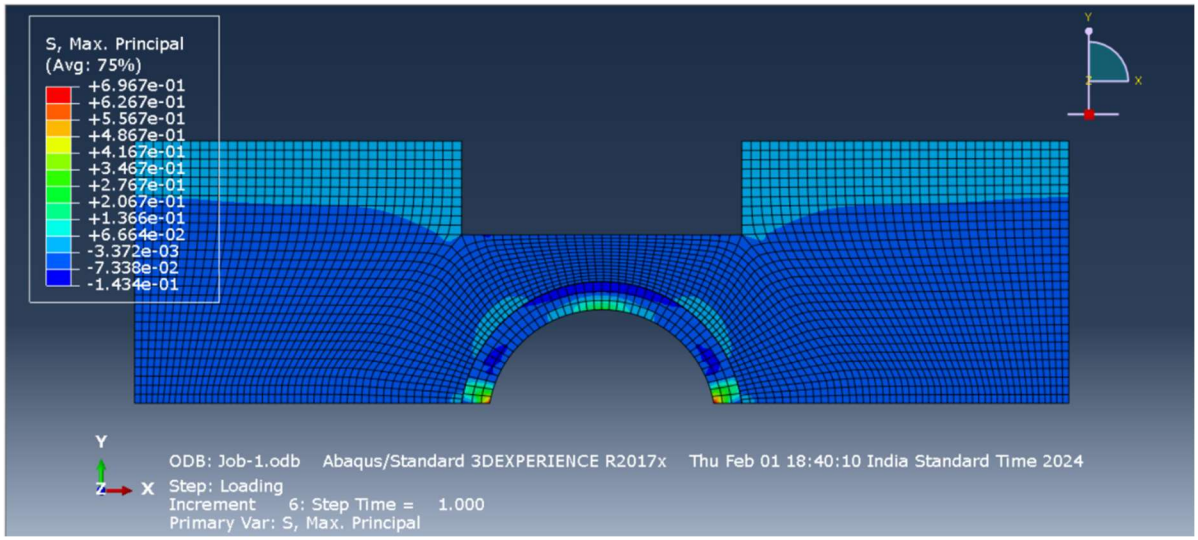

Fig.B.36. Maximum principal stress (MPa) contour corresponding to symmetric loading by footing of size 3 m x 3 m

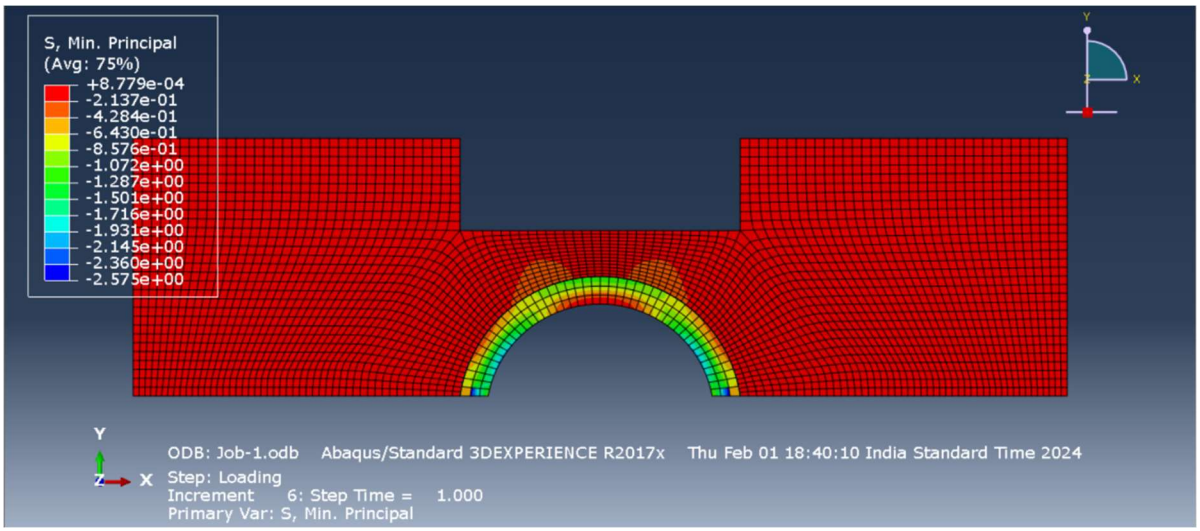

Fig.B.37. Minimum principal stress (MPa) contour corresponding to symmetric loading by footing of size 3 m x 3 m

4.B.4.3.6. Case 6: Unsymmetric loading of masonry tunnel using footing of size 3.0 m x 3.0 m

Total pressure corresponding to 1.5 (DL + LL) combination = 0.20 MPa.

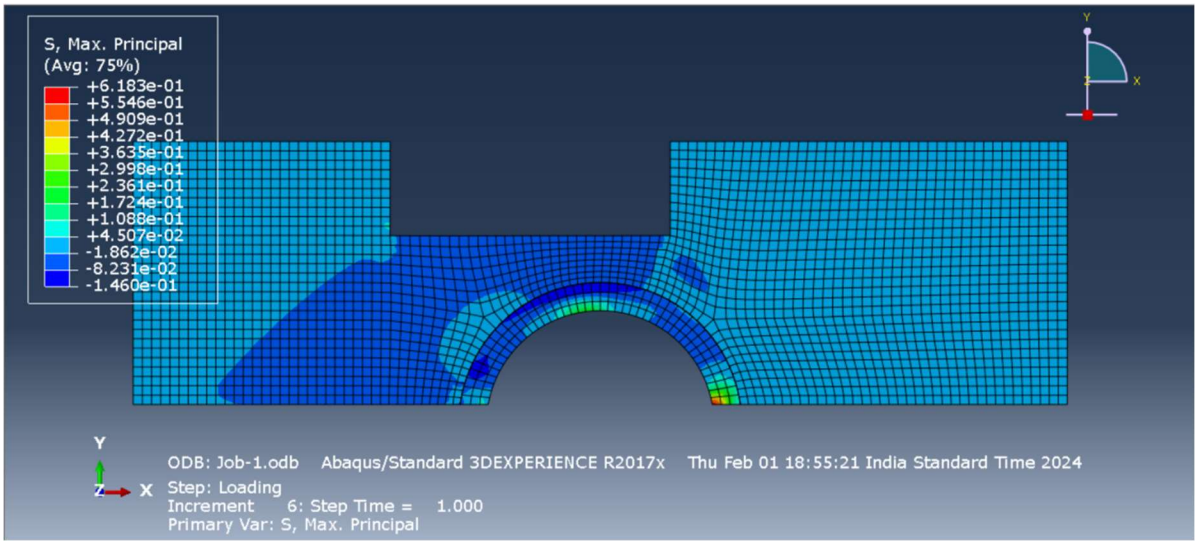

Fig.B.38. Maximum principal stress (MPa) contour corresponding to unsymmetric loading by footing of size 3 m x 3 m

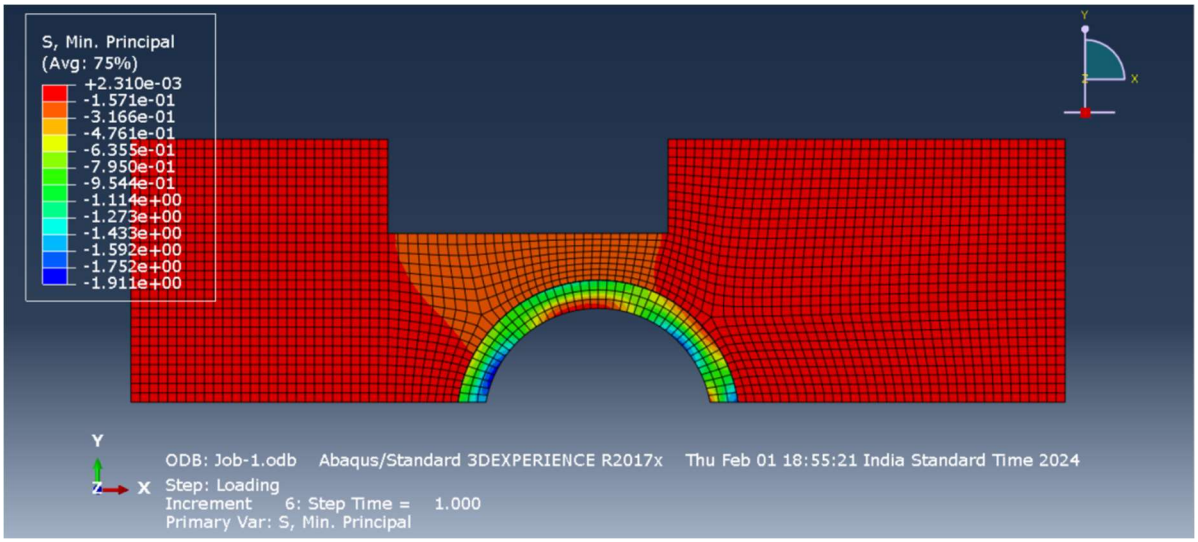

Fig.B.39. Minimum principal stress (MPa) contour corresponding to unsymmetric loading by footing of size 3 m x 3 m

Table B. 5. Consolidated test results of static analysis : Load Case – 1.5 (DL+LL)

Footing Size	Symmetric Loading		Unsymmetric loading	
	Maximum principal stress (MPa)	Minimum principal stress (MPa)	Maximum principal stress (MPa)	Minimum principal stress (MPa)
1.5 m x 1.5 m	+ 1.01	- 5.16	+ 1.40	- 5.110
2.0 m x 2.0 m	+ 0.40	- 3.58	+ 0.78	- 3.75
3.0 m x 3.0 m	+ 0.35	- 1.93	+ 0.30	- 1.911

4. B.4.4. Inferences:

Considering the various load positions and footing sizes in Table B.5, for all analysis cases, the ultimate compressive stress in the material of the arch is less than the tested strength of brick samples. But considering a material partial safety factor of 1.5, the maximum permissible compressive stress in bricks can be approximately taken as 4 MPa.

With reference to Table B.5, the minimum principal stress (representative of the maximum compressive stress from FE analysis) is less than 4 MPa (with sufficient safety margin) only for the case with footing size exceeding 3 m x 3 m. For footing size below 3 m, the maximum compressive stress is close to or exceeding 4 MPa.

For all footings and load positions analysed, tensile stresses are developed in the arch, but only for the column with footing size 3 m x 3 m, the ultimate tensile stresses developed in the material of arch is significantly small with minor spreading. For all other loading cases, tensile stress value and its spreading is considerable.

The masonry arch tunnel is seen to be not safe in the dead load plus live load combinations of column load with footing size 1.5 m x 1.5 m and 2 m x 2m placed above. However, for 3 m size footings and above, the arch seems to be safe under the dead load plus live load combinations. Similar observations were made with reference to estimation of tunnel collapse load using limit analysis in section 4.B.3.2.4. Hence, with reference to the static analysis results, it can be concluded that stability of the arch tunnel is questionable for footing sizes less than 3 m.

For unsymmetric loading scenario involving 3 m x 3 m size footing, though the stress levels are seen to be close to that for the case of symmetric loading scenario, the spread of tension zone is seen to be more and unsymmetric, making the 3 m unsymmetric loading scenario more vulnerable to failure.

4. B. 5. Analysis of masonry tunnel for seismic load using FEA

Tunnel structures are constrained by the surrounding soil. Hence, in general, tunnel structures cannot be excited independent of the ground or be subjected to strong vibratory amplification, such as the inertial response of a bridge structure during earthquake. As a result, tunnels, in general, have performed better during earthquakes compared to above-ground structures such as buildings and bridges.

An equivalent static approach, similar to the seismic analysis of retaining walls subjected to dynamic earth pressures due to soil backfill, resulting from ground motions [IS 1893, Part 3, 2014] has been attempted in the present study.

4.B. 5. 1. Quasi-static analysis methodology for seismic effects

The methodology involves estimation of the dynamic increment in active earth pressure over the static effects. The static effects being already accounted in the analysis by incorporating soil structure interaction effects in the finite element model.

Once the dynamic increment in active earth pressure is estimated, the same in introduced as an additional loading step in the ABAQUS model, after the geostatic load step and the load step which includes the vertical loading from the building structure. The load definitions in various steps are properly scaled to include the following load combination rules:

1. 1.5 (DL + EL)
2. 1.2 (DL + LL + EL)

Here, DL represents the dead load component of the static vertical pressure transmitted from the footing. LL represents the live load component of the static vertical pressure transmitted from the footing and EL represents the earthquake forces, i.e., the lateral pressure on the tunnel walls resulting from the dynamic increment in active earth pressure.

Estimation of dynamic active earth pressure due to backfill [IS 1893, Part 3, 2014]

Dynamic active earth pressure due to backfill $\left(P_{A\gamma}\right)_{dyn} = \frac{1}{2}\gamma h^2 C_{a,Tot}$

$\left(P_{A\gamma}\right)_{dyn} =$ dynamic total active earth pressure in kN/m length of the wall.

Where $C_{a,Tot}$ is the total active earth pressure coefficient

$\gamma =$ soil unit weight in kN/m^3 = 18 kN/m^3

$h =$ 1.3 m projected height of arch (height of wall in m)

$$C_{a,Tot} = \frac{(1 \pm A_v)cos^2(\emptyset - \lambda - \alpha)}{cos\lambda\, cos^2\alpha\, cos(\delta + \alpha + \lambda)} \times \left[\frac{1}{1 + \left\{\frac{sin(\emptyset+\delta)\, sin(\emptyset - i - \lambda)}{cos(\alpha - i)cos(\delta+\alpha+\lambda)}\right\}^{1/2}}\right]^2$$

$A_v =$ vertical seismic coefficient

$$A_v = \frac{2}{3}A_h$$

$A_h =$ horizontal seismic coefficient.

$\emptyset =$ Angle of internal friction of soil = 30°

$$\lambda = tan^{-1}\left(\frac{A_h}{1 \pm A_v}\right) = tan^{-1}\left(\frac{A_h}{1 \pm A_v}\right)$$

$\alpha =$ angle which the earth face of the wall makes with the vertical.

$i =$ slope of earth fill

$\delta =$ angle of friction between wall and earth fill.

$$\delta = tan^{-1}\mu = tan^{-1}0.4 = 21.8^\circ$$

$$A_h = \frac{Z}{2}\frac{I}{R}\frac{S_a}{g}$$

Note: R = 1.0 for masonry piers.

$\frac{S_a}{g}$ depends on the fundamental time period of the tunnel soil system,

Estimation of fundamental time period was made from the eigen value analysis of the finite element model of soil-tunnel system developed in ABAQUS (Figure B.40). The fundamental frequency came to 2.85 Hz or fundamental time period = 0.35 s.

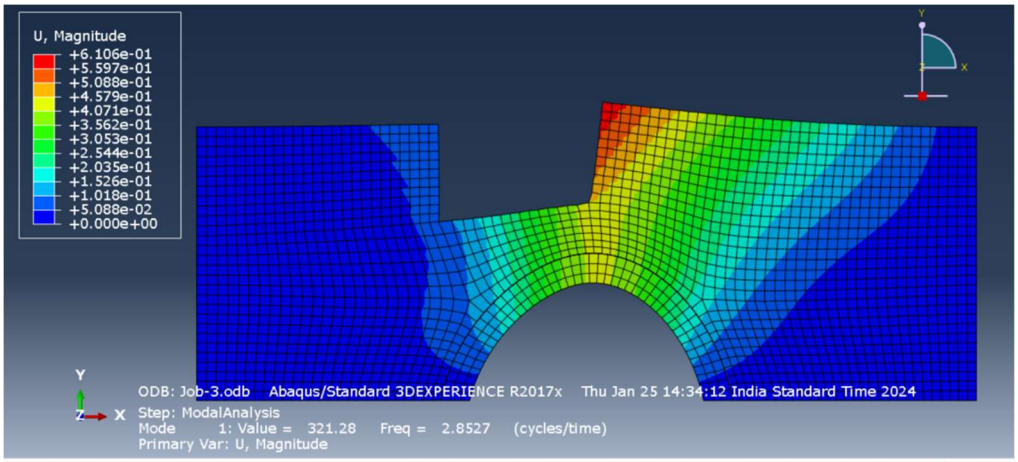

Fig. B.40. Fundamental mode of vibration of tunnel-soil system

Hence from Fig.1 of IS 1893, part 3 (2014), corresponding to a fundamental period of 0.35 s, $\frac{S_a}{g} = 2.5$

Hence, $A_h = \ 0.2$

$$A_v = \frac{2}{3}A_h = \ 0.1333$$

$$\lambda = \ tan^{-1}\left(\frac{A_h}{1 \pm A_v}\right) = \ 10.01\ , 12.99$$

$$C_{a,Tot} = \frac{(1 + A_v)cos^2(\emptyset - \lambda - \alpha)}{cos\lambda\ cos^2\alpha\ cos(\delta + \alpha + \lambda)} \times \left[\frac{1}{1 + \left\{\frac{sin(\emptyset+\delta)\ sin(\emptyset-i-\lambda)}{cos(\alpha-i)cos(\delta+\alpha+\lambda)}\right\}^{1/2}}\right]^2$$

$$\therefore C_{a1,Tot} = \ 0.49$$

$$C_{a2,Tot} = \frac{(1 - A_v)cos^2(\emptyset - \lambda - \alpha)}{cos\lambda\ cos^2\alpha\ cos(\delta + \alpha + \lambda)} \times \left[\frac{1}{1 + \left\{\frac{sin(\emptyset+\delta)\ sin(\emptyset-i-\lambda)}{cos(\alpha-i)cos(\delta+\alpha+\lambda)}\right\}^{1/2}}\right]^2$$

$$C_{a2,Tot} = 0.4236$$

$$\therefore C_{a,Tot} = \max\left(C_{a1,Tot}, C_{a2,Tot}\right) = 0.49$$

$$\left(P_{A\gamma}\right)_{dyn} = \frac{1}{2}\gamma h^2 C_{a,Tot} = 7.453\ kN/m$$

Total pressure ordinate at base = $C_{a,Tot}\ \gamma\ h = 11.466\ kN/m^2 = 0.0115MPa$

Static active earth pressure

Static active earth pressure can be obtained by substituting $A_v = \ A_h = \ \lambda = 0$

$$C_{a,Stat} = \frac{cos^2(\emptyset - \alpha)}{cos^2\alpha\ cos(\delta + \alpha)} \times \left[\frac{1}{1 + \left\{\frac{sin(\emptyset+\delta)\ sin(\emptyset-i)}{cos(\alpha-i)cos(\delta+\alpha)}\right\}^{1/2}}\right]^2$$

$$C_{a,Stat} = 0.29651$$

$$\left(P_{A\gamma}\right)_{stat} = \frac{1}{2}\gamma h^2 C_{a,Stat} = \ 4.5099\ kN/m$$

Static pressure ordinate at base = $C_{a,Stat}\ \gamma h = 6.94\ kN/m^2$ =0.00694 MPa

Applied at an elevation of 1.3/3 = 0.4333 m from the base of the wall

Dynamic increment in active earth pressure due to ground motion = difference between total active earth pressure including dynamic effects and static active earth pressure = $C_{a,Tot} - C_{a,Stat}$

i.e., dynamic increment = $7.453 - 4.5099 = 2.943\ kN/m$ (Applied at an elevation of 1.3/2= 0.65 m from the base of the wall)

Therefore, dynamic increment in active earth pressure ordinate at the tunnel base = 11.46-6.94 = 4.52 kN/m^2 = 0.00452 MPa

Active pressure due to uniform surcharge

The active pressure against the tunnel wall due to a uniform surcharge of intensity *q*, kN per unit area of the inclined earth fill surface shall be:

$$\left(P_{Aq}\right)_{dyn} = \frac{qhcos\alpha}{cos(\alpha - i)} C_a$$

Estimation of Seismic weight of structure for calculation of surcharge pressure

DL per floor = 217.55 kN

LL per floor = 64 kN

Therefore, Total DL from four floors = 870.2 kN

Total LL from four floors = 256 kN

Hence, seismic weight transferred to column footing = 870.2 + 0.5 x 256 = 998.2 ≅ 1000 kN

Calculation of surcharge pressure due to column footings of various sizes.

(i) 1.5 m x 1.5 m footing: $q = \frac{1000}{1.5x1.5} = 444.44\ kN/m^2$

(ii) 2m x 2 m footing: $q = \frac{1000}{2x2} = 250\ kN/m^2$

(iii) 3m x 3m footing: $q = \frac{1000}{3\ x\ 3} = 111.11\ kN/m^2$

Increment in dynamic pressure due to surcharge $=qh\left(C_{a,Tot} - C_{a,stat}\right)$

(i) 1.5 m x 1.5 m footing:

$$\left(P_{Aq}\right)_{dyn,inc\_1.5x1.5} = 444.44 \times 1.3 \times (0.49 - 0.29651) = 111.79\ kN/m^2 = 0.112\ MPa$$

(ii) 2 m x 2m footing:

$$\left(P_{Aq}\right)_{dyn,inc\_2x2} = 250 \times 1.3 \times (0.49 - 0.29651) = 62.88\ kN/m^2 0.0629\ MPa$$

(iii) 3m x 3m footing:

$$\left(P_{Aq}\right)_{dyn,inc\_3x3} = 133.33 \times 1.3 \times (0.49 - 0.29651) = 33.537\ kN/m^2 0.03354\ MPa$$

Combining the surcharge effects with the lateral dynamic pressures:

(i) Dynamic increment in 1.5 m x 1.5 m footing = $(P)_{dyn,inc\_1.5x1.5} = 0.11652\ MPa$

(ii) Dynamic increment in 2 m x 2 m footing = $(P)_{dyn,inc\_2x2} = 0.06742\ MPa$

(iii) Dynamic increment in 3 m x 3 m footing = $(P)_{dyn,inc\_3x3} = 0.03806\ MPa$

4.B.5.2. Results of quasi-static analysis for seismic load effects in the lateral direction

Seismic Case 1: Symmetric loading of masonry tunnel using footing of size 1.5 m – load case: 1.5 (DL + EL)

Load calculation:

1.5 DL = 870.2 = 1305.3 kN; Pressure = 0.58 MPa ;

Lateral Pressure due to 1.5 EL = $1.5 \times 0.11652 = 0.175\ MPa$

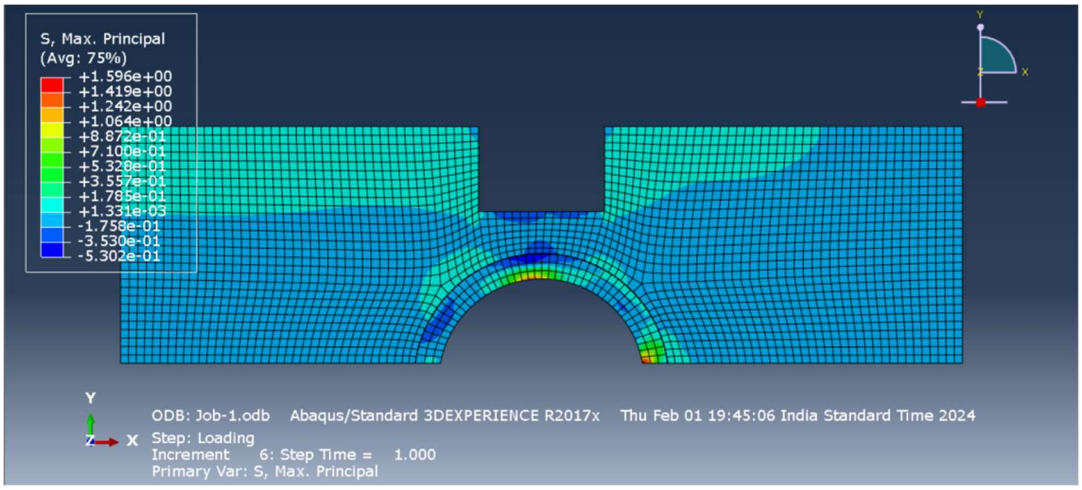

Fig.B.41. Maximum principal stress (MPa) contour corresponding to symmetric loading for footing of size 1.5 m x 1.5 m. Load case: 1.5 (DL + EL)

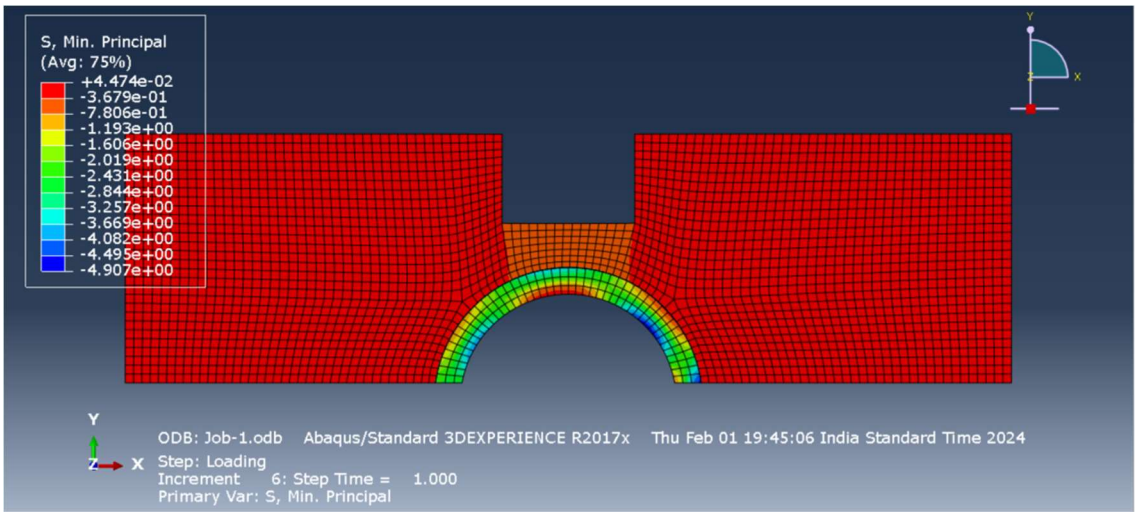

Fig. B. 42. Minimum principal stress (MPa) contour corresponding to symmetric loading for footing of size 1.5 m x 1.5 m. Load case: 1.5 (DL + EL)

Seismic Case 2: Symmetric loading of masonry tunnel using footing of size 1.5 m – load case: 1.2 (DL +LL+ EL)

Load calculation:

1.2 (DL + LL) = = 0.64 MPa

1.2 EL = 0.1398 MPa

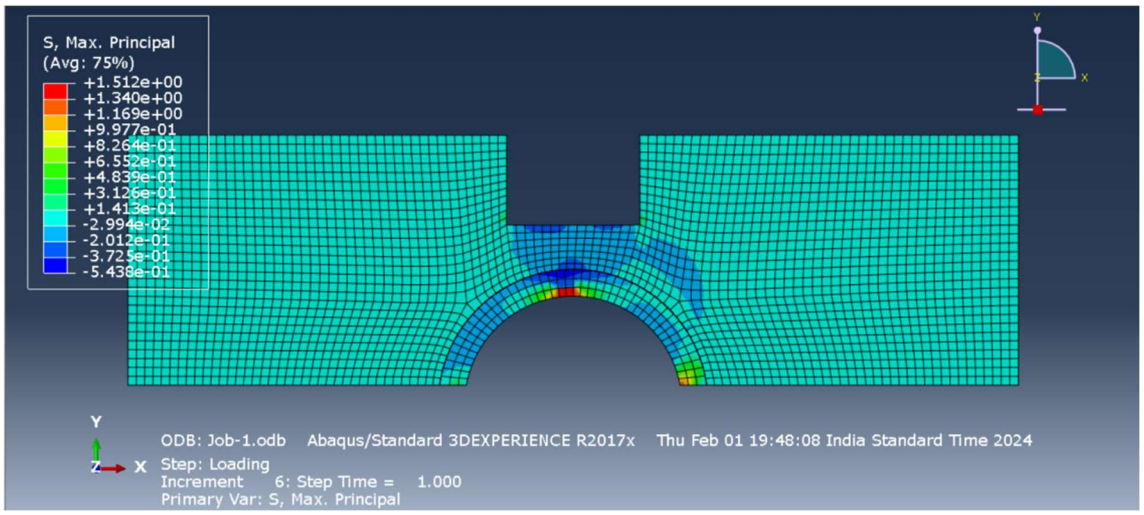

Fig.. B.43. Maximum principal stress (MPa) contour corresponding to symmetric loading for footing of size 1.5 m x 1.5 m. Load case: 1.2 (DL + LL+ EL)

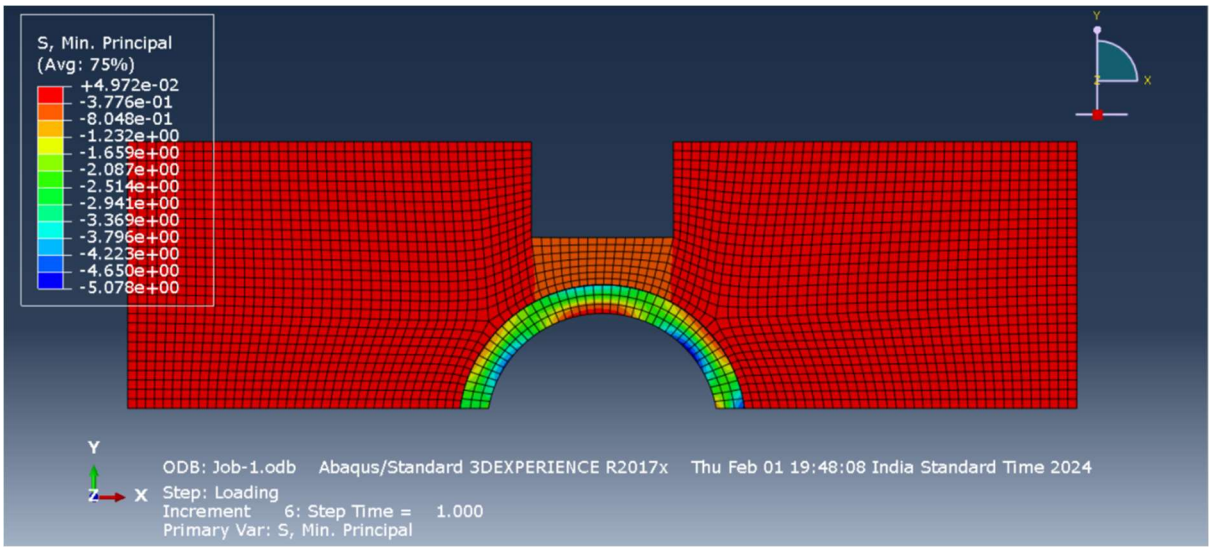

Fig.B.44. Minimum principal stress (MPa) contour corresponding to symmetric loading for footing of size 1.5 m x 1.5 m. Load case: 1.2 (DL + LL+ EL)

Seismic Case 3: Unsymmetric loading of masonry tunnel using footing of size 1.5 m – load case: 1.5 (DL + EL)

Load calculation:

1.5 DL = 0.58 MPa

Pressure due to 1.5 EL = $0.175\ MPa$

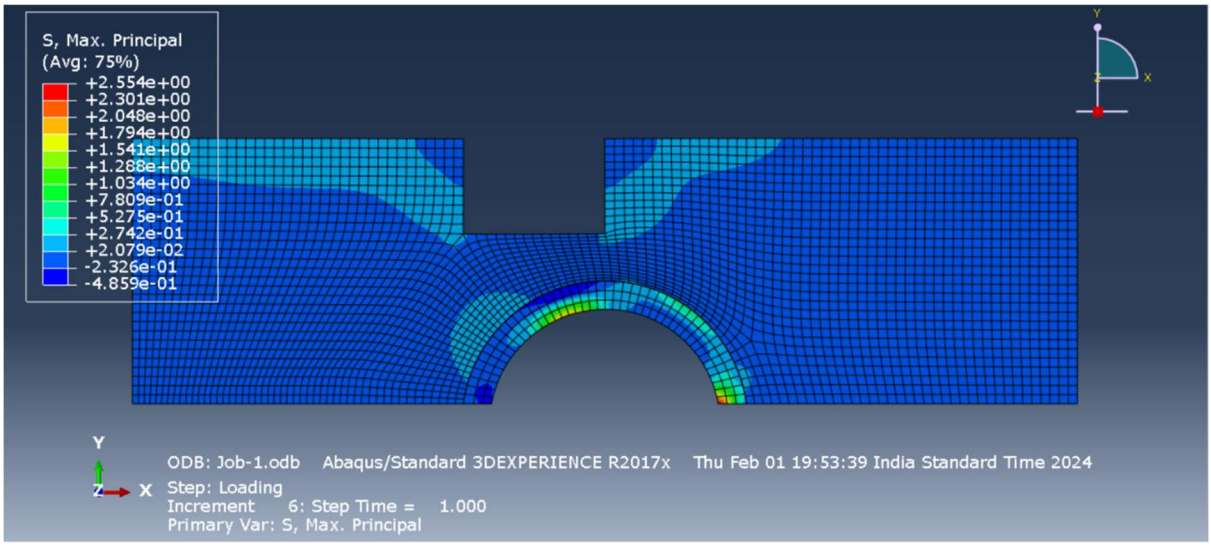

Fig.B.45. Maximum principal stress (MPa) contour corresponding to unsymmetric loading for footing of size 1.5 m x 1.5 m. Load case: 1.5 (DL + EL)

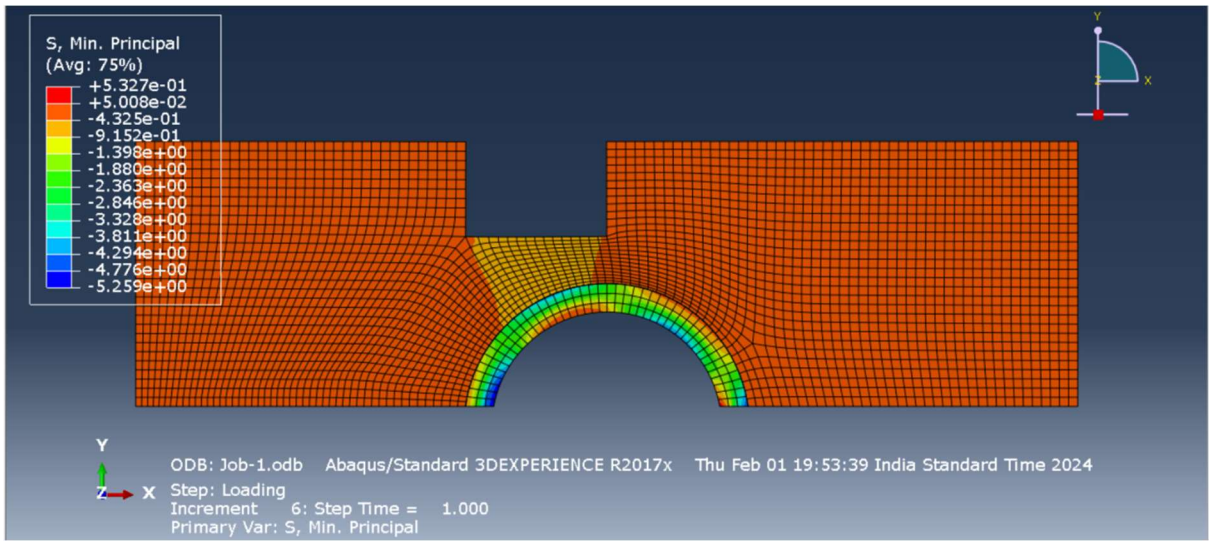

Fig.B.46. Minimum principal stress (MPa) contour corresponding to unsymmetric loading for footing of size 1.5 m x 1.5 m. Load case: 1.5 (DL + EL)

Seismic Case 4: Unsymmetric loading of masonry tunnel using footing of size 1.5 m – load case: 1.2 (DL + LL+ EL)

Load calculation:

1.2 (DL + LL) = 0.64 MPa

1.2 EL = 0.1398 MPa

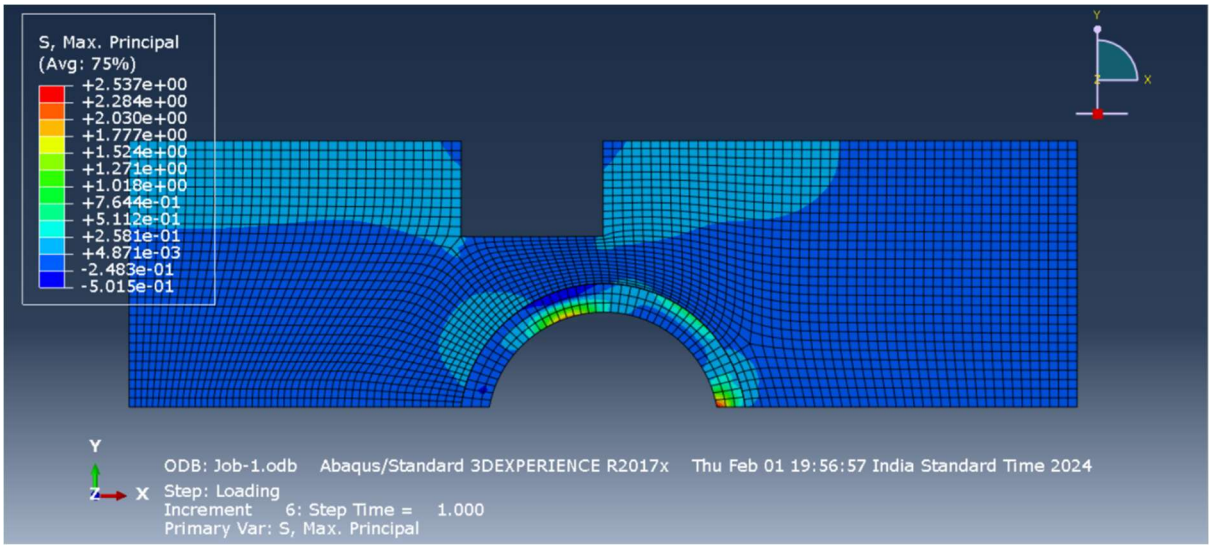

Fig.B.47. Maximum principal stress (MPa) contour corresponding to unsymmetric loading for footing of size 1.5 m x 1.5 m. Load case: 1.2 (DL + LL+ EL)

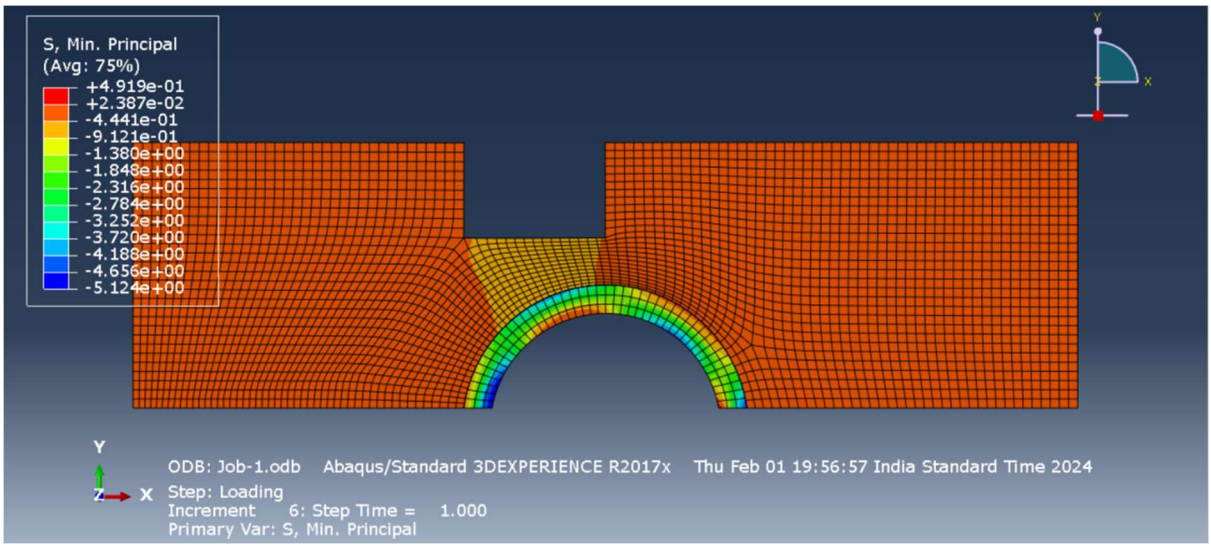

Fig.B.48. Minimum principal stress (MPa) contour corresponding to unsymmetric loading for footing of size 1.5 m x 1.5 m. Load case: 1.2 (DL+ LL + EL)

Seismic Case 5: Symmetric loading of masonry tunnel using footing of size 2.0x 2.0 m m – load case: 1.5 (DL + EL)

Load calculation:

Pressure corresponding to 1.5 DL = 0.326 MPa.

Pressure due to 1.5 EL = $0.1011\ MPa$

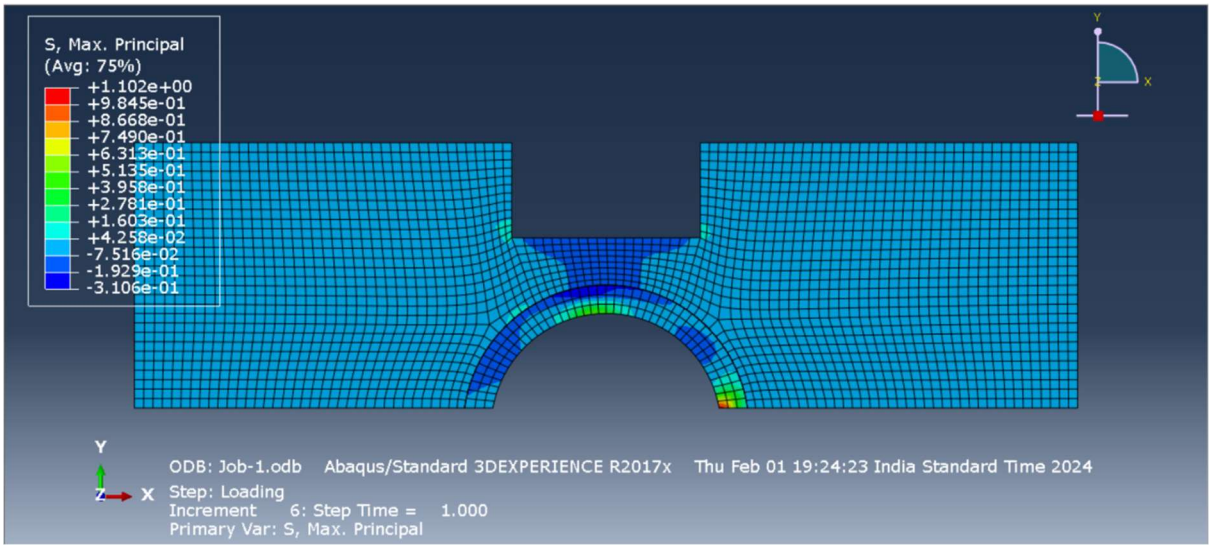

Fig.B.49. Maximum principal stress (MPa) contour corresponding to symmetric loading for footing of size 2.0 m x 2.0 m. Load case: 1.5 (DL+ EL)

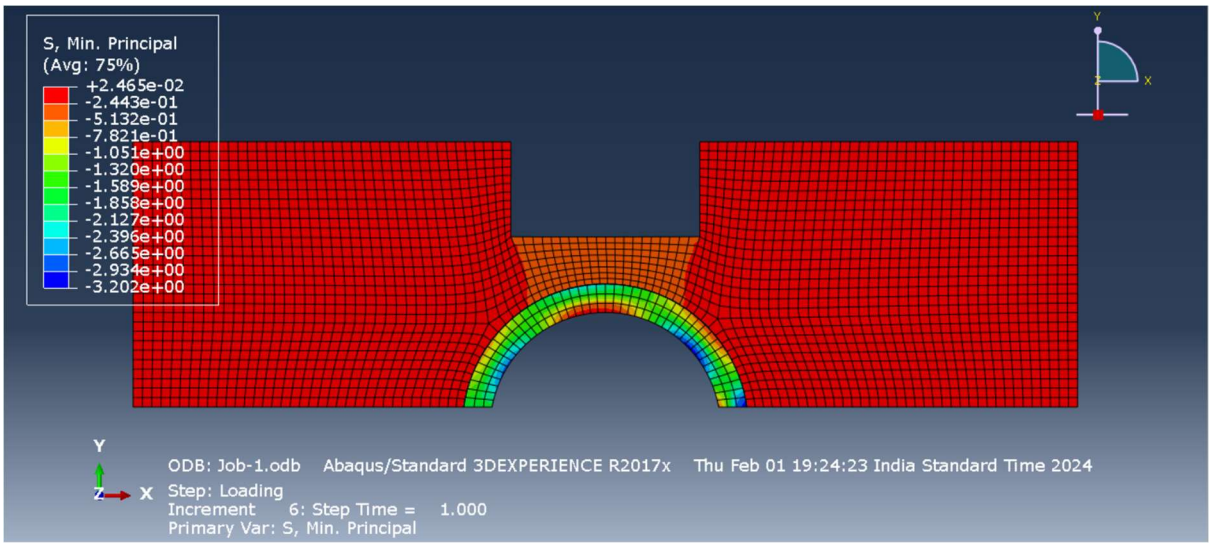

Fig.B.50. Minimum principal stress (MPa) contour corresponding to symmetric loading for footing of size 2.0 m x 2.0 m. Load case: 1.5 (DL+ EL)

Seismic Case 6: Symmetric loading of masonry tunnel using footing of size 2.0 m – load case: 1.2 (DL + LL+ EL)

Load calculation:

1.2(DL+LL) = 0.36 MPa

Pressure due to 1.2 EL = $0.0809\ MPa$

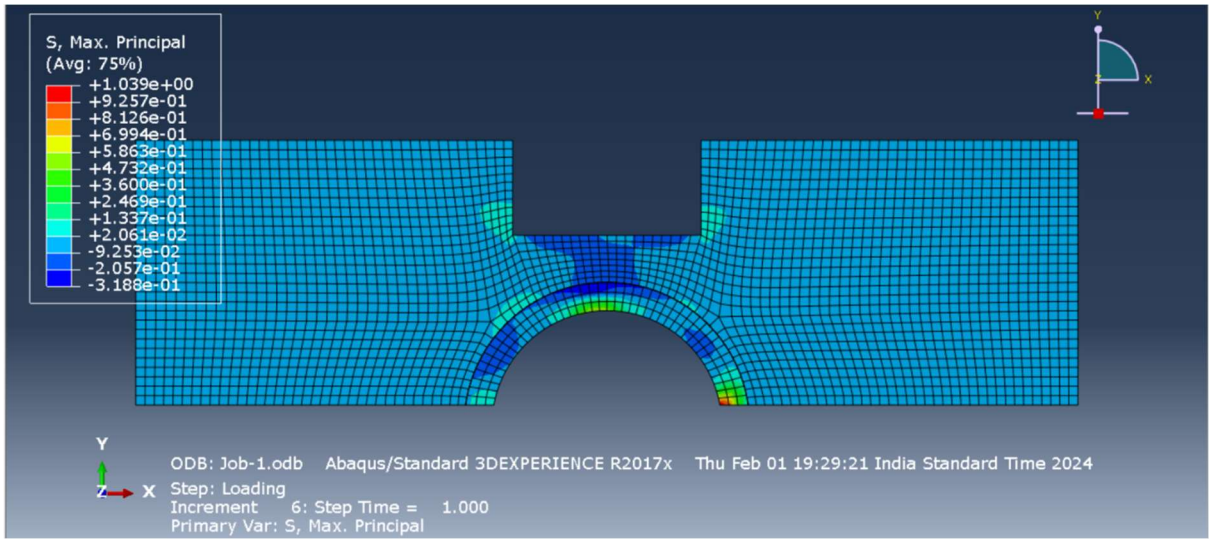

Fig.B.51. Maximum principal stress (MPa) contour corresponding to symmetric loading for footing of size 2.0 m x 2.0 m. Load case: 1.2 (DL+ LL+ EL)

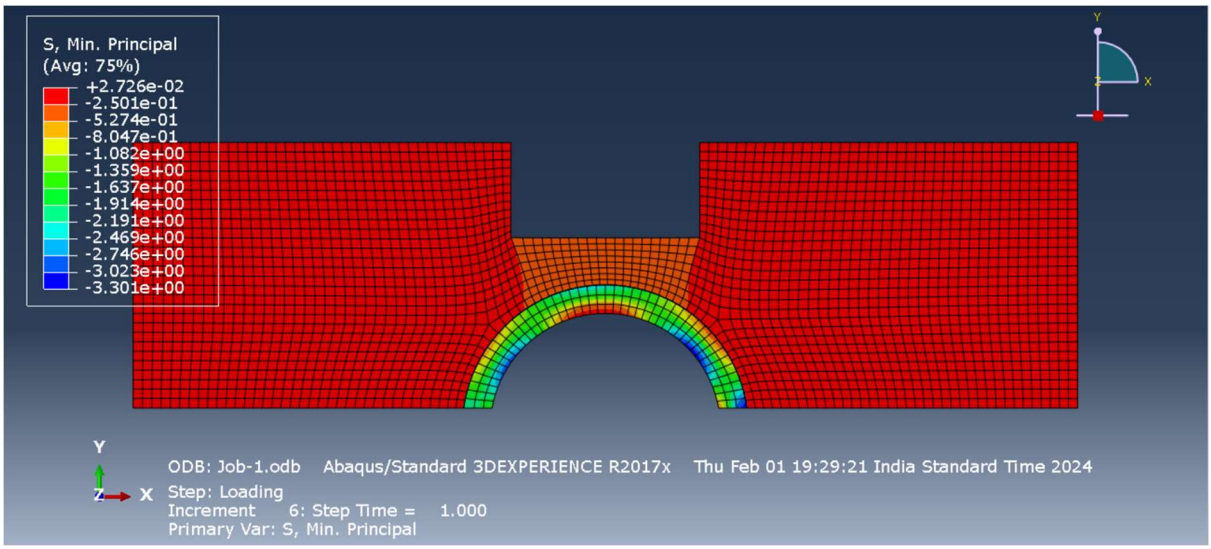

Fig.B.52. Minimum principal stress (MPa) contour corresponding to symmetric loading for footing of size 2.0 m x 2.0 m. Load case: 1.2 (DL+ LL+ EL)

Seismic Case 7: Unsymmetric loading of masonry tunnel using footing of size 2.0 m – load case: 1.5 (DL + EL)

Load calculation:

1.5 x DL = 0.326 MPa

Pressure due to 1.5 EL = $0.1011\ MPa$

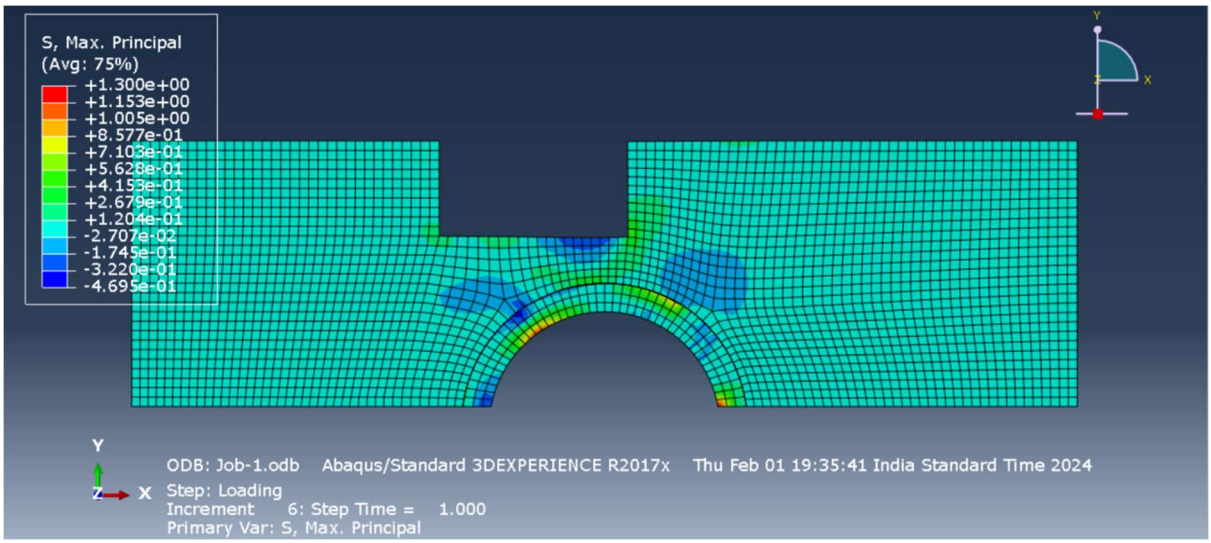

Fig.B.53. Maximum principal stress (MPa) contour corresponding to unsymmetric loading for footing of size 2.0 m x 2.0 m. Load case: 1.5 (DL+ EL)

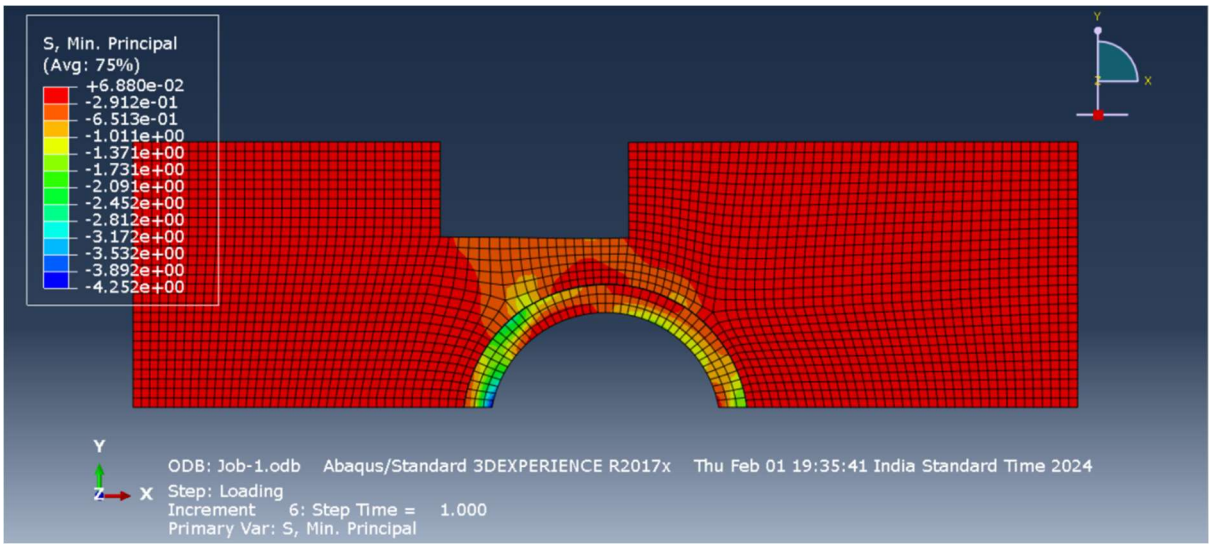

Fig.B.54. Minimum principal stress (MPa) contour corresponding to unsymmetric loading for footing of size 2.0 m x 2.0 m. Load case: 1.5 (DL + EL)

Seismic Case 8: Unsymmetric loading of masonry tunnel using footing of size 2.0 m – load case: 1.2 (DL + LL+ EL)

Load calculation:

1.2(DL+LL) = 0.36 MPa

1.2 x EL = $0.0809\ MPa$

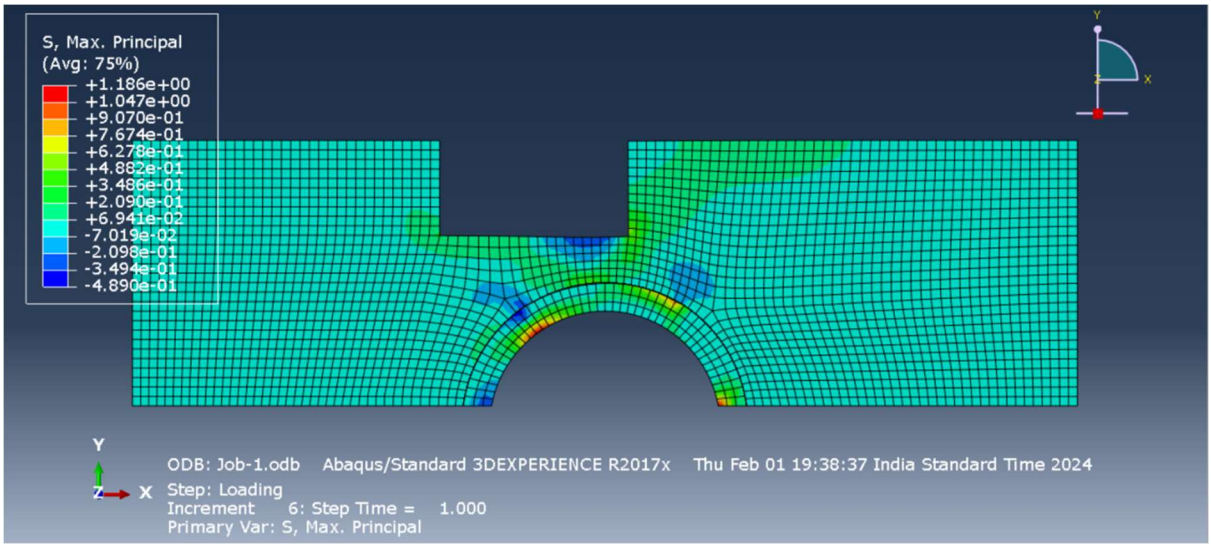

Fig.B.55. Maximum principal stress (MPa) contour corresponding to unsymmetric loading for footing of size 2.0 m x 2.0 m. Load case: 1.2 (DL+ LL+ EL)

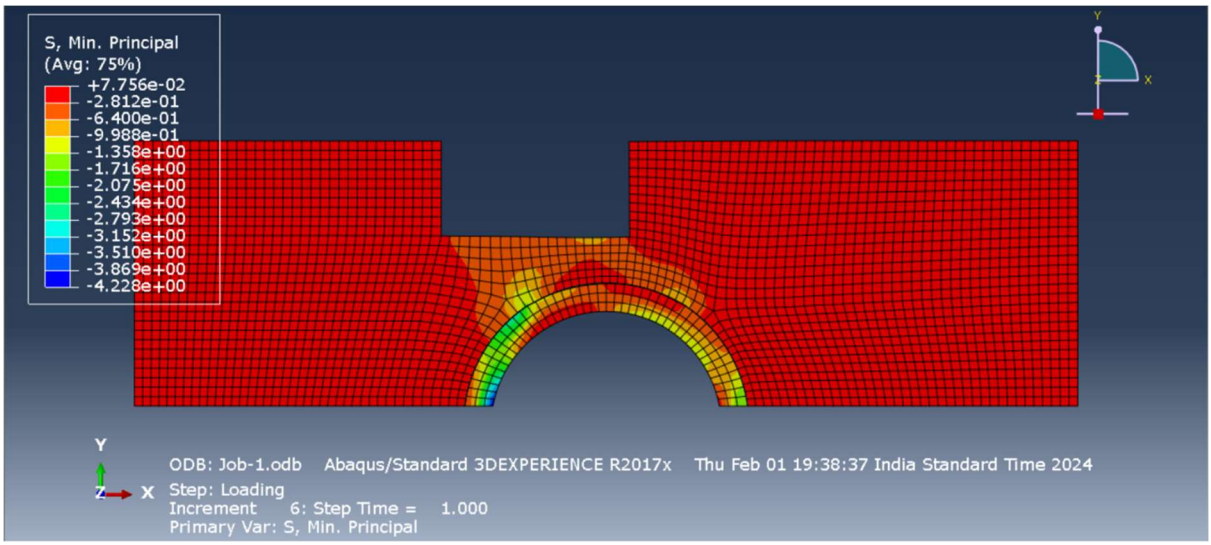

Fig.B.56. Minimum principal stress (MPa) contour corresponding to unsymmetric loading for footing of size 2.0 m x 2.0 m. Load case: 1.2 (DL+ LL+ EL)

Seismic Case 9: Symmetric loading of masonry tunnel using footing of size 3.0 m – load case: 1.5 (DL + EL)

Load calculation:

Pressure corresponding to 1.5 DL = 0.145 MPa.

Pressure due to 1.5 EL = $0.0571\ MPa$

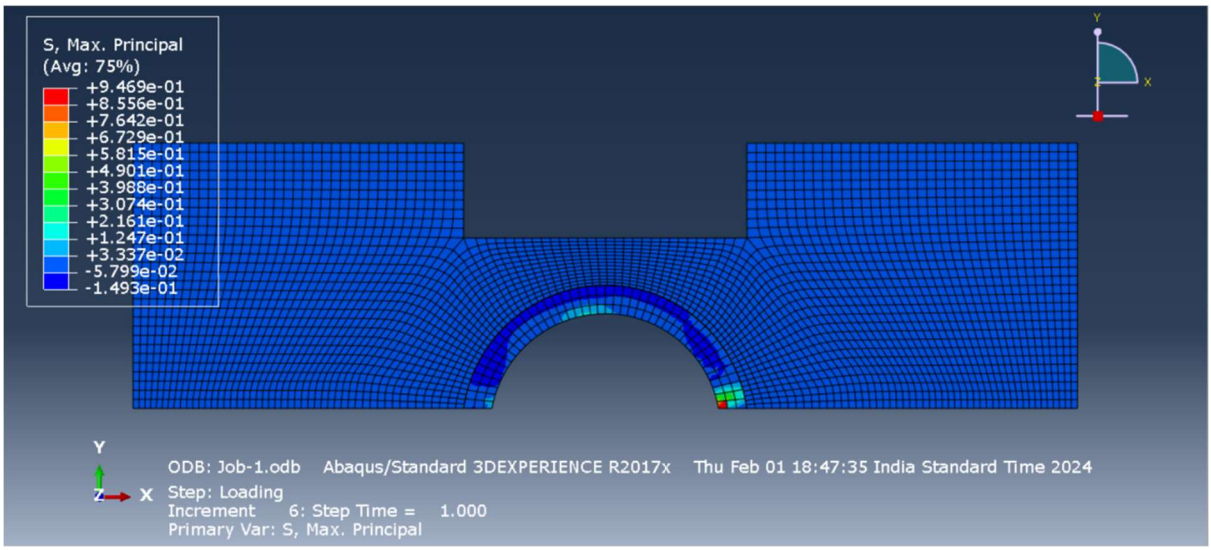

Fig.B.57. Maximum principal stress (MPa) contour corresponding to symmetric loading for footing of size 3.0 m x 3.0 m. Load case: 1.5 (DL+EL)

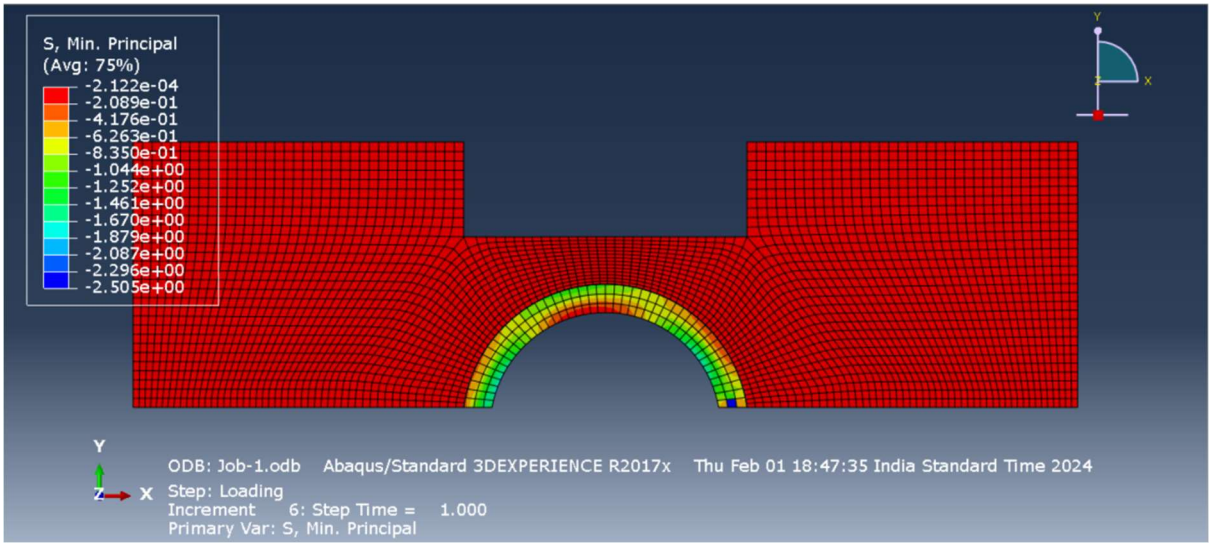

Fig.B.58. Minimum principal stress (MPa) contour corresponding to symmetric loading by footing of size 3.0 m x 3.0 m. Load case: 1.5 (DL + EL)

Seismic Case 10: Symmetric loading of masonry tunnel using footing of size 3.0 m – load case: 1.2 (DL +LL+ EL)

Load calculation:

1.2(DL + LL) = 1 0.16 MPa

1.2 EL = 0.04567 MPa

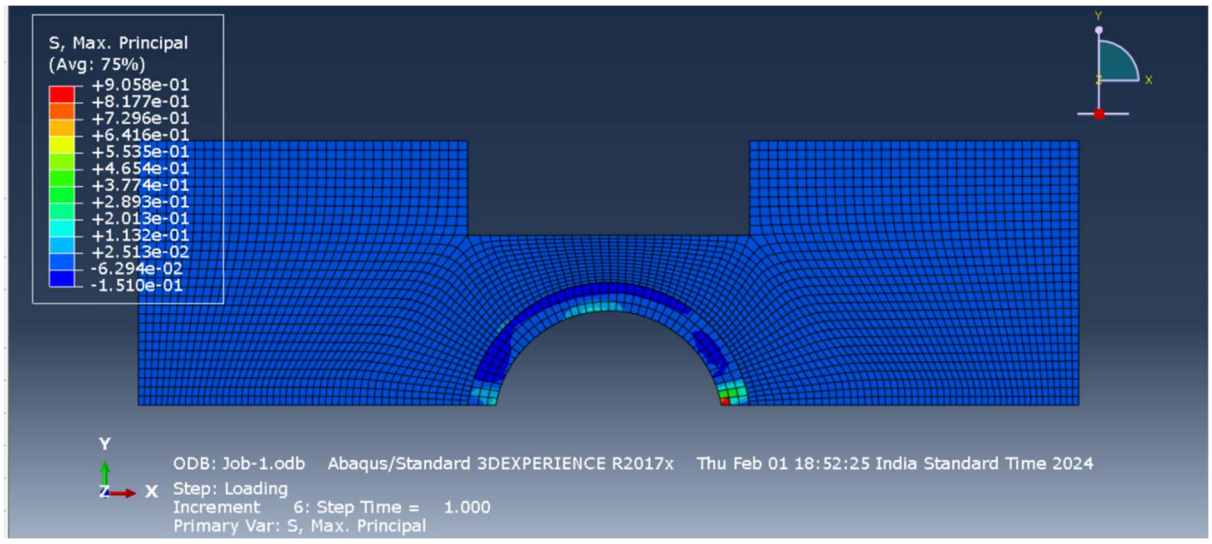

Fig.B.59. Maximum principal stress (MPa) contour corresponding to symmetric loading by footing of size 3.0 m x 3.0 m. Load case: 1.2 (DL+ LL+ EL)

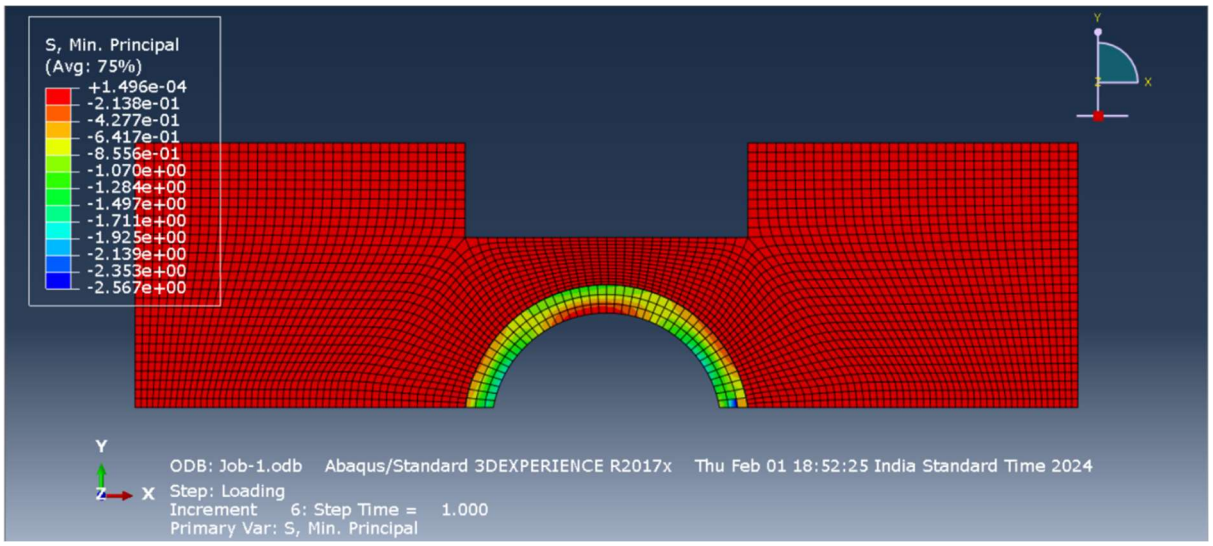

Fig.B.60. Minimum principal stress (MPa) contour corresponding to symmetric loading for footing of size 3.0 m x 3.0 m. Load case: 1.2 (DL+LL+EL)

Seismic Case 11: Unsymmetric loading of masonry tunnel using footing of size 3.0 m – load case: 1.5 (DL + EL)

Load calculation:

Pressure corresponding to 1.5 DL = 0.145 MPa.

Pressure due to 1.5 EL = $0.0571\ MPa$

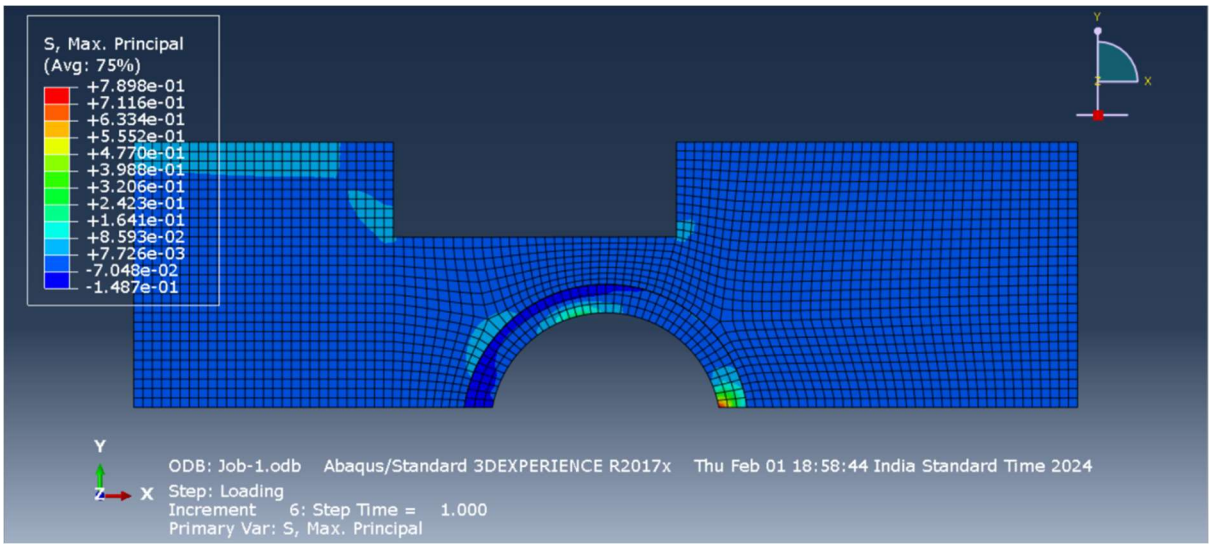

Fig.B.61. Maximum principal stress (MPa) contour corresponding to unsymmetric loading for footing of size 3.0 m x 3.0 m. Load case: 1.5 (DL+ EL)

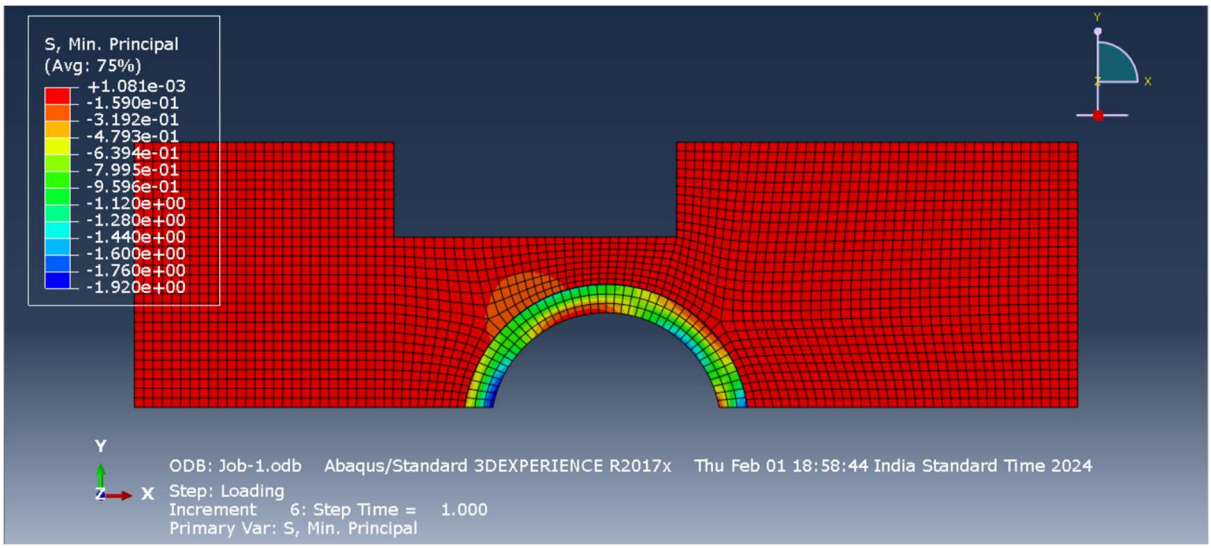

Fig.B.62. Minimum principal stress (MPa) contour corresponding to unsymmetric loading for footing of size 3.0 m x 3.0 m. Load case: 1.5 (DL+ EL)

Seismic Case 12: Unsymmetric loading of masonry tunnel using footing of size 3.0 m – load case: 1.2 (DL + LL+ EL)

Load calculation:

1.2(DL + LL) = 0.16 MPa

1.2 EL = 0.04567 MPa

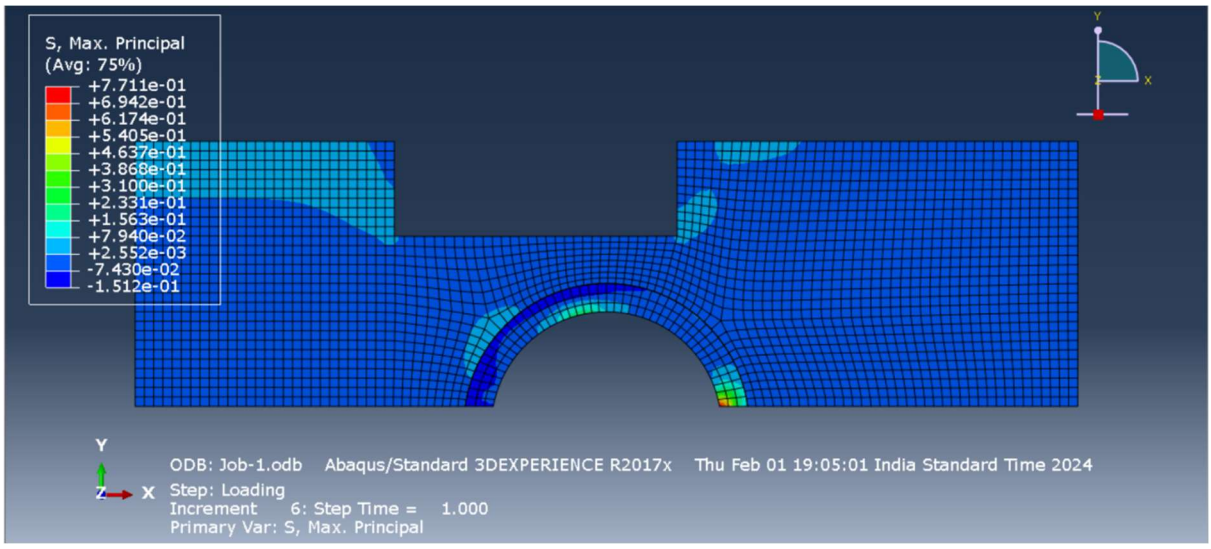

Fig.B.63. Maximum principal stress (MPa) contour corresponding to unsymmetric loading by footing of size 3.0 m x 3.0 m. Load case: 1.2 (DL+ LL+ EL)

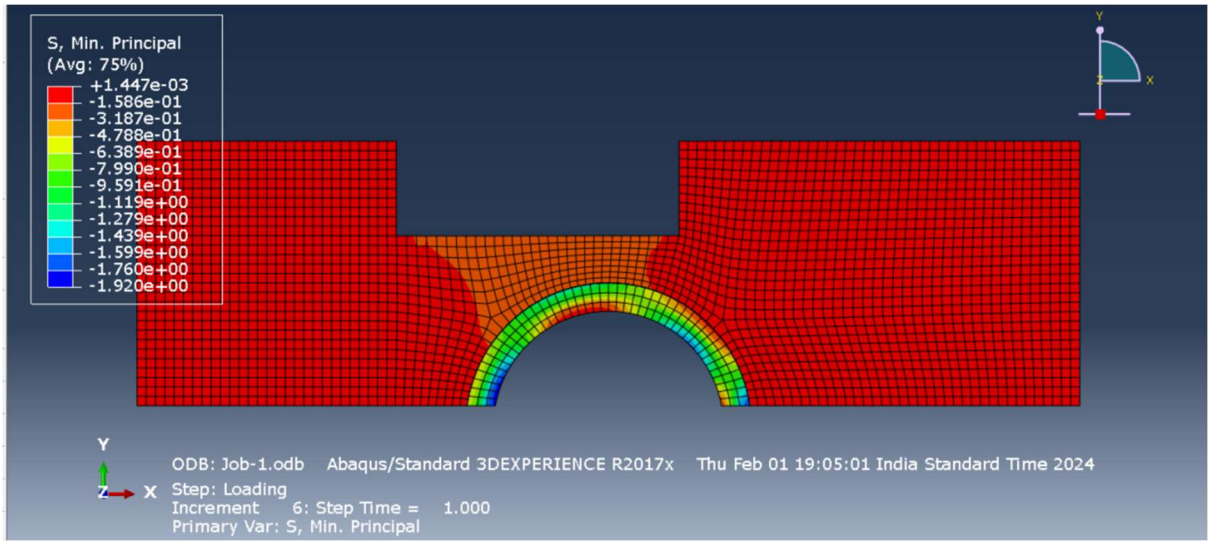

Fig.B.64. Minimum principal stress (MPa) contour corresponding to unsymmetric loading by footing of size 3.0 m x 3.0 m. Load case: 1.2 (DL+ LL+ EL)

Table B.6. Consolidated test results of seismic analysis: Load Case – 1.5 (DL+EL)

Footing Size	Symmetric Loading		Unsymmetric loading	
	Maximum principal stress (MPa)	Minimum principal stress (MPa)	Maximum principal stress (MPa)	Minimum principal stress (MPa)
1.5 m x 1.5 m	+0.71	-4.91	+1.30	-5.26
2.0 m x 2.0 m	+0.51	-3.02	+0.71	-4.25
3.0 m x 3.0 m	+0.49	-1.87	+0.40	-1.92

Table B.7. Consolidated test results of seismic analysis: Load Case – 1.2 (DL+LL+EL)

Footing Size	Symmetric Loading		Unsymmetric loading	
	Maximum principal stress (MPa)	Minimum principal stress (MPa)	Maximum principal stress (MPa)	Minimum principal stress (MPa)
1.5 m x 1.5 m	+1.52	-5.07	+1.30	-5.13
2.0 m x 2.0 m	+0.48	-3.30	+1.19	-4.23
3.0 m x 3.0 m	+0.50	-1.92	+0.40	-1.92

NB: localized peak stresses in the stress contours, developed in single elements, are discarded and stress magnitudes which has a considerable spread (over multiple elements) alone are included in the above tables.

4.B.5.3. Inferences from seismic analysis

Considering the various analysis involving gravity and seismic load cases, the following inferences are drawn:

For the symmetric loading of masonry tunnel involving footing of various sizes, the maximum principal compressive stress induced in the masonry tunnel section is due to the gravity loading case of 1.5(DL+LL). Whereas, the maximum principal tension induced in the tunnel section is due to the seismic loading cases (1.5DL+1.5EL or 1.2DL + 1.2LL+ 1.2EL).

For the unsymmetrical loading of masonry tunnel involving footing of various sizes, the maximum principal compression induced in the masonry tunnel section is due to the seismic loading scenario of 1.5(DL+EL). Whereas, the maximum principal tension induced in the tunnel section is due to the seismic loading case of 1.2(DL+LL+EL).

Considering the symmetric and unsymmetric loading scenarios of masonry tunnel by column footings, the seismic loading cases considered are seen to induce principal compression and principal tension in the masonry tunnel, exceeding the limits, for the case of 1.5 m and 2.0 m size square footing. Whereas, for the case of 3 m size square footing, the induced stresses due to seismic loads are seen to be within the limits.

Hence it can be concluded that considering the various gravity and seismic loading scenarios included in the analysis, columns with square footing of size 3 m or above, under a symmetric loading scenario, is expected to be safe. Unsymmetric loading from square footing of size 3 m is seen to induce a distributed tension at one of the supports of the tunnel, making the case vulnerable to failure.

5. Concluding Remarks of the Study

1. It is observed that many lateral canals have been constructed under peration Anatha and other schemes and joined to the main Thekkinikkara canal, at different stretches, so as to drain off the water and alleviate the flooding problem in the study area.
2. The major stretch of Thekkinikkara canal is silted up thereby having lesser carrying capacity when compared to its design carrying capacity.

3. It is observed that the existing network of Thekkinikkara canal is subjected to flooding for rainfall with return periods of 25-year, 50-year and 100-year and PMP values.
4. The canal is not subjected to flooding for rainfall having return period of 5 years and 10 years, being commonly used in the design of urban storm water drainage design.
5. The flood situation reported in the study is with the hydraulic particulars for the designed section of the canal. The flooding situation will be worse with the silted section of the canal, due to reduction in carrying capacity.
6. Following the limit state analysis of masonry structures, for column loading case, the masonry tunnel is found to be safe with a factor of safety 2, only in the case of column with footing dimension 3 m x 3 m or more, symmetrically placed, covering the entire channel width. For column footings with dimensions less than 3 m, the masonry tunnel was found to be unsafe. Under the action of traffic loads, the tunnel is safe with a safety margin of the order of 3.5.
7. Following the finite element analysis, the masonry arch tunnel is seen to be not safe in the dead load plus live load combinations of column load with footing size 1.5 m x 1.5 m and 2 m x 2 m placed above. However, for 3 m size footings above, the arch seems to be safe under the dead load plus live load combinations, provided the column footing is symmetrically placed over the masonry tunnel. For unsymmetric loading scenario involving 3 m x 3 m size footing, though the stress levels are seen to be close to that for the case of symmetric loading scenario, the spread of tension zone is seen to be more and unsymmetric, making the 3 m unsymmetric loading scenario more vulnerable to failure.
8. The principal compression induced on tunnel under unsymmetrical loading from column footing is governed by the seismic loading scenario, whereas the principal compression induced in symmetrical loading from column footing case is governed by gravity loading scenario.
9. Considering the symmetric and unsymmetric loading scenarios of masonry tunnel by column footings, the seismic loading cases considered are seen to induce principal compression and principal tension in the masonry tunnel, exceeding the limits, for the case of 1.5 m and 2.0 m size square footing.

Whereas, for the case of 3 m size square footing, the induced stresses due to seismic loads are seen to be within the limits.

10. The principal compressive and tensile stresses resulting from the various seismic loading cases is seen to be close to the stresses resulting from gravity loading scenario. This observation falls in line with the general notion that underground tunnels perform better during earthquakes compared to above ground structures, since tunnel structures cannot be excited independent of the ground.

References

1. Heyman, J. 1982 The masonry arch. Ellis Horwood, Chichester, United Kingdom
2. Livesley, R. K. A. 1978 Limit analysis of structures formed from rigid blocks. International Journal for Numerical Methods in Engineering **12**, 1853–1871
3. Gilbert, M. & Melbourne, C. 1994 Rigid-block analysis of masonry structures. The StructuralEngineer **72**, 356–360.
4. Limit State: Ring manual version 3.2 c, Limit state inc., Sheffield, UK, 2020.
5. Kezdi,A. (1974) Handbook of Soil Mechanics. Ed.1, Elsevier, Amsterdam
6. Amedia F. and B.Kuriakose (2017) Non-linear Finite Element Analysis of Unreinforced masonry walls, Applied Mechanics and Materials, 857, pp 142-147.
7. Naqvi, M.W., M.F. Akhtar, M. Zaid and M.R. Sadique (2020) Effect of superstructure on stability of underground tunnels, Transportation Infrastructure geotechnology, Springer Nature. https://doi.org/10.1007/s40515-020-00119-6.
8. Abdulla K.F., L.S. Cunningham and M. Gillie (2017) Simulating masonry wall behaviour using simplified micro model approach, Engineering Structures, 150, pp. 349-365.
9. Sarangapani G., B. V. Venkatarama Reddy and K. S. Jagadish (2005) Brick mortar bond and masonry compressive strength, Journal of Materials in Civil Engineering (ASCE), 17(2), pp- 229-237.
10. IS 1893 (part3):2014 Criteria for Earthquake resistant Design of Structures: Part 3: Bridges and retaining walls., Bureau of Indian Standards, NewDelhi.

11. Dam Safety assurance and Rehabilitation Project – Generalized PMP Atlas Phase 2 (Stage 1) : Report of the West flowing rivers of Western Ghats, WAPCOS, New Delhi.
12. Soumya R, Anjitha, U G, Smitha Mohan, Adarsh S, Gopakumar R (2020), IOP Conf. Ser.: Earth Environ. Sci. 491012013
13. Hazard and Vulnerability assessment report: Thiruvananthapuram city, Kerala state disaster management authority, 2015